

**EXPLORING THE IMPACT OF THE TUMOR MICROENVIRONMENT
ON NUCLEAR MORPHOMETRY: LESSONS LEARNED FOR
SENSITIVITY TO CYTOTOXIC TREATMENT**

by

Apekshya Chhetri

A Thesis

Submitted to the Faculty of Purdue University

In Partial Fulfillment of the Requirements for the degree of

Master of Science



Department of Basic Medical Sciences

West Lafayette, Indiana

May 2021

THE PURDUE UNIVERSITY GRADUATE SCHOOL
STATEMENT OF COMMITTEE APPROVAL

Dr. Sophie A. Lelièvre, Chair

College of Veterinary Medicine

Dr. Brittany Lee Allen-Petersen

College of Science

Dr. Joseph V. Rispoli

College of Engineering

Dr. Kinam Park

College of Pharmacy and College of Engineering

Approved by:

Dr. Laurie Jaeger

*Dedicated with love to my parents, Goma and Than, to my sister, Samikshya
and to my beloved, Ashu.*

ACKNOWLEDGMENTS

I would like to express my sincere gratitude and appreciation to my advisor, Prof. Sophie Lelièvre, for her support, guidance, and indispensable feedbacks. They taught me how to pursue a research interest and more importantly, interpret the findings like a researcher. I am grateful to my colleagues in the Cell Nucleus Laboratory – Dr. Shirisha Chittiboyina, for her constant cheer, advices and for my training in cell culture ; Dr. Yunfeng Bai for his support. I thank my committee members - Dr. Brittany Allen-Peterson and Dr. Joseph Rispoli for their invaluable feedbacks and encouragements. I also thank Garima Baral, a fellow graduate student working in the Allen-Peterson laboratory for her help with the microscopy and cheer her friendship. I extend my gratitude to the faculties and staff members from the department of Basic Medical Sciences, Weldon School of Biomedical Engineering, and the graduate school dissertation office at Purdue university for their support.

I am equally grateful and overjoyed to receive the love and support of my family and friends, to hear their refreshing perspectives and to feel their constant presence in my life. Successful completion of my master's research and its compilation into this dissertation would not have been possible without their encouragements.

TABLE OF CONTENTS

LIST OF TABLES.....	7
LIST OF FIGURES	8
ABSTRACT.....	9
CHAPTER 1. INTRODUCTION.....	10
1.1 Breast cancer.....	10
1.1.1 Triple negative breast cancer	11
1.1.2 Cisplatin treatment for patients with aggressive forms of cancer.....	11
1.1.3 Pathological investigation of cancer involves nuclear atypia	11
1.2 In vitro cell culture in cancer research	13
1.3 References:	14
CHAPTER 2. 3D CELL CULTURE FOR THE STUDY OF MICROENVIRONMENT-MEDIATED MECHANOSTIMULI TO THE CELL NUCLEUS: AN IMPORTANT STEP FOR CANCER RESEARCH.....	17
2.1 Introduction	18
2.2 Evidence of mechanotransduction to the genome in cell culture	20
2.3 Cell culture models for ECM-mediated mechanical forces in cancer progression.....	24
2.4 Integration of microfluidics in the study of mechanotransduction in tumors	27
2.5 A bright future for 3D cell culture in mechanomedicine.....	28
2.6 References.....	34
CHAPTER 3. MATERIALS AND METHODS	44
3.1 Cell culture and medium.....	44
3.2 3D cell culture and collagen matrix preparation	44
3.2.1 The following sections are included from pages 4 – 9 of the article: Basic protocol 1	45
3.2.2 Support protocol 1	53
3.2.3 Support protocol 2	56
3.3 Treatments with conditioned medium and cisplatin	60
3.4 DAPI staining	60
3.5 Nuclear morphometry and cell death assessment	61

3.6 References:	63
CHAPTER 4. RESULTS.....	64
4.1 References:	89
CHAPTER 5. DISCUSSION	90
5.1 References:	97
CHAPTER 6. CONCLUSION.....	102

LIST OF TABLES

Table 3.1. Stock, Working and Final Concentrations of Cell Culture Additives with their Storage Conditions	47
Table 3.2. Example of Cell Seeding Depending on the Culture Mode	49
Table 4.1. Percentage of cell death in MDA-MB-231 and T4-2 tumors based on microenvironmental conditions	79
Table 4.2. Percentages of cytotoxicity response to cisplatin in collagen (900 Pa and 2000 Pa stiffnesses) for MDA-MB-231 cells in control conditioned medium.	81
Table 4.3. Percentage of cytotoxicity response to cisplatin in collagen I (900 Pa and 2000 Pa stiffnesses) for MDA-MB-231 cells in the presence of S1 conditioned medium:	83
Table 4.4. Percentage of cytotoxicity response to cisplatin in collagen I (2000 Pa and 3300 Pa stiffnesses) for T4-2	87

LIST OF FIGURES

Figure 2.1. Mechanotransduction in response of mechanostimuli	22
Figure 2.2. Heterogeneity within and outside tumors influences cancer behavior.....	30
Figure 3.1. Influence of matrix stiffness on cancer cells.	58
Figure 3.3.2 T4-2 tumors cultured in collagen I (2000 Pa) on H14 medium	62
Figure 4.1. Tumor obtained from MDA-MB-231 and T4-2 cell lines are distinct.	65
Figure 4.2. Mean nuclear area in MDA-MB-231(top panel) and T4-2 (bottom panel) is dependent on the stiffness of collagen I.	66
Figure 4.3. Mean nuclear circularity in MDA-MB-231(top panel) and T4-2 (bottom panel) is dependent on the stiffness of collagen I	68
Figure 4.4. The distribution of nuclear area is influenced by the stiffness of collagen I in opposite manner depending on the degree of aggressiveness of the tumors.....	70
Figure 4.5. The distribution of nuclear circularity appears poorly responsive to increased matrix stiffness, especially in less aggressive tumors.	71
Figure 4.6. S1 cells monolayer culture on top of laminin 111 precoated with collagen I (770 Pa).	72
Figure 4.7. Conditioned medium from non-neoplastic cells prevents the effect of increasing collagen I stiffness on nuclear circularity.	74
Figure 4.8. The impact of ECM stiffness on the distribution of nuclear circularity in cancer cells is prevented by paracrine factors from the non-neoplastic cells.....	76
Figure 4.10. Increasing stiffness does not alter the sensitivity of T4-2 cell to LD50 of cisplatin.	88

ABSTRACT

Breast cancer remains the leading cause of death among females worldwide. While systemic therapy for breast cancer may work effectively in the early phases, for more than 10% of primary and 50% of metastatic cases, the disease eventually progresses, resisting treatments. To overcome this issue, recognizing markers of resistance as early as possible is critical. However, the underlying mechanisms of resistance remains elusive. The influence of microenvironmental factors of the extracellular matrix (ECM) on tumor behavior has been revealed relatively recently and increased stiffness of ECM is associated with cancer progression. Additionally, impacts of other matrix components such as non-neoplastic epithelial cells (that may constitute an important portion of the tumor microenvironment -TME) are suspected to influence tumors but they have not been investigated in detail. Besides, it is not known whether the response to increasing stiffness depends on the subtypes of breast cancer. Here, using breast models in 3D cell culture we have shown that the non-neoplastic epithelial compartment can influence the effect of matrix stiffness even for tumors recognized as highly aggressive. The degree of tumor aggressiveness recognizable via tumor architecture is associated with a differential behavior when ECM stiffness changes. In a 3D microenvironmental context, which provides an optimal level of constraints for tumors to display their phenotype, we report stiffness and paracrine influence impact on cisplatin-mediated cytotoxicity, which correlates with distinct nuclear morphometry and distribution pattern associated with population heterogeneity. The response pattern varies across cell lines representing higher and lower levels of aggressiveness in the basal-like subtypes of breast cancer. Our results also highlight the need for integrating biochemical and physical components of the TME in future designs of *in vitro* drug screening platforms.

Keywords: breast cancer, ECM, microenvironment, 3D cell culture, matrix stiffness, nuclear morphometry, heterogeneity

CHAPTER 1. INTRODUCTION

1.1 Breast cancer

Worldwide, breast cancer affects 2.3 million persons each year and remains the primary cause of cancer-associated deaths among women (1). In the last 40 years since the disease received the warranted attention of the policy makers, [which initiated with the National Cancer Act in the USA (1971)], effective intervention and screening strategies rose tremendously. The survival rates of patients with all types of cancer in the US has improved significantly (by 27%) in the last two decades (2). In terms of improved breast cancer survivorship, early detection, increased awareness about breast cancer, early screening and evolving effective treatments are the primary reasons for the achievement. Even with these positive strides, currently, resistance to treatment remains a sustained problem in breast cancer management.

While the systemic therapy may work effectively in the early phases, for more than 10% of primary and 50% of metastatic cases, the disease eventually progresses, resisting treatments (3). Moreover, metastatic recurrences are largely difficult to treat. To overcome this issue, recognizing markers of resistance as early as possible is critical in addition to designed therapies that prevent and/or overcome resistance mechanisms. Resistance is a multi-factorial process governed by genetic and epigenetic changes (4-6); however, the underlying mechanism(s) of resistance remains unknown. Assessment of resistance at the time of cancer detection and before the use of neoadjuvant therapies could be useful in countering the development of cancer resistance; biomarkers of resistance are currently being explored on multiple levels, both inside and outside the cells.

Breast cancer being a heterogenous disease requires different therapeutic approaches for effective treatment. Most types of breast cancers display overexpressed hormone receptors, including estrogen receptor (ER), progesterone receptor (PR) and Human epidermal growth factor receptor 2 (HER2), and are treated with therapies that target these receptors. There are certain types of breast cancers that do not exhibit such overexpression of receptors, often indicating aggressive phenotypes, and requiring strong treatment alternatives. Early detection via effective screenings and evolving treatments have improved the chances of breast cancer patients' survival (2). Thus, it is crucial to continue identifying techniques to detect and treat aggressive cancers in

early stages and find new avenues to better treat cancers in later stages when resistance to chemotherapy is a major risk.

1.1.1 Triple negative breast cancer

Breast cancer is known to be heterogenous with classifications into multiple subtypes. Triple negative breast cancer (TNBC) is one of the most aggressive forms amongst these cancer subtypes. It is molecularly characterized by the absence of all three types of growth receptors: ER, HER2 and PR and accounts for 15-20% of breast cancer incidence (3). Newer evidence indicates that the TNBC is a heterogenous group, notably of ~three to five molecular subtypes (4). Each of these subtypes responds varyingly to treatments, many of which are still under clinical phases of research. For patients diagnosed with TNBC, cytotoxic chemotherapy is the first line of treatment and often includes cisplatin, although research is underway to identify new therapeutic targets (4).

1.1.2 Cisplatin treatment for patients with aggressive forms of cancer

“Apoptosis” or programmed cell death of is a major mechanism of action of effective chemotherapeutic agents (5). Platinum derived chemotherapeutics are one of the strongest choices for treating aggressive cancers, including cancers of pancreas, lungs, and breast (6). The triple negative breast cancers that lack targeted therapies are often treated using cytotoxic drug combinations, which includes the very potent Cisplatin. A type of platinum-based drug, cisplatin binds to the DNA, forming platinum-DNA-adduct and causing DNA damage. Such lesions in the DNA result in the activation of the DNA repair machinery that ultimately induces apoptosis. Newer evidence suggests that cisplatin can even target the cell death programming machinery in the nucleus in an independent manner, through Ca^{2+} and endoplasmic reticulum mediated stress (6,7,8).

1.1.3 Pathological investigation of cancer involves nuclear atypia

Treatment decisions for cancer patients require collective information from clinical, pathological and genomics analyses to screen and characterize the state of the tumor. The state of cancer in patients is evaluated pathologically through tumor grading and staging, which mostly

involves comparing the physical and cellular attributes of the cancerous sites with the normal histology. The histological grading factors vary between different types of cancers. In breast cancer, the grading factors are derived based on the Nottingham grading index for breast cancers (9).

Nuclear atypia scoring is one of the histological analyses that is currently in use for pathological confirmation of diseases like cancer. The scoring involves comparing the nuclear dimensions (size and shape) and visible characteristics of diseased (cancerous) nuclei with that of a noncancerous nucleus. The more deviated the nuclei from normal histology, the higher its score, suggesting a more aggressive type of tumor. The nucleus being the main center for relaying information and action, owing to the presence of genetic information, nuclear changes are essential in capturing the diseased state. One of the criticisms that the current method of nuclear atypia scoring faces is the variability during data collection. To overcome this issue, research is underway to standardize the method of data capturing. Newer imaging technologies that provide higher resolution and improved software, with the added strengths of bioinformatics, might aid in limiting the variability in assessments of patient samples (10-13).

It is debatable whether nuclear volume and nuclear size are affected by the genomic density known to change in cancer (14). Nuclear shape and function remain an interesting puzzle, with evidence supporting an influence of shape on function, but the underlying path remains elusive (15). Most of the characterizations of specific nuclear shape are linked to cell division. Such as the rounding of the nucleus during mitosis is of great importance to the cells, as it ensures a symmetric division to form daughter cells. Further, nuclear shape changes to minimize internal stress accumulated in response to external stress, such as those felt during migratory movements of metastatic cancers or during any damages to DNA (16). Also, distinct features of nuclear size and shape are observed with specific patterns of chromatin (17) and long non-coding RNAs that mediate transcription levels (18), suggesting that these features should be explored as potential biomarkers of diseases.

The shape of a nucleus is determined by a bidirectional force, experienced between the external cytoskeleton and internal chromosomal rearrangements. Which among these two forces impact the maintenance of nuclear shape most remains unknown. Newer evidences from mechanotransduction emphasize the role of external stimuli on the nuclear components through membrane linking via microtubules/filamented proteins. These changes in external stimuli also influence distinct chromatin distribution and change its linkage to nuclear membrane as well as

gene expression (19-21). Based on the arguments that shape maintenance is equally affected by external cytoskeletal components connected to the nucleus, we hypothesized in our study that changing a physical component (stiffness) of the ECM, influences nuclear shape (circularity) and size (area) differently depending on tumor aggressiveness illustrated by tumor architecture. This hypothesis is based on a unifying principle proposed 20 years ago by Bissell and colleagues (22) stating that “the unit of function in higher organisms is neither the genome nor the cell alone but the complex, three-dimensional tissue”.

1.2 In vitro cell culture in cancer research

The current state-of-knowledge of cancer and the advanced therapeutics developed against this disease were possible thanks to the progressive advancement of basic science research and its partnership with the rapidly evolving engineering research. At the heart of this interdisciplinary knowledge and the resulting sophisticated techniques, remains the basic principle of replicating the *in vivo* ‘human-body like environment’ to culture cells using appropriate *in vitro* microenvironments. Identified more than a century ago, the methods and techniques used for *in vitro* cell culture have evolved to create more physiologically relevant models. Current cell culture techniques recreating the complexity of a tissue matrix and its environment have applications in basic and translational research. Such tissue matrices are recreated in a laboratory by utilizing commercially available synthetic gels, such as collagen I, which is a major protein of the ECM in the stroma and is directly linked to the increased stiffness that accompanies cancer progression (23). In real tissues, the ECM is a dynamic compartment with constant remodeling (24). Proteins like collagens are involved in this remodeling and result in ECM’s stiffness changes. Adding this physical complexity of the ECM thanks to the synthetic collagen I based gel in the laboratory is dependent on its pH dependent polymerization. A range of collagen I stiffnesses can be obtained by varying the concentrations of collagen I obtained from manufacturers as Advanced Biomatrix (<https://advancedbiomatrix.com/collagen/>). A detailed protocol describing the physiologically relevant cell culture technique (more commonly termed 3D cell culture, due to the ease of forming a three-dimensional morphology in porous substrates), along with obtaining collagen I gels of varying stiffnesses, is described in the MATERIALS & METHODS section.

Since the ECM and its physical and biochemical components are linked to internal cellular components reaching the nucleus through a direct physical linkage (mechanotransduction) as well

as continuous biochemical exchanges, effective strategies to screen resistance would have to consider this interplay and bidirectional communication. Increasing evidence suggests a remodeled matrix, with an elevated stiffness, in cancer. Specifically, as cancer progresses into a more aggressive form, the matrix further stiffens (25). Compared to a healthy breast tissue which has a Young's modulus (a measure of stiffness) of ~900-1200 Pa, a cancerous tissue is projected to have a Young's modulus of ~3000 to 5000 Pa. In our study, we have looked at how the tumor's responses adapt with respect to stiffness-mediated physical change, especially in the early phases of cancer growth (corresponding to stiffness of 900 - 3000 Pa) in aggressive and less aggressive forms of triple negative breast tumors. Further, we were also interested to see if there were any influences from the non-neoplastic epithelial cells (from which the carcinomas are derived) to such stiffness-mediated interaction. Any influence of stiffness modulated by paracrine factors from non-neoplastic epithelial cells on tumor phenotypes would be invaluable information to include to other parameters already studied in developing therapeutic approaches and predicting the outcomes of therapeutic interventions. The first part of our study presents these physical and biochemical interactions through nuclear phenotypic changes (spread of nuclear morphometric parameters and the heterogeneity of the spread) and the second part, using cytotoxic treatment with Cisplatin, we investigate the impact of physical (stiffness) and paracrine influences on the behavior of the aggressive TNBC tumors.

1.3 References:

1. Sung, H., Ferlay, J., Siegel, R. L., Laversanne, M., Soerjomataram, I., Jemal, A., & Bray, F. (2021). Global cancer STATISTICS 2020: GLOBOCAN estimates of incidence and mortality worldwide for 36 cancers in 185 countries. *CA: A Cancer Journal for Clinicians*. doi:10.3322/caac.21660
2. CDCBreastCancer. (2021, February 23). An update on cancer deaths in the United States. Retrieved April 17, 2021, from <https://www.cdc.gov/cancer/dcpc/research/update-on-cancer-deaths/index.htm>
3. Marra, A., Trapani, D., Viale, G., Criscitiello, C., & Curigliano, G. (2020). Practical classification of triple-negative breast cancer: intratumoral heterogeneity, mechanisms of drug resistance, and novel therapies. *npj Breast Cancer*, 6(1), 1-16.
4. Nedeljković, M., & Damjanović, A. (2019). Mechanisms of chemotherapy resistance in triple-negative breast cancer—how we can rise to the challenge. *Cells*, 8(9), 957.

5. Marczak, A., Denel-Bobrowska, M., Rogalska, A., Łukawska, M., & Oszczapowicz, I. (2015). Cytotoxicity and induction of apoptosis by formamidinodoxorubicins in comparison to doxorubicin in human ovarian adenocarcinoma cells. *Environmental toxicology and pharmacology*, 39(1), 369-383.
6. Al-Bahlani, S., & Al-Jaaidi, S. (2018). Triple-Negative Breast Cancer, Cisplatin and Calpain-1. In *Breast Cancer and Surgery*. IntechOpen.
7. Han, J., Lim, W., You, D., Jeong, Y., Kim, S., Lee, J. E., ... & Park, S. (2019). Chemoresistance in the human triple-negative breast cancer cell line MDA-MB-231 induced by doxorubicin gradient is associated with epigenetic alterations in histone deacetylase. *Journal of oncology*, 2019.
8. Yu, F., Megyesi, J., & Price, P. M. (2008). Cytoplasmic initiation of cisplatin cytotoxicity. *American Journal of Physiology-Renal Physiology*, 295(1), F44-F52.
9. Elston, C. W., & Ellis, I. O. (1991). Pathological prognostic factors in breast cancer. I. The value of histological grade in breast cancer: experience from a large study with long-term follow-up. *Histopathology*, 19(5), 403-410.
10. Horlings, H. M., Savci-Heijink, C. D., & van de Vijver, M. J. (2010). Translating the Genomic Architecture of Breast Cancer into Clinical Applications. *Science translational medicine*, 2(38), 38ps32-38ps32. Khan, A. M., Sirinukunwattana, K., & Rajpoot, N. (2015). A global covariance descriptor for nuclear atypia scoring in breast histopathology images. *IEEE journal of biomedical and health informatics*, 19(5), 1637-1647.
11. Gutman, D. A., Khalilia, M., Lee, S., Nalisnik, M., Mullen, Z., Beezley, J., ... & Cooper, L. A. (2017). The digital slide archive: A software platform for management, integration, and analysis of histology for cancer research. *Cancer research*, 77(21), e75-e78.
12. Amgad, M., Atteya, L. A., Hussein, H., Mohammed, K. H., Hafiz, E., Elsebaie, M. A., ... & Cooper, L. A. (2021). NuCLS: A scalable crowdsourcing, deep learning approach and dataset for nucleus classification, localization and segmentation. *arXiv preprint arXiv:2102.09099*.13.
13. Khan, A. M., Sirinukunwattana, K., & Rajpoot, N. (2015). A global covariance descriptor for nuclear atypia scoring in breast histopathology images. *IEEE journal of biomedical and health informatics*, 19(5), 1637-1647.14.
14. Zimmermann, A. (2017). Nucleus, Nuclear Structure, and Nuclear Functional Changes in Liver Cancer. In A. Zimmermann (Ed.), *Tumors and Tumor-Like Lesions of the Hepatobiliary Tract: General and Surgical Pathology* (pp. 3043–3069). Springer International Publishing. https://doi.org/10.1007/978-3-319-26956-6_169
15. Webster, M., Witkin, K. L., & Cohen-Fix, O. (2009). Sizing up the nucleus: nuclear shape, size and nuclear-envelope assembly. *Journal of cell science*, 122(10), 1477-1486.

16. Mukherjee, A., Barai, A., Singh, R. K., Yan, W., & Sen, S. (2020). Nuclear plasticity increases susceptibility to damage during confined migration. *PLoS computational biology*, 16(10), e1008300.
17. Damodaran, K., Crestani, M., Jokhun, D. S., & Shivashankar, G. V. (2019). Nuclear morphometrics and chromatin condensation patterns as disease biomarkers using a mobile microscope. *PloS one*, 14(7), e0218757.
18. Grosch, M., Ittermann, S., Rusha, E., Greisle, T., Ori, C., Truong, D. J. J., ... & Drukker, M. (2020). Nucleus size and DNA accessibility are linked to the regulation of paraspeckle formation in cellular differentiation. *BMC biology*, 18, 1-19.
19. Dahl, K. N., Ribeiro, A. J. S., & Lammerding, J. (2008). Nuclear shape, mechanics, and mechanotransduction. *Circulation Research*, 102(11), 1307–1318. <https://doi.org/10.1161/CIRCRESAHA.108.173989>
20. Jain, N., Iyer, K. V., Kumar, A., & Shivashankar, G. V. (2013). Cell geometric constraints induce modular gene-expression patterns via redistribution of HDAC3 regulated by actomyosin contractility. *Proceedings of the National Academy of Sciences*, 110(28), 11349–11354. JSTOR.
21. Guerreiro, I., & Kind, J. (2019). Spatial chromatin organization and gene regulation at the nuclear lamina. *Current Opinion in Genetics & Development*, 55, 19–25. <https://doi.org/10.1016/j.gde.2019.04.008>
22. Bissell, Weaver, V., Lelièvre, S. A., Wang, F., Petersen, O. W., & Schmeichel, K. L. (1999). Tissue structure, nuclear organization, and gene expression in normal and malignant breast—PubMed. *Cancer Res*, 59(7), 1757–1764s.
23. Lu, P., Weaver, V. M., & Werb, Z. (2012). The extracellular matrix: a dynamic niche in cancer progression. *Journal of cell biology*, 196(4), 395-406.
24. Winkler, J., Abisoye-Ogunniyan, A., Metcalf, K. J., & Werb, Z. (2020). Concepts of extracellular matrix remodelling in tumour progression and metastasis. *Nature communications*, 11(1), 1-19.
25. Paszek, M. J., Zahir, N., Johnson, K. R., Lakins, J. N., Rozenberg, G. I., Gefen, A., ... & Weaver, V. M. (2005). Tensional homeostasis and the malignant phenotype. *Cancer Cell*, 8(3), 241–254. <https://doi.org/10.1016/j.ccr.2005.08.010>

CHAPTER 2. 3D CELL CULTURE FOR THE STUDY OF MICROENVIRONMENT-MEDIATED MECHANOSTIMULI TO THE CELL NUCLEUS: AN IMPORTANT STEP FOR CANCER RESEARCH

The content of this chapter is published as a perspective article in:

(Chhetri A., Rispoli J.V. and Lelièvre S.A. (2021). 3D Cell culture for the study of microenvironment-mediated mechanostimuli to the cell nucleus: an important step for cancer research. *Front. Mol. Biosci.* 8:628386. doi: 10.3389/fmolb.2021.628386.

The article is presented in the format required for Frontier's electronic submission.

Apekshya Chhetri^{1,2}, Joseph V. Rispoli^{1,3}, Sophie A. Lelièvre^{2,3,*}

(1) Department of Biomedical Engineering; (2) Department of Basic Medical Sciences; (3) Center for Cancer Research, Purdue University, West Lafayette, IN, United States of America

Abstract:

The discovery that the stiffness of the tumor microenvironment (TME) changes during cancer progression motivated the development of cell culture involving extracellular mechanostimuli, with the intent of identifying mechanotransduction mechanisms that influence cell phenotypes. Collagen I is a main extracellular matrix (ECM) component used to study mechanotransduction in three-dimensional (3D) cell culture. There are also models with interstitial fluid stress that have been mostly focusing on the migration of invasive cells. We argue that a major step for the culture of tumors is to integrate increased ECM stiffness and fluid movement characteristic of the TME. Mechanotransduction is based on the principles of tensegrity and dynamic reciprocity, which requires measuring not only biochemical changes, but also physical changes in cytoplasmic and nuclear compartments. Most techniques available for cellular rheology were developed for a 2D, flat cell culture world, hence hampering studies requiring proper cellular architecture that, itself, depends on 3D tissue organization. New and adapted measuring techniques for 3D cell culture will be worthwhile to study the apparent increase in physical plasticity of cancer cells with disease progression. Finally, evidence of the physical heterogeneity of the TME, in terms of ECM composition and stiffness and of fluid flow, calls for the investigation of its impact on the cellular heterogeneity proposed to control tumor phenotypes. Reproducing, measuring and controlling TME heterogeneity should stimulate collaborative efforts between biologists and engineers.

Studying cancers in well-tuned 3D cell culture platforms is paramount to bring mechanomedicine into the realm of oncology.

Keywords (5-8): mechanotransduction, mechanosensing, extracellular matrix, microfluidics, tensegrity, epigenome, nucleoskeleton, phenotypic heterogeneity

2.1 Introduction

Force variations at the cellular level are a source of biological modifications that influence organ development and homeostasis (Eckes and Krieg, 2004; Mammoto and Ingber, 2010; Humphrey et al., 2014; Schroer and Merryman, 2015; Barnes et al., 2017). The extracellular matrix (ECM), the protein network of which connects the different parts of an organ and belongs to the cells' microenvironment, is considered to regulate and propagate mechanical forces (Frantz et al., 2010).

The central role of the ECM in tissue homeostasis had been suggested early on and motivated its inclusion in cell-based research (Bissell, 1981; Ingber et al., 1981). It was the birth of three-dimensional (3D) cell culture, for which the organization of cells into recognizable tissue structures, whether normal or sickly, is paramount. The tumor microenvironment (TME) has been extensively studied with 3D cell culture models. It encompasses noncancerous cells (fibroblasts, endothelial cells, epithelial cells, immune cells like macrophages and dendritic cells) and molecules that sculpt the ECM (e.g., collagen, laminin, elastin, fibronectin, matrix metalloproteinases, elastases, cathepsins). The type and amount of TME components are characteristics of each specific form of cancer (Balkwill et al., 2012; Lu et al., 2012; Hirata and Sahai, 2017). Importantly, dynamic remodeling of the TME associated with stiffening favors aggressive cancer phenotypes (Cheng et al., 2009; Zhao et al., 2014). For instance, increased collagen I deposition and stiffer stroma distinguish aggressive (Basal-like; Her2) from less aggressive (Luminal A and B) breast cancer subtypes (Acerbi et al., 2015). Thus, exploring, *in vitro*, the mechanisms of ECM-cell interactions that control phenotypes requires 3D cell culture.

The concept of tensegrity states that cells are in an active prestress condition secured by a cable-like physical linkage between the ECM and cytoskeletal proteins (Ingber, 1993). Such condition stabilizes and counterbalances forces between intracellular and extracellular compartments. This concept was initially demonstrated by the stiffening response transmitted to the cytoskeleton as a result of mechanical stress directly applied to integrins (Wang et al., 1993).

The mammalian cell nucleus was also shown to react to mechanical stressors in the microenvironment (McGregor et al., 2016; Stephens et al., 2019). Reciprocally, cells exert traction on the ECM, as it was shown through deformations on silicone and collagen substrates by chicken fibroblasts (Harris et al., 1980). Constant communication between the ECM and the cells may be viewed as dynamic reciprocity (Bissell et al., 1982), a theory originally substantiated by results from Ingber and Bissell laboratories (Maniotis et al., 1997; Lelièvre et al., 1998). Dynamic reciprocity outlines a model for force-mediated interactions between the ECM and the cell nucleus via transmembrane proteins, cytoskeletal components, centrioles involved in the regulation of cell division, and nuclear components, including the genome, to ultimately affect gene transcription; conversely, changes in gene expression could modify the composition of the ECM.

The conversion of physical forces into biochemical signals, termed mechanotransduction, has been considered a major structure-function relation in cells ultimately leading to a biological outcome (Watson, 1991). The opening of membrane ion channels in response to stretch provided an early demonstration of cellular mechanotransduction (Craelius et al., 1988). Since then, standard 2D culture has confirmed the existence of intracellular mediators of forces, including cytoskeletal elements (e.g., vimentin, talin, microfilaments, microtubules, intermediate filaments) (Liu et al., 2015; Tapia-Royo and Fernandez, 2020), and at the level of the nuclear envelope, linker of nucleoskeleton and cytoskeleton (LINC) complexes and lamins (Buxboim et al., 2014; Guilluy et al., 2014; Janota et al., 2020). In the cell nucleus, mechanotransduction studies are complicated by an organization exquisitely determined by tissue architecture (Chandramouly et al., 2007; Lelièvre and Chittiboyina, 2018), which requires using 3D cell culture to recapitulate the assembly and phenotype of cells as *in vivo*.

In this article, we are placing cell culture models in perspective to illustrate how mechanotransduction to the cell nucleus may be studied beyond standard 2D culture. Microenvironmental forces have been focused on ECM network remodeling, notably in cancer. Yet, current considerations of fluid flow in the microenvironment should provide critical additional information on the impact of TME-mediated mechanical forces on phenotypes (Rothbauer et al., 2018). Cell culture models that integrate ECM and microfluidics to study cancer progression via an influence on the phenotypic heterogeneity of cancers are discussed to highlight how they might feed information necessary for the development of mechanomedicine.

2.2 Evidence of mechanotransduction to the genome in cell culture

The transfer of mechanostimuli from the microenvironment to the genes encompasses two major modes, the coupling protein complexes, like LINC, that bridge cytoskeleton and nucleoskeleton, and nuclear pore complexes (NPC) that control the passage of signaling molecules above 35 kDa. Proteins that translocate to the cell nucleus through NPCs in response to mechanostimuli are mechanosensors if they react to cytoskeletal rearrangement when the ECM stiffens or their expression increases on rigid substrates (Moreno-Vicente et al., 2018). They are mechanotransducers via their interaction with transcription factors in the cell nucleus, leading to changes in gene transcription (Foster et al., 2017; Sidorenko and Vartiainen, 2019; Pocaterra et al., 2020). Here, mechanotransduction to the genes may be compared to delivery modes for which mechanical forces are converted into biochemical signals in the cytoplasm (Figure 1A).

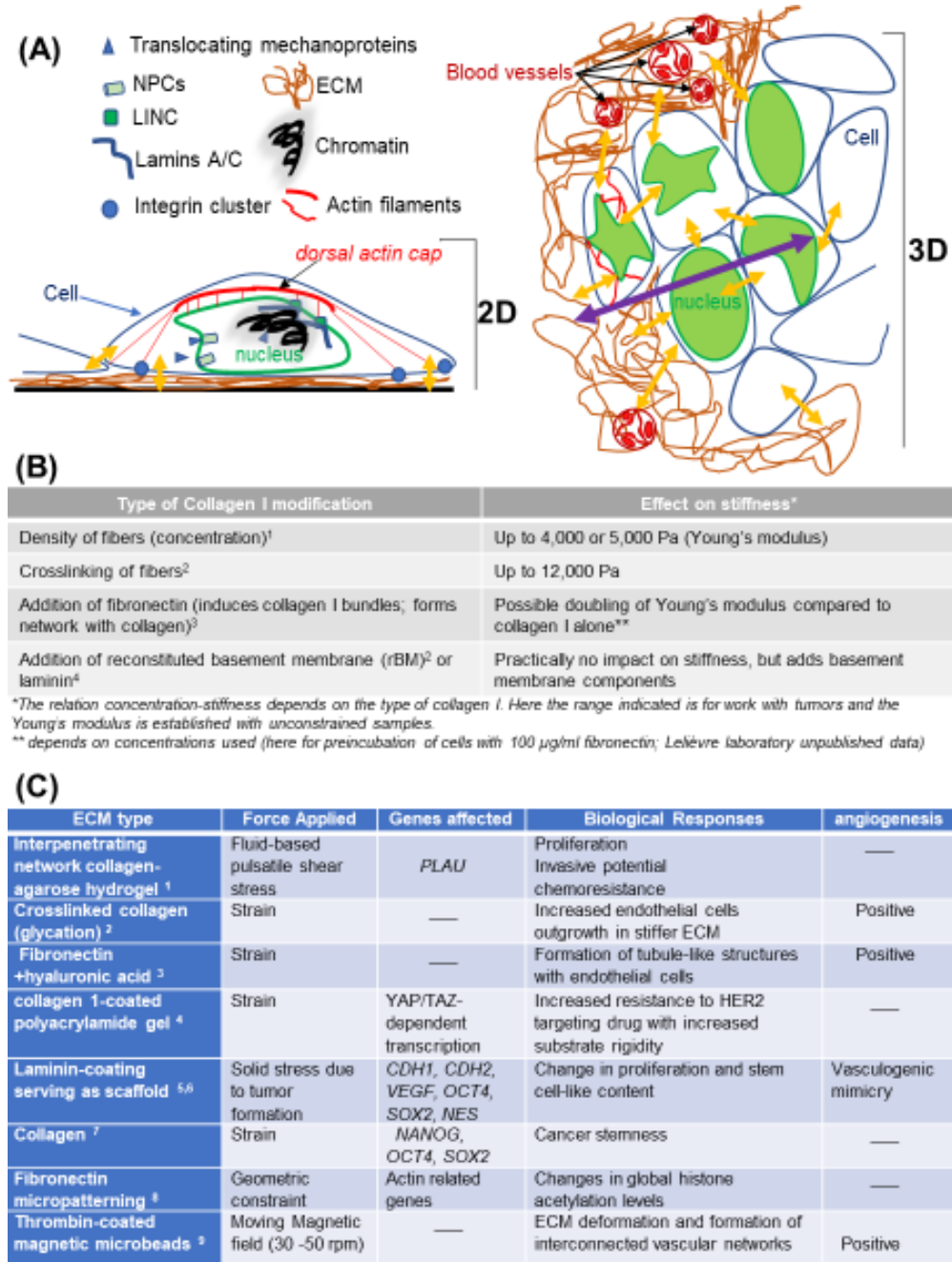
Mechanotransduction via LINC is based on balancing intracellular tension. The structural proteins SUN and Nesprin connect actin microfilaments and the outer nuclear envelope (Stewart-Hutchinson et al., 2008). Then, the propagation of mechanical forces to the genome might include structural proteins that span the nuclear interior and form small networks and/or organize chromatin, like nuclear actins (Plessner et al., 2015) and lamins A/C. These and other fibrous proteins along with ribonucleoproteins shape the scaffold of the nucleus that is compared to a nucleoskeleton (Pederson, 2000). The lamins regulate the organization of the genome via an influence on chromatin binding to the nuclear envelope (Makatsori et al., 2004); lamins A/C expression varies depending on ECM stiffness, with resulting effects on gene transcription and phenotypic differentiation (Swift et al., 2013). The cytoskeletal network influences protein translocation and nuclear stiffness (itself linked to the nucleoskeleton and chromatin) (Janota et al., 2020). The nucleus is 2-10 times stiffer than the cytoplasm; yet, it is dynamic and its envelope is in direct contact with chromatin, allowing for an influence on genome architecture and the translation of physical signals into biochemical changes (Uhler and Shivashankar, 2017) (Figure 1A). The direct connection between integrins, the cytoskeleton, chromatin stretching, and the expression of a GFP-tag reporter gene was elegantly demonstrated using magnetic twisting cytometry (Tajik et al., 2017). Moreover, transcriptional modifications associated with the application of mechanical forces via integrins involve changes in H3K9 methylation that depend on the location within the cell nucleus (Sun et al., 2020).

Many experiments on mechanosensing and mechanotransduction did not reproduce the tissue context for which cell shape and intracellular organization are essential characteristics. Yet, the nucleus can acquire specific roles within a 3D collagen I gel, as shown by its control of contractility, in contrast to cells cultured on top of the gel (Graham et al., 2018). The importance of 3D cell culture to study the nucleus was initially demonstrated via the dynamic distribution of the nuclear structural protein NuMA that responds to ECM signaling (Lelièvre, et al., 1998; Vidi et al., 2012), and itself controls phenotypically normal differentiation via an action on the epigenome (Abad et al., 2007). Epigenetic organization also depends on tissue architecture (Plachot et al., 2004; Chandramouly et al., 2007), reinforcing the value of 3D cell culture to unravel the influence of mechanotransduction to the cell nucleus on phenotypes. As an encouraging step towards ECM-based cell culture to study mechanotransduction to the epigenome, deformation of mouse oligodendrocytes seeded on stretchable silicone rubber-coated with Matrigel revealed the involvement of SYNE1, a component of LINC, in increased expression of the epigenetic silencing marker H3K9me3 (Hernandez et al., 2016). For the epigenetic disorder that is cancer, it is essential to study mechanotransduction in tumor models in 3D cell culture.

Figure 2.1. Mechanotransduction in response of mechanostimuli

(A). *Left*: In 2D culture, cancer cells deposit their own ECM on the plastic surface, with focal adhesion (integrin clusters) on the ECM against the hard culture surface; there are also possible tension forces between cells. Two interacting modes of mechanotransduction include (1) the translocation of mechanoproteins (YAP/TAZ, myocardin-related transcription factor; MRTF; muscle LIM protein, MLP, etc.) upon cytoskeletal rearrangement that influence gene transcription and (2) the balance of forces between cytoskeleton and the network of lamins and other nuclear proteins via the LINC complexes, ultimately influencing chromatin compaction and gene transcription. *Right*: In 3D culture, the organization of cancer cells into a tumor changes not only the type of forces involved but also the intracellular architecture (e.g., different organization of actin microfilaments and no more dorsal actin cap; great variations in nuclear morphometry depending on the epigenome of cells and their location in the tumor). There are variations in the forces received if cells are at the periphery or deep within the tumor. Yellow arrows indicate a sample of areas of mechanostimuli (the impact from the cell culture medium is not included); the purple arrow indicates increasing distances between cells inside the tumor (with multilayering of cells) and the bulk of the ECM that might create heterogeneity in mechanostimuli. Finally, matrix stiffening also increases angiogenesis via an influence on endothelial cells. (B). Example of ECM stiffness tuning based on collagen I (¹Chhetri et al., 2019, ²Levental et al., 2009, ³Paten et al., 2019, ⁴Chittiboyina et al., 2018). Other matrices of nonmammalian origin may also be used (e.g., agar, alginate, polyacrylamide) and are sometime mixed with ECM molecules (e.g., collagen I, fibronectin). (C). Cell culture-based examples of the impact of different types of matrices and forces that result in changes in gene transcription and angiogenesis as they relate to cancer aggressiveness (¹Novak et al., 2019, ²Bordeleau et al., 2016, ³Seidlits et al., 2011, ⁴Lin et al., 2015, ⁵Larson et al., 2014, ⁶Brodaczewska et al., 2019, ⁷Pankova et al., 2019, ⁸Jain et al., 2013, ⁹Sewell-Loftin et al., 2017).

Figure 2.1 continued



2.3 Cell culture models for ECM-mediated mechanical forces in cancer progression

The discovery that tumors are stiffer than healthy tissues has encouraged the study of mechanotransduction in 3D cell culture. Overall, models employing collagen I-based control of ECM stiffness have demonstrated that mechanotransduction might play an essential role in phenotypic switches throughout the neoplastic process, from an ‘at risk’ phenotype to an invasive cancer phenotype. For instance, increasing collagen I density to augment stiffness by a factor of 2 altered normal mammary morphogenesis, as evidenced by loss of polarity, although basement membrane components that are important to maintain differentiation were also included (Paszek et al., 2005). It was accompanied with the activation of Rho kinase, a regulator of the cytoskeleton known to respond to mechanical stress (Wojciak-Stothard and Ridley, 2003). Noticeably, increased collagen density is considered an aggravating factor of breast cancer risk (Turashvili et al., 2009), and loss of polarity is necessary for cancer onset as shown in 3D cell culture (Chandramouly et al., 2007; Bazzoun et al., 2019). Stiffening the ECM via collagen I cross-linking also disrupted epithelial organization, and in combination with oncogenes, drove invasive behavior via integrin clustering (Levental et al., 2009). Stiffening may be further increased by collagen I and fibronectin interaction; however, the organization of the ECM also depends on cellular traction forces (Kubow et al., 2015), which nicely illustrates the dynamic reciprocity concept. Mechanotransduction equally occurs in the stromal cells that secrete interstitial ECM and influence cancer development, as shown by the involvement of focal adhesion kinase (FAK) in fibroblast migration through a dense collagen I matrix (Mierke et al., 2017).

Importantly, mechanotransduction in tumor cells may be induced not only through cell-ECM interaction but also by cell-cell interaction. Cell-mediated mechanical stress has been measured by cell-sized oil microdroplets with defined mechanical and adhesion properties introduced between cells (Campàs et al., 2014). Mechanotransduction induced by an increased matrix stiffness also influences endothelial cells. Using 3D matrices made of collagen, it was shown that a stiffer ECM promoted by glycation (but not a denser matrix) increased angiogenesis via the upregulation of matrix metalloproteinases and that the stiffness corresponding to a TME altered the integrity of the endothelial barrier as *in vivo* (Bordeleau et al., 2017) (Figure 1A). For details we refer the readers to a well-documented summary of the literature on the impact of mechanical forces on tumor angiogenesis, notably highlighting the mechanosensory complexes activated in response to mechanical forces in endothelial cells (Zanotelli and Reinhart-King, 2018).

A simple initial approach to introduce ECM stiffness in 3D cell culture is to use collagen I hydrogel that can be fine-tuned to a selected Young's modulus (Chhetri et al., 2019) and mixed with other ECM molecules to further alter stiffness or stimulate diverse biochemical signaling pathways (Figure 1B). However, setting 3D cell culture conditions requires information on *in vivo* stromal Young's modulus. For instance, a parallel increase in collagen deposition (Trichome staining) and matrix stiffness (atomic force microscopy-AFM) was observed from healthy to cancerous preinvasive and cancerous invasive human breast tissues, with a 4-5 fold stiffness increase for the latter corresponding to a Young's modulus of 3,000 Pa on average based on unconfined compression analysis (Acerbi et al. 2015). It is important to understand that not only the stiffness of the matrix, but also its type play critical roles in 3D cell culture. For instance, using solely a fibronectin network has been shown to promote epithelial to mesenchymal transition (Jordahl et al., 2019) and the addition of hyaluronic acid to fibronectin stimulates angiogenesis (Seidlits et al., 2011). Reproducing TME characteristic of specific types of cancer is especially important to study cancer therapies, as shown with the production of different types of HA-rich ECM emulating the brain parenchyma (Blehm et al., 2015). Stabilizing the high stiffness level of collagen I and fibronectin necessary for 3D culture of tumors may be achieved with photocrosslinking (Seidlits et al., 2011; Nguyen et al., 2019). Synthetic polyhydrogels are also being developed for use in 3D cell culture. They can be crosslinked physically (ionic/H-bonding/hydrophobic forces) or chemically by covalent process in order to provide the degree of elasticity necessary for a TME. The reversibility and thus, poor mechanical properties of physically crosslinked polymers is their major limitation affecting the overall stiffness of the matrix (Parhi, 2017). Examples of synthetic hydrogels usable for tumor culture include Polyethylene glycol (PEG) and Polycaprolactone (PCL) that can be crosslinked chemically and provide stiffness conditions within the wide range of mechanical properties of many tumors (0.4-10 kPa). However, these hydrogels lack the essence of biological signaling unless they are functionalized, for instance by adding peptide sequences of ECM components. The great capabilities for architectural modeling or patterning and for functionalization of these types of matrix usually leads to highly specialized uses like therapeutic approaches (e.g., for use *in vivo* for drug delivery), controlled matrix degradation, study of migration in complex matrix densities, cancer stem cell enrichment (Singh et al. 2014; Palomeras et al., 2016).

Rheology (i.e., the deformation and flow of materials that give viscoelastic information) governs physical cellular responses to mechanical stress that occur over time (Bonfanti et al., 2020), and tensegrity is one of the rheological models (Van Citters et al., 2006). The complexity of cellular mechanical properties lies in part on different reactions depending on cortical and deep locations and requires various models and advanced measurement tools like particle-tracking microrheology, optical tweezers, AFM, traction force microscopy, magnetic bead cytometry, optical stretchers, micropipette aspiration and microplate rheometer. Unfortunately, studying rheology in 3D cell culture is short of a magical process, since most measurement and mathematical tools have been established with standard 2D cell culture and do not accommodate for the thickness and depth of tumors. Importantly, 2D cell culture on plastic artificially increases stiffness (via “bottom effects”) measured with AFM indentation; 3D culture that can be done on top of ECM for certain tissues provides greatly improved measurement conditions (Guimarães et al. 2020). An optical trap that senses thermal fluctuations of lipid granules was used to compare the intracellular viscoelastic properties of invasive breast, colon and pancreatic cancer cells with noninvasive cells cultured in low (1 mg/ml) and increased (4 mg/ml) collagen I density in 3D culture of tumor nodules. A statistically significant adjustment in cellular viscoelasticity was observed within 24 hours of exposure to increased ECM stiffness, but only in the invasive cells and with increased viscosity at the invasive edge (Wullkopf et al., 2018).

Even more difficult is to apprehend the physics of the cell nucleus. Magnetic tweezers that nicely revealed the involvement of nuclear lamins in nucleus resistance to shear forces are not an easy option for 3D cell culture (Guilluy et al., 2014). In tumors, we have used nuclear morphometry as evidence of a physical impact of increased collagen I stiffness (Chittiboyina et al., 2018). There was a significant nuclear deformation (via a decrease in circularity) when comparing 1500 to 800 Pa for the ECM. Nuclear deformation appears to influence the ATR protein that controls chromatin association to the nuclear envelope, as shown by cell stretching in 2D culture, which might provide a means for the genome to cope with mechanical stress (Kumar et al., 2014). As further evidence of an impact of mechanical forces on the cell nucleus we have included examples of alterations in gene expression depending on the type of ECM and forces (Figure 1C).

2.4 Integration of microfluidics in the study of mechanotransduction in tumors

In vivo, cell nutrition and oxygenation rely on fluid extravasation from blood vessels. In tumors, cells are subjected to strong solid and shear stresses. Rapid tumor growth contributes to solid stress, which in turn, subjects the TME to both tensile and compressive stresses and increases interstitial fluid pressure (Griffon-Etienne et al., 1999). Interstitial flow causes shear stress ranging from pulsatile and turbulent (near capillaries) to primarily laminar convection, with fluid velocity influenced by interstitial porosity and pressure as well as capillary density, permeability, and viscoelastic properties (Follain et al., 2020). In breast tumors, where local vascularization is highly modified, with leaky vessels for instance, fluid flow is increased approximately five-fold in the interstitium compared to normal tissue and results in higher hydrostatic pressure (Butler and Grantham, 1975). Dynamic contrast-enhanced magnetic resonance imaging of murine xenografts of primary tumors has revealed higher interstitial fluid pressure in metastatic compared to nonmetastatic cancers (Hompland et al., 2012).

Cell culture platforms engineered with microfluidic channels are revealing that fluid movement is an important contributor to the mechanostimulation that influences tissue phenotypes. They may be single or multi-chambered and are built with biocompatible substrata, like the popular silicon-based organic polymer polydimethylsiloxane (PDMS). In addition to the speed of delivery into, and retrieval from the platform, the width and depth of the microchannels contribute to the control of shear stress (Cioffi et al. 2010). Since the interstitial fluid goes through a matrix that influences diffusion depending on the density of ECM fibers, mechanotransduction experiments should integrate information from both fluid movement and ECM stiffness; in such case, it is valuable to integrate stiffness biosensors within the cell culture platform (Zareei et al., 2020). Specialized microfluidic platforms, like the gradient-on-a-chip, that generate gradients of molecules in the ECM permit the identification of thresholds for their action depending on ECM stiffness and fluid movements, hence combining physical and chemical stimuli in the microenvironment (Chittiboyina et al., 2018).

Fluid impact in cancer research *in vitro* has been mostly studied in the context of cell motion, a necessary precursor to metastasis. For instance, physiological levels of fluid shear stress (0.1-0.75 dynes/cm² for flow rate 3.9-26 µl/min) experienced by glioma cells embedded in 2 mg/ml collagen I in a modified Boyden chamber, prevented migratory and invasive capabilities for some of the cell types (Qazi et al., 2011). High speed (4.6 µm/s) of interstitial fluid was shown to control

the direction of migration of breast invasive tumor cells embedded in 2 mg/ml collagen I gel towards regions of high fluid pressure (that would normally correspond to leaky blood vessels) by influencing asymmetric cell-matrix adhesion and the location of cytoskeletal molecules (Polacheck et al., 2014). Biological responses included standard mechanotransduction pathways, with activation of integrins and autophosphorylation of FAK. Other studies attempted to mimic shear stress in a vessel for metastatic cells. Translocation of YAP, in response to fluid wall shear stress, was associated with the control of genes that promote metastasis (Lee et al., 2017); whereas the translocation of TAZ seemed to control cell proliferation (Lee et al., 2018).

For work on primary tumors, fluid-mediated mechanical impact will be best investigated in 3D cell culture, with tumors grown with appropriate ECM stiffness, since high interstitial fluid pressure may drive fluid efflux from the tumor core, hence inducing fluid stress within tumors too. Systems based on the generation of hydrostatic pressure might be applicable to whole tumors (Figure 2A). The study of fluid impact on a tumor will require measuring global tumor deformation as well as intracellular modifications. The study of solid stress performed with tumors grown in agarose matrices, in which confining environments might limit tumor growth and increase cellular packing density (Helmlinger et al., 1997), has revealed that tumor cell size might be used as a measurement of solid stress inside a tumor (Roose et al., 2003). Such architectural response would result from the combination of pressure from the TME, cell-cell interaction and fluid fluxes through the tumor. The study of solid stress has also revealed that increased pressure in the TME, linked not only to tumor growth but also to the deposition of collagen I and hyaluronan, constrains blood vessels, hence not only further increasing interstitial fluid pressure but also preventing optimal delivery of anticancer drugs (Griffon-Etienne et al., 1999) (Figure 2B). This early observation illustrates the need to consider mechanical properties in cancer for the design of therapies.

2.5 A bright future for 3D cell culture in mechanomedicine

Mechanomedicine has been defined as the art of mechanobiology-based medicine (Wang, 2017). Thus, it may be applied to pathological conditions for which mechanobiology is either paramount for organ and tissue functions (e.g., cardiovascular, reproductive and respiratory systems), or maybe used to study and possibly target diseased tissues and cells, as it is the case in cancer (Ma et al., 2016; Özkale et al., 2021). Cancer mechanomedicine is illustrated for instance

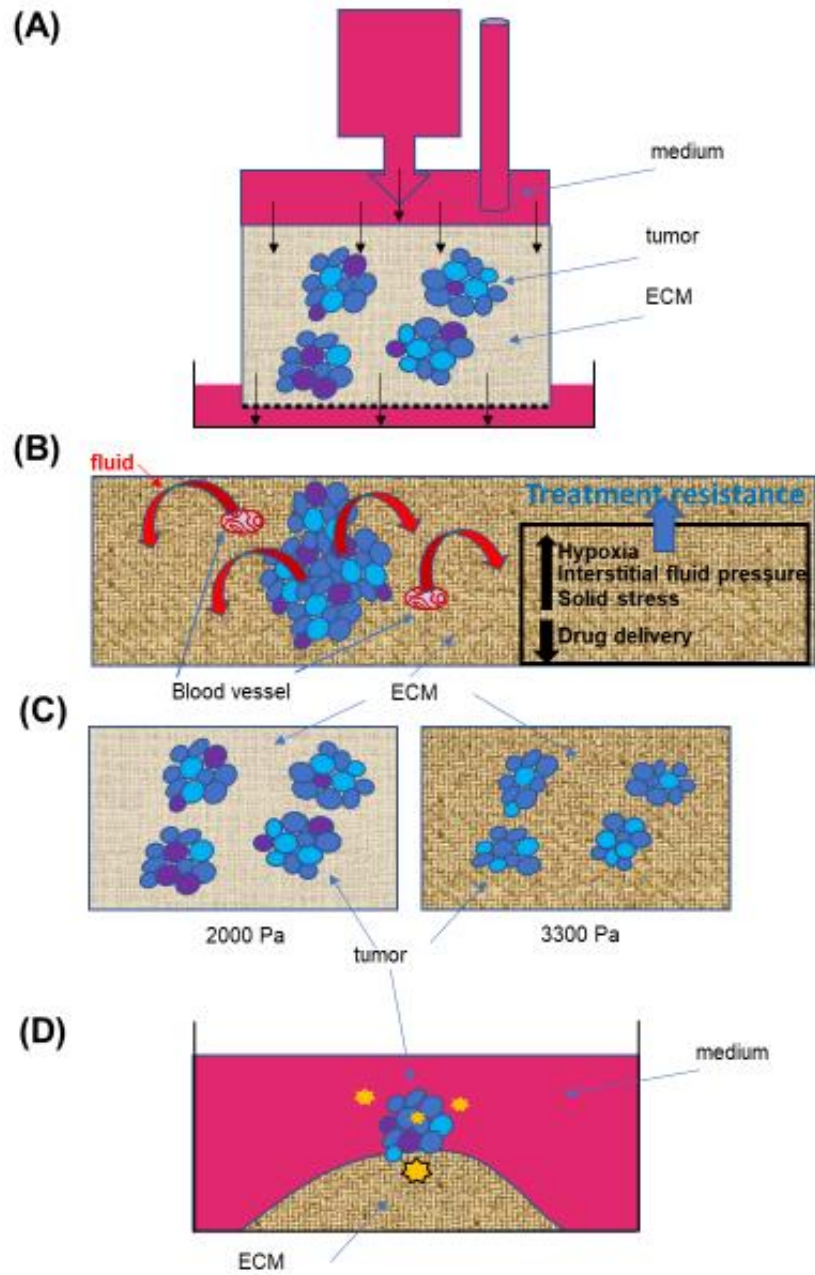
by research on modifying tumor vasculature to improve drug efficacy. Indeed, intratumor fluid pressure mediated by solid stress not only leads to hypoxia, hence promoting invasion, metastasis and treatment resistance, but it also prevents proper drug delivery, which also contributes to chemoresistance (Stylianopoulos et al., 2018) (Figure 2B).

A fundamental question to address with 3D cell culture is whether increased TME stiffness during cancer progression modifies the intratumor phenotypic heterogeneity that defines aggressiveness; indeed, we measured potential selective pressure in light of a higher apoptotic rate in breast tumors cultured in 3300 Pa compared to 2000 Pa (Figure 2C), confirming observations made previously of a link between high mechanical stress, measured in an agarose matrix with fluorescent microbeads, and apoptosis (Cheng et al., 2009). Moreover, we demonstrated that phenotypic intratumor heterogeneity occurred even when starting from a single cell to produce a tumor on top of an island of collagen I of 3300 Pa (Jain et al. 2020). One possible explanation for the induction of heterogeneity is the evolving force gradient within the tumor (Figure 2D). The importance of the impact of matrix stiffness on creating phenotypic heterogeneity is also supported by the fact that certain types of cancer cells, notably those involved in tumorigenesis require a soft microenvironment to proliferate (Liu et al., 2012).

Figure 2.2. Heterogeneity within and outside tumors influences cancer behavior.

(A). Example of fluid stress induced by hydrostatic pressure on isolated cells (Qazi et al. 2011), but that might be applied to tumors in 3D culture. Even if the hydrostatic pressure is homogenous at the top of the device, the phenotypic heterogeneity within tumors (represented by different colors of cells) as well as the heterogeneity in the size of pores (0.1-30 microns) in the ECM are likely to induce different cell responses and thus, behaviors of tumors. Black arrows indicate flow direction. (B). Solid stress linked to tumor growth will also create intratumor heterogeneity by influencing intratumor pressure which pushes fluid out of the tumor, and increasing interstitial fluid pressure, which contributes to hypoxia in different regions of the tumor. Moreover, solid stress and increased matrix stiffness also lead to the compression of blood vessels. Altogether, intratumor heterogeneity, hypoxia and a decreased efficacy in drug delivery (due to blood vessel compression and increased interstitial fluid pressure) contribute to treatment resistance. (C). There might also be selective pressure from mechanostimuli, simply based on an increased matrix stiffness, that would modify intratumor heterogeneity by inducing cell death, as we measured when culturing triple negative breast cancer T4-2 cells for 10 days in 2000 Pa compared to 3300 Pa collagen I matrix (% increase between 25 and 50%, depending on the biological replicate; $n=3$). (D). Even when starting from one individual cell, without purposefully inducing a mechanostimulus, the tumor that forms on an island of collagen I (3300 Pa) presents cellular heterogeneity (Jain et al., 2020). We propose that in addition to inherent genetic instability of cancer cells during division, as the tumor develops, cells are experiencing different degrees of mechanical forces (represented here by orange stars of various sizes) from within and outside the tumor, depending on their location. Such heterogeneity in mechanostimuli contributes to different levels of mechanotransduction to the cell nucleus and thus, differential gene transcription and phenotypic switch

Figure 2.2 continued



Our current understanding of the impact of mechanotransduction on cancer phenotypes is limited to a correlation between TME and metastatic potential. Tensegrity and dynamic reciprocity models have brought enough incentives to consider that changes in stiffness within cells are also essential to study in order to fully develop mechanomedicine, especially since, opposite to the situation in the interstitium, invasive cells appear softer compared to nonmalignant and preinvasive cells; however, upon cancer progression cells acquire increased plasticity that might render them stiffer depending on external stimuli (Baker et al., 2010; Plodinec et al., 2012). Following incubation with anticancer drugs, treatment-resistant prostate cancer cells and leukemia cells display higher stiffness compared to untreated cells, as measured with AFM in 2D culture (Raudenska et al., 2019). If changes in intracellular stiffness control the sensitivity to anticancer drugs, further experiments will require 3D cell culture for validation, since such sensitivity is notoriously different between 2D and 3D cultures. It will also be necessary to identify targets of mechanostimuli responsible for resistance to treatment. For instance, shear stress applied to breast cancer cells with cell culture medium run through the ECM (agarose-collagen I) led to the activation of *PLAU* and linked this gene to increased resistance to paclitaxel (Novak et al. 2019). A wound healing system with compression with a rigid weight disc on an agar cushion on top of glioblastoma cells was used to mimic solid stress of cells detaching from the tumor within a confined skull. Results revealed a link between miR548 and increased migration as well as an influence on genes associated with chemoresistance (*TMEM45Q*) and angiogenesis (*CTGF*, *VEGFA*, *VEGFB*) (Calhoun et al., 2020). However, these results were obtained with different types of matrices, which makes it difficult to identify strict mechanical impact from a combination of mechanical and biochemical signaling. Further understanding of nuclear homeostasis in response to mechanical impact from well-characterized TME would strengthen the field of cancer mechanomedicine.

Another topic of importance for mechanotransduction to the cell nucleus that will influence mechanomedicine is tissue geometry. Physical constraints associated with a specific geometry were shown to control tissue morphogenesis, by locally influencing the concentration of morphogens in the microenvironment (Nelson et al., 2006), and the organization of the cell nucleus (Lelièvre and Chittiboyina, 2018). Regarding cancer, we have shown different levels of drug sensitivity for tumors depending on their location on flat vs. curved geometry (Vidi et al., 2014). Geometry-induced mechanotransduction to the cell nucleus has been clearly demonstrated in 2D

culture on supports with defined geometry (Gomez et al., 2010). However, it is difficult to separate the effect of tissue geometry and that of matrix stiffness on cells cultured in 3D. Indeed, direct force application (which could be linked to matrix stiffness) influences tissue geometry and the composition of the ECM (Matsugaki et al., 2013; Muncie et al., 2020). Moreover, tumor proliferation and invasion are stimulated within a duct made of non-neoplastic epithelial cells only when mechanical stress is high, hence showing that mechanical stress acts independently on (or on top of) tissue geometry (Bogheart et al., 2012). Our preliminary studies with non-neoplastic breast epithelial cells suggest that a duct-like curved geometry modifies the effect of increasing matrix stiffness on cell phenotypes compared to increasing matrix stiffness on a flat geometry, which suggests that both physical aspects (geometry and matrix stiffness) have complementary impacts on phenotypes (Lelièvre laboratory, unpublished data).

In conclusion, the investigation of ECM-mediated mechanotransduction in a physiologically relevant context is crucial in furthering research aimed to overcome cancer progression and treatment resistance. In the above text, we have illustrated possibilities to induce intratumor phenotypic heterogeneity, a driver towards resistance. There is evidence that heterogeneity also exists in the cells' capabilities to exert compressive stresses within a population (Mohagheghian et al., 2018). The 3D cell culture platforms will need to integrate different physical characteristics and physical stress measurement methods to best render the phenotypic heterogeneity of cancers. Actually, the TME is likely to contribute to the mixture of phenotypes because of the heterogeneity in matrix stiffness at the tumor periphery (Acerbi et al., 2015) and in fluid flow (Evje & Waldeland, 2019). Moreover, to properly tune ECM and fluid flows, tumor models should include stromal cells like fibroblasts that greatly contribute to cancer progression via their modulation of the TME.

Acknowledgements

This work is supported by a Showalter Award to JVR and SAL. Publication fees are covered by the Drug Delivery & Molecular Sensing program of the Purdue Center for Cancer Research. JR and SL are members of International Breast Cancer & Nutrition (IBCN).

Conflict of interest

The authors declare no conflict of interest.

Contributions

SAL and AC wrote the manuscript and prepared the figures. JVR participated in discussions and edits.

2.6 References

1. Abad, P. C., Lewis, J., Mian, I. S., Knowles, D. W., Sturgis, J., Badve, S., et al. (2007). NuMA Influences Higher Order Chromatin Organization in Human Mammary Epithelium. *J. Mol. Cell Bio.* 18:2. doi:10.1091/mbc.e06-06-0551
2. Acerbi, I., Cassereau, L., Dean, I., Shi, Q., Au, A., Park, C., et al. (2015). Human Breast Cancer Invasion and Aggression Correlates with ECM Stiffening and Immune Cell Infiltration. *Integr. Biol. (Camb).* 7:10. doi:10.1039/c5ib00040h
3. Baker, E. L., Lu, J., Yu, D., Bonnecaze, R. T., and Zaman, M. H. (2010). Cancer cell stiffness: integrated roles of three-dimensional matrix stiffness and transforming potential. *Biophys. J.* 99:7. doi:10.1016/j.bpj.2010.07.051
4. Balkwill, F.R., Capasso, M., and Hagemann, T. (2012). The tumor microenvironment at a glance. *J. Cell Sci.* 125:23. doi: 10.1242/jcs.116392
5. Barnes, J.M., Przybyla, L., and Weaver, V.M. (2017). Tissue mechanics regulate brain development, homeostasis and disease. *J. Cell Sci.* 130:1. doi:10.1242/jcs.191742
6. Bayer, S. V., Grither, W. R., Brenot, A., Hwang, P. Y., Barcus, C. E., Ernst, M. et al. (2019). DDR2 controls breast tumor stiffness and metastasis by regulating integrin mediated mechanotransduction in CAFs. *ELife.* 8:e45508. doi:10.7554/eLife.45508
7. Bazzoun, D., Adissu, H. A., Wang, L., Urazaev, A., Tenvooren, I., Fostok, S. F. et al. (2019). Connexin 43 maintains tissue polarity and regulates mitotic spindle orientation in the breast epithelium. *J. Cell Sci.* 132:10. doi:10.1242/jcs.223313
8. Bissell, M.J. (1981). The differentiated state of normal and malignant cells or how to define a “normal” cell in culture. *Int. Rev. Cyt.* 70. 27–100. doi: 10.1016/S0074-7696(08)61130-4
9. Bissell, M.J., Hall, H.G., and Parry, G. (1982). How does the extracellular matrix direct gene expression? *J.Theor. Bio.* 99:1. Doi:10.1016/0022-5193(82)90388-5
10. Blehm, B.H., Jiang, N., Kotobuki Y., Tanner K. (2015). Deconstructing the role of the ECM microenvironment on drug efficacy targeting MAPK signaling in a pre-clinical platform for cutaneous melanoma. *Biomaterials.* 56:129–139. doi:10.1016/j.biomaterials.2015.03.041

11. Boghaert, E., Gleghorn, J.P., Lee, K., Gjorevski, N., Radisky, D.C., Nelson C.M. (2012). Host epithelial geometry regulates breast cancer cell invasiveness. *Proc. Natl. Acad. Sci.* 109:19632. doi:10.1073/pnas.1118872109
12. Bonfanti, A., Fouchard, J., Khalilgharibi, N., Charras, G., and Kabla, A. (2020). A unified rheological model for cells and cellularised materials. *R. Soc. Open Sci.* 7:1. <https://doi.org/10.1098/rsos.190920>
13. Bordeleau, F., Mason, B.N., Lollis, E.M., Mazzola M., Zanutelli M.R., et al. (2017). Matrix stiffening promotes a tumor vasculature phenotype. *Proc. Natl. Acad. Sci.* 114:492. doi:10.1073/pnas.1613855114
14. Brodaczewska, K.K., Bielecka, Z.F., Maliszewska-Olejniczak, K., Szczylik, C., Porta, C., Bartnik E, et al. (2019). Metastatic renal cell carcinoma cells growing in 3D on poly-D-lysine or laminin present a stem-like phenotype and drug resistance. *Oncol Rep.* 42:1878. doi: 10.3892/or.2019.7321
15. Butler, T. P., and Grantham, F. H. (1975). Bulk Transfer of Fluid in the Interstitial Compartment of Mammary Tumors. *Cancer Res.* 35. 3084–3088.
16. Buxboim, A., Swift, J., Irianto, J., Spinler, K.R., Dingal, P.C.D.P., Athirasala, A. et al. (2014). Matrix elasticity regulates lamin-A,C phosphorylation and turnover with feedback to actomyosin. *Curr. Biol.* 24:16. [doi:10.1016/j.cub.2014.07.001](https://doi.org/10.1016/j.cub.2014.07.001)
17. Calhoun, M.A., Cui, Y., Elliott, E.E., Mo, X., Otero, J.J., Winter, J.O. (2020). MicroRNA-mRNA Interactions at Low Levels of Compressive Solid Stress Implicate mir-548 in Increased Glioblastoma Cell Motility. *Sci Rep.* 10:311. doi: 10.1038/s41598-019-56983-x
18. Campàs, O., Mammoto, T., Hasso, S., Sperling, R.A., O'Connell, D., Bischof A.G., et al. (2014). Quantifying cell-generated mechanical forces within living embryonic tissues. *Nat Methods.* 2014 Feb;11(2):183-9. doi: 10.1038/nmeth.2761
19. Chandramouly, G., Abad, P. C., Knowles, D. W., and Lelièvre, S. A. (2007). The control of tissue architecture over nuclear organization is crucial for epithelial cell fate. *J. Cell Sci.* 120:9. Doi: 10.1242/jcs.03439
20. Cheng, G., Tse, J., Jain, R.K., and Munn, L.L. (2009). Micro-environmental mechanical stress controls tumor spheroid size and morphology by suppressing proliferation and inducing apoptosis in cancer cells. *PLoS One.* 4:2. [doi :10.1371/journal.pone.0004632](https://doi.org/10.1371/journal.pone.0004632)
21. Chhetri, A., Chittiboyina, S., Atrian, F., Bai, Y., Delisi, D. A., Rahimi, R. et al. (2019). Cell culture and coculture for oncological research in appropriate microenvironments. *Curr. Protoc. Chem. Bio.* 11:2. doi:10.1002/cpch.65
22. Chittiboyina, S., Rahimi, R., Atrian, F., Ochoa, M., Ziaie, B., and Lelièvre, S. A. (2018). Gradient-on-a-Chip with Reactive Oxygen Species Reveals Thresholds in the Nucleus Response of Cancer Cells Depending on the Matrix Environment. *ACS Biomater. Sci. Eng.* 4:2. [doi: 10.1021/acsbiomaterials.7b00087](https://doi.org/10.1021/acsbiomaterials.7b00087)

23. Cioffi, M., Moretti, M., Manbachi, A., Chung, B. G., Khademhosseini, A., and Dubini, G. (2010). A computational and experimental study inside microfluidic systems: The role of shear stress and flow recirculation in cell docking. *Biomed. Microdevices.* 12:6. doi:10.1007/s10544-010-9414-5
24. Craelius, W., Chen, V., el-Sherif, N. (1988). Stretch activated ion channels in ventricular myocytes.
25. *Biosci. Rep.* 8:407. doi: 10.1007/BF01121637.
26. Eckes, B., and Krieg, T. (2004). Regulation of connective tissue homeostasis in the skin by mechanical forces. *Clin. Exp. Rheumatol.* 22: (Suppl 33): 573-576.
27. Evje, S., and Waldeland, J. O. (2019). How Tumor Cells Can Make Use of Interstitial Fluid Flow in a Strategy for Metastasis. *Cell. Mol. Bioeng.* 12:3. Doi:10.1007/s12195-019-00569-0
28. Follain, G., Herrmann, D., Harlepp, S., Hyenne, V., Osmani N., Warren, S.C., et al. Fluids and their mechanics in tumour transit: shaping metastasis. *Nat. Rev. Cancer.* 20:107 (2020). <https://doi.org/10.1038/s41568-019-0221-x>
29. Foster, C.T., Gualdrini, F., and Treisman, R. (2017). Mutual dependence of the MRTF-SRF and YAP-TEAD pathways in cancer-associated fibroblasts is indirect and mediated by cytoskeletal dynamics. *Genes Dev.* 31:23. doi:10.1101/gad.304501.117
30. Frantz, C., Stewart, K.M., and Weaver, V.M. (2010). The extracellular matrix at a glance. *J. Cell Sci.* 123: 24. doi:10.1242/jcs.023820
31. Gomez, E.W., Chen, Q.K., Gjorevski, N., Nelson, C.M. (2010). Tissue geometry patterns epithelial-mesenchymal transition via intercellular mechanotransduction. *J Cell Biochem.* 110:44. doi: 10.1002/jcb.22545
32. Graham, D. M., Andersen, T., Sharek, L., Uzer, G., Rothenberg, K., Hoffman, B. D., et al. (2018). Enucleated cells reveal differential roles of the nucleus in cell migration, polarity, and mechanotransduction. *J. Cell Biol.* 217:3. doi:10.1083/jcb.201706097
33. Griffon-Etienne, G., Boucher, Y., Brekken, C., Suit, H.D., Jain, R.K. (1999). Taxane-induced apoptosis decompresses blood vessels and lowers interstitial fluid pressure in solid tumors: clinical implications. *Cancer Res.* 59:3776.
34. Guilluy, C., Osborne, L.D., Van Landeghem, L., Sharek, L., Superfine, R., Garcia-Mata, R. et al. (2014). Isolated nuclei adapt to force and reveal a mechanotransduction pathway in the nucleus. *Nat. Cell Biol.* 16:4. doi:10.1038/ncb2927
35. Guimarães, C. F., Gasperini, L., Marques, A. P., and Reis, R. L. (2020). The stiffness of living tissues and its implications for tissue engineering. *Nat. Rev. Mater.* 5:5. doi:10.1038/s41578-019-0169-1

36. Harris, A. K., Wild, P., and Stopak, D. (1980). Silicone rubber substrata: a new wrinkle in the study of cell locomotion. *Science*. 208:4440. Doi: 10.1126/science.6987736
37. Helmlinger, G., Netti, P.A., Lichtenbeld, H.C., Melder, R.J., Jain, R.K. (1997). Solid stress inhibits the growth of multicellular tumor spheroids. *Nat Biotechnol*. 5:778. doi: 10.1038/nbt0897-778
38. Hernandez, M., Patzig, J., Mayoral, S.R., Costa, K.D., Chan, J.R., and Casaccia, P. (2016). Mechanostimulation Promotes Nuclear and Epigenetic Changes in Oligodendrocytes. *J. Neurosci*. 36:3. doi: 10.1523/JNEUROSCI.2873-15.2016
39. Hirata, E., and Sahai, E. (2017). Tumor Microenvironment and Differential Responses to Therapy. *Cold Spring Harb. Perspect. Med*. 7:7. doi:10.1101/cshperspect.a026781
40. Hompland, T., Ellingsen, C., Øvrebø, K. M., and Rofstad, E. K. (2012). Interstitial Fluid Pressure and Associated Lymph Node Metastasis Revealed in Tumors by Dynamic Contrast-Enhanced MRI. *Cancer Res*. 72:19. doi:10.1158/0008-5472.CAN-12-0903
41. Humphrey, J.D., Dufresne, E.R., and Schwartz, M.A. (2014). Mechanotransduction and extracellular matrix homeostasis. *Nat. Rev. Mol. Cell Biol*. 15:12. doi:10.1038/nrm3896
42. Ingber, D.E. (1993). Cellular tensegrity: defining new rules of biological design that govern the cytoskeleton. *J. Cell Sci*. 104: 613-627.
43. Ingber, D.E., Madri, J.A., and Jamieson, J.D. (1981). Role of basal lamina in neoplastic disorganization of tissue architecture. *PNAS*. 78:6. doi:10.1073/pnas.78.6.3901
44. Jain, R., Chittiboyina, S., Chang, C.-L., Lelièvre, S. A., and Savran, C. A. (2020). Deterministic culturing of single cells in 3D. *Scientific Rep*. 10:1. Doi:10.1038/s41598-020-67674-3
45. Jain, N., Venkatesan Iyer, K., Kumar, A., Shivashankar, G.V. (2013). Cell geometric constraints induce modular gene-expression patterns via redistribution of HDAC3 regulated by actomyosin contractility. *Proc Natl Acad Sci U S A*. 110:11349. doi: 10.1073/pnas.1300801110
46. Janota, C. S., Calero-Cuenca, F. J., and Gomes, E. R. (2020). The role of the cell nucleus in mechanotransduction. *Curr. Opin. Cell Biol*. 63:204 doi:10.1016/j.ceb.2020.03.001
47. Jordahl, S., Solorio, L., Neale, D.B., McDermott, S., Jordahl, J.H., Fox A., et al. (2019). Engineered fibrillar fibronectin networks as three-dimensional tissue scaffolds. *Advanced Materials*. 31:1904580. doi: 10.1002/adma.201904580
48. Kubow, K. E., Vukmirovic, R., Zhe, L., Klotzsch, E., Smith, M. L., Gourdon, D. et al. (2015). Mechanical forces regulate the interactions of fibronectin and collagen I in extracellular matrix. *Nat. Commun*. 6:1. doi:10.1038/ncomms9026

49. Kumar, A., Mazzanti, M., Mistrik, M., Kosar, M., Beznoussenko, G. V., Mironov, A. et al. (2014). ATR Mediates a Checkpoint at the Nuclear Envelope in Response to Mechanical Stress. *Cell*. 158:3. doi:10.1016/j.cell.2014.05.046
50. Larson, A.R., Lee, C.W., Lezcano, C., Zhan, Q., Huang, J., Fischer, A.H., et al. (2014). Melanoma spheroid formation involves laminin-associated vasculogenic mimicry. *Am J Pathol*. 184:71. doi: 10.1016/j.ajpath.2013.09.020
51. Lee, H. J., Diaz, M. F., Price, K. M., Ozuna, J. A., Zhang, S., Sevic-Muraca, E. M. et al. (2017). Fluid shear stress activates YAP1 to promote cancer cell motility. *Nat. Commun*. 8:1. doi:10.1038/ncomms14122
52. Lee, H. J., Ewere, A., Diaz, M. F., & Wenzel, P. L. (2018). TAZ responds to fluid shear stress to regulate the cell cycle. *Cell Cycle*. 17:2. doi:10.1080/15384101.2017.1404209
53. Lee, J. Y., Chang, J. K., Dominguez, A. A., Lee, H., Nam, S., Chang, J. et al. (2019). YAP-independent mechanotransduction drives breast cancer progression. *Nat. Commun*.10:1. doi:10.1038/s41467-019-09755-0
54. Lelièvre, S.A., and Chittiboyina, S. (2018). Microphysiological systems to study microenvironment-cell nucleus interaction: importance of tissue geometry and heterogeneity. *Microphysiol. Syst*. 2:0. doi: 10.21037/mps.2018.11.02.
55. Lelièvre, S.A., Weaver, V. M., Nickerson, J. A., Larabell, C. A., Bhaumik, A., Petersen, O. W., et al. (1998). Tissue phenotype depends on reciprocal interactions between the extracellular matrix and the structural organization of the nucleus. *PNAS*. 95:25. Doi: 10.1073/pnas.95.25.14711
56. Levental, K. R., Yu, H., Kass, L., Lakins, J. N., Egeblad, M., Erler, J. T., et al. (2009). Matrix crosslinking forces tumor progression by enhancing integrin signaling. *Cell*. 139:5. doi:10.1016/j.cell.2009.10.027
57. Lin, C-H., Pelissier, F.A., Zhang, H., Lakins, J., Weaver, V.M., Park C., et al. (2015). Microenvironment rigidity modulates responses to the HER2 receptor tyrosine kinase inhibitor lapatinib via YAP and TAZ transcription factors. *Mol. Biol. Cell*. 26:3946. doi:10.1091/mbc.E15-07-0456
58. Liu, C.-Y., Lin, H.-H., Tang, M.-J., Wang, Y.-K. (2015). Vimentin contributes to epithelial-mesenchymal transition cancer cell mechanics by mediating cytoskeletal organization and focal adhesion maturation. *Oncotarget*. 6:18. doi: 10.18632/oncotarget.3862
59. Liu, J., Tan, Y., Zhang, H., Zhang, Y., Xu, P., Chen, J. et al., (2012). Soft fibrin gels promote selection and growth of tumorigenic cells. *Nat Mater*. 11:734. doi: 10.1038/nmat3361
60. Lu, P., Weaver, V.M., and Werb, Z. (2012). The extracellular matrix: A dynamic niche in cancer progression. *J. Cell Biol*. 196:4. doi:10.1083/jcb.201102147

61. Ma, J., Zhang, Y., Tang, K., Zhang, H., Yin, X., Li, Y., et al. (2016). Reversing drug resistance of soft tumor-repopulating cells by tumor cell-derived chemotherapeutic microparticles. *Cell Res* . 26:713. doi: 10.1038/cr.2016.53
62. Makatsori, D., Kourmouli, N., Polioudaki, H., Shultz, L. D., Mclean, K., Theodoropoulos, P. A. et al. (2004). The inner nuclear membrane protein lamin b receptor forms distinct microdomains and links epigenetically marked chromatin to the nuclear envelope. *J. Biol. Chem.* 279:25567. doi: 10.1074/jbc.M313606200
63. Mammoto, T., and Ingber, D.E. (2010). Mechanical control of tissue and organ development. *Development*. 137: 9. [doi:10.1242/dev.024166](https://doi.org/10.1242/dev.024166)
64. Maniotis, A. J., Chen, C.S., and Ingber, D.E. (1997). Demonstration of mechanical connections between integrins, cytoskeletal filaments, and nucleoplasm that stabilize nuclear structure. *PNAS*. 94: 3. doi:10.1073/pnas.94.3.849
65. Matsugaki, A., Fujiwara, N., Nakano T. (2013) Continuous cyclic stretch induces osteoblast alignment and formation of anisotropic collagen fiber matrix. *Acta Biomater.* 9:7227. doi:10.1016/j.actbio.2013.03.015
66. McGregor, A.L., Hsia, C.-R., and Lammerding, J. (2016). Squish and squeeze — the nucleus as a physical barrier during migration in confined environments. *Curr. Opin. Cell Biol.* 40:32. [doi:10.1016/j.ceb.2016.01.011](https://doi.org/10.1016/j.ceb.2016.01.011)
67. Mierke, C. T., Fischer, T., Puder, S., Kunschmann, T., Soetje, B., and Ziegler, W. H. (2017). Focal adhesion kinase activity is required for actomyosin contractility-based invasion of cells into dense 3D matrices. *Sci. Rep.* 7: 42780. doi:10.1038/srep42780
68. Mohagheghian, E., Luo, J., Chen, J., Chaudhary, G., Sun J., Ewoldt R.H. et al. (2018). Quantifying compressive forces between living cell layers and within tissues using elastic round microgels. *Nature Comm.* 9:1878. doi:10.1038/s41467-018-04245-1
69. Moreno-Vicente, R., Pavón, D. M., Martín-Padura, I., Català-Montoro, M., Díez-Sánchez, A., Quílez-Álvarez, A. et al. (2018). Caveolin-1 modulates mechanotransduction responses to substrate stiffness through actin-dependent control of YAP. *Cell Rep.* 25:6. doi:10.1016/j.celrep.2018.10.024
70. Muncie, J.M., Ayad, N.M.E., Lakins, J.N., Xue, X., Fu, J., Weaver, V.M. (2020). Mechanical tension promotes formation of gastrulation-like nodes and patterns mesoderm specification in human embryonic stem cells. (2020). *Dev Cell*. 55:679.e11. doi: 10.1016/j.devcel.2020.10.015
71. Naruse, K. (2018). Mechanomedicine. *Biophys Rev.* 10:5. doi:10.1007/s12551-018-0459-7
72. Nelson, C.M., VanDuijn, M.M., Inman, J.L., Fletcher, D.A., Bissell, M.J. (2006). Tissue geometry determines sites of mammary branching morphogenesis in organotypic cultures. *Science*. 314:298. doi:10.1126/science.1131000

73. Nguyen, T-U., Watkins, K.E., and Kishore V. (2019). Photochemically crosslinked cell-laden methacrylated collagen hydrogels with high cell viability and functionality. *J. Biomed. Mater. Res. Part A*. 107:1541–1550. doi: 10.1002/jbm.a.36668
74. Novak, C. M., Horst, E. N., Taylor, C. C., Liu, C. Z., and Mehta, G. (2019). Fluid shear stress stimulates breast cancer cells to display invasive and chemoresistant phenotypes while upregulating *PLAU* in a 3D bioreactor. *Biotechnol. Bioeng.* 116:11. doi:10.1002/bit.27119
75. Ondeck, M. G., Kumar, A., Placone, J. K., Plunkett, C. M., Matte, B. F., Wong, K. C. et al. (2019). Dynamically stiffened matrix promotes malignant transformation of mammary epithelial cells via collective mechanical signaling. *Proc. Natl Acad. Sci. (USA)*. 116:9. doi:10.1073/pnas.1814204116
76. Özkale, B., Sakar, M.S., Mooney, D.J. (2021). Active biomaterials for mechanobiology. *Biomaterials*. 267:120497. doi: 10.1016/j.biomaterials.2020.120497
77. Palomeras, S., Rabionet, M., Ferrer, I., Sarrats, A., Garcia-Romeu, M.L., Puig, T. et al. (2016). Breast cancer stem cell culture and enrichment using poly(ϵ -caprolactone) scaffolds. *Molecules*. 21: doi:10.3390/molecules21040537
78. Pankova, D., Jiang, Y., Chatzifrangkeskou, M., Vendrell, I., Buzzelli, J., Ryan, A., et al. (2019). RASSF1A controls tissue stiffness and cancer stem-like cells in lung adenocarcinoma. *EMBO J*. 38:e100532. doi:10.15252/embj.2018100532
79. Parhi R. (2017). Cross-linked hydrogel for pharmaceutical applications: a review. *Adv Pharm Bull*. 7:515–530. doi:10.15171/apb.2017.064
80. Paszek, M. J., Zahir, N., Johnson, K. R., Lakins, J. N., Rozenberg, G. I., Gefen, A. et al. (2005). Tensional homeostasis and the malignant phenotype. *Cancer Cell*, 8:3. doi:10.1016/j.ccr.2005.08.010
81. Paten, J.A., Martin, C.L., Wanis, J.T., Siadat, S.M., Figueroa-Navedo, A.M., Ruberti, J.W. et al. (2019). Molecular interactions between collagen and fibronectin: A reciprocal relationship that regulates de novo fibrillogenesis. *Chem.* 5:2126. doi.org/10.1016/j.chempr.2019.05.011
82. Pederson, T. (2000). Half a Century of “The Nuclear Matrix.”. *Mol. Biol. Cell*. 11:3. doi:10.1091/mbc.11.3.799
83. Plachot, C., and Lelièvre, S. A. (2004). DNA methylation control of tissue polarity and cellular differentiation in the mammary epithelium. *Exp. Cell Res.* 298:1. doi:10.1016/j.yexcr.2004.04.024
84. Plessner, M., Melak, M., Chinchilla, P., Baarlink, C., and Grosse, R. (2015). Nuclear F-actin Formation and Reorganization upon Cell Spreading. *J. Biol. Chem.* 290:18. doi:10.1074/jbc.M114.627166

85. Plodinec, M., Loparic, M., Monnier, C.A., Obermann, E.C., Zanetti-Dallenbach, R., Oertle, P., et al. (2012). The nanomechanical signature of breast cancer. Nat. Nanotechnol. 7:757. doi: 10.1038/nnano.2012.167
86. Pocaterra, A., Romani, P. Dupont, S. (2020). YAP/TAZ functions and their regulation at a glance. *J Cell Sci.* 133:jcs230425. doi: 10.1242/jcs.230425
87. Polacheck, W. J., German, A. E., Mammoto, A., Ingber, D. E., and Kamm, R. D. (2014). Mechanotransduction of fluid stresses governs 3D cell migration. *Proc. Natl. Acad. Sci. (USA)*. 111:7. doi:10.1073/pnas.1316848111
88. Provenzano, P. P., Inman, D. R., Eliceiri, K. W., and Keely, P. J. (2009). Matrix density-induced mechanoregulation of breast cell phenotype, signaling and gene expression through a FAK–ERK linkage. *Oncogene*. 28:49. doi:10.1038/onc.2009.299
89. Qazi, H., Shi, Z.-D., and Tarbell, J. M. (2011). Fluid shear stress regulates the invasive potential of glioma cells via modulation of migratory activity and matrix metalloproteinase expression. *PLoS ONE*. 6:5. doi:10.1371/journal.pone.0020348
90. Raudenska, M., Kratochvilova, M., Vicar, T., Gumulec, J., Balvan, J., Polanska, H. et al. (2019). Cisplatin enhances cell stiffness and decreases invasiveness rate in prostate cancer cells by actin accumulation. *Sci. Rep.* 9:1. doi:10.1038/s41598-018-38199-7
91. Roose, T., Netti, P.A., Munn, L.L., Boucher, Y., Jain, R.K. (2003). Solid stress generated by spheroid growth estimated using a linear poroelasticity model. *Microvasc Res.* 66:204-12. doi: 10.1016/s0026-2862(03)00057-8
92. Rothbauer, M., Zirath, H., and Ertl, P. (2018). Recent advances in microfluidic technologies for cell-to-cell interaction studies. *Lab Chip*. 18:2. doi:10.1039/C7LC00815E
93. Schroer, A.K., and Merryman, W.D. (2015). Mechanobiology of myofibroblast adhesion in fibrotic cardiac disease. *J. Cell Sci.* 128:10. doi:10.1242/jcs.162891
94. Schwager, S. C., Bordeleau, F., Zhang, J., Antonyak, M. A., Cerione, R. A., and Reinhart-King, C. A. (2019). Matrix stiffness regulates microvesicle-induced fibroblast activation. *Am. J. Physiol. Cell Physiol.* 317:1. doi:10.1152/ajpcell.00418.2018
95. Seidlits, S.K., Drinnan, C.T., Petersen, R.R., Shear, J.B., Suggs, L.J., and Schmidt C.E. (2011). Fibronectin-hyaluronic acid composite hydrogels for three-dimensional endothelial cell culture. *Acta Biomater.* 7:2401–2409. doi:10.1016/j.actbio.2011.03.024
96. Sewell-Loftin, M. K., Bayer, S. V. H., Crist, E., Hughes, T., Joison, S. M., Longmore, G. D. et al. (2017). Cancer-associated fibroblasts support vascular growth through mechanical force. *Sci. Rep.* 7. doi:10.1038/s41598-017-13006-x
97. Sidorenko, E., and Vartiainen, M. K. (2019). Nucleoskeletal regulation of transcription: actin on MRTF. *Exp. Biol. Med.* 244:15. doi:10.1177/1535370219854669

98. Singh, N., Liu, X., Hulitt, J., Jiang, S., June, C.H., Grupp, S.A. et al. (2014). Nature of tumor control by permanently and transiently modified gd2 chimeric antigen receptor t cells in xenograft models of neuroblastoma. *Cancer Immunol Res.* 2:1059–1070. doi:10.1158/2326-6066.CIR-14-0051
99. Stephens, A.D., Liu, P.Z., Kandula, V., Chen, H., Almassalha, L.M., Herman, C. et al. (2019). Physicochemical mechanotransduction alters nuclear shape and mechanics via heterochromatin formation. *Mol. Biol. Cell.* 30:17. doi:10.1091/mbc.E19-05-0286-T
100. Stewart-Hutchinson, P.J., Hale, C.M., Wirtz, D., and Hodzic, D. (2008). Structural requirements for the assembly of LINC complexes and their function in cellular mechanical stiffness. *Exp. Cell Res.* 314:8. doi:10.1016/j.yexcr.2008.02.022
101. , T., Munn, L.L., Jain, R.K. (2018). Reengineering the Tumor Vasculature: Improving Drug Delivery and Efficacy. *Trends Cancer.* 4:258. doi: 10.1016/j.trecan.2018.02.010
102. Sun, J., Chen, J., Mohagheghian, E., Ning Wang. (2020). Force-induced gene up-regulation does not follow the weak power law but depends on H3K9 demethylation. *Sci Adv.* 6(14):eaay9095. doi: 10.1126/sciadv.aay9095
103. Swift, J., Ivanovska, I.L., Buxboim, A., Harada, T., Dingal, P.C.D.P., Pinter, J. et al. (2013). Nuclear lamin-a scales with tissue stiffness and enhances matrix-directed differentiation. *Science.* 341:6149. doi:10.1126/science.1240104
104. Tajik A., Zhang, Y., Wei, F., Sun, J., Jia, Q., Zhou, W., et al. (2016). Transcription upregulation via force-induced direct stretching of chromatin. *Nat Mater.* 15:1287. doi: 10.1038/nmat4729
105. Tapia-Rojo, R., and Fernandez, J.M. (2020). Talin folding: the tuning fork of cellular mechanotransduction. *PNAS.* 117:35. doi:10.1073/pnas.2004091117.
106. Turashvili, G., McKinney, S., Martin, L., Gelmon, K. A., Watson, P., Boyd, N. et al. (2009). Columnar cell lesions, mammographic density and breast cancer risk. *Breast Cancer Res. Treat.* 115:3. doi: 10.1007/s10549-008-0099-x
107. Uhler, C., and Shivashankar, G. V. (2017). Regulation of genome organization and gene expression by nuclear mechanotransduction. *Nat. Rev. Mol. Cell Biol.* 18:12. doi:10.1038/nrm.2017.101
108. Van Citters, K. M., Hoffman, B. D., Massiera, G., and Crocker, J. C. (2006). The Role of F-Actin and Myosin in Epithelial Cell Rheology. *Biophys. J.* 91:10. doi:10.1529/biophysj.106.091264
109. Vidi, P.A., Chandramouly, G., Gray, M., Wang, L., Liu, E., Kim, J. J. et al. (2012). Interconnected contribution of tissue morphogenesis and the nuclear protein NuMA to the DNA damage response. *J. Cell Sci.,* 125:2. doi:10.1242/jcs.089177

110. Vidi, P.A., Maleki, T., Ochoa, M., Wang, L., Clark, S.M., Leary, J.F., et al. Disease-On-Chip: Mimicry of Tumor Growth in Mammary Ducts. *Lab chip*. 14:172-7, 2014. doi: 10.1039/c3lc50819f
111. Wang, N. (2017). Review of cellular mechanotransduction. (2017). *J Phys. D. Appl. Phys.* 50:233002. doi: 10.1088/1361-6463/aa6e18
112. Wang, N., Butler, J. P., and Ingber, D. E. (1993). Mechanotransduction across the cell surface and through the cytoskeleton. *Science*. 3:8. doi:10.1016/0962-8924(93)90050-B
113. Watson, P. A. (1991). Function follows form: Generation of intracellular signals by cell deformation. *FASEB J*. 5:7. doi:10.1096/fasebj.5.7.1707019
114. Wojciak-Stothard, B., and Ridley, A. J. (2003). Shear stress–induced endothelial cell polarization is mediated by Rho and Rac but not Cdc42 or PI 3-kinases. *J. Cell Biol.* 161:2. doi:10.1083/jcb.200210135
115. Wullkopf, L., West, A.K. V., Leijnse, N., Cox, T. R., Madsen, C. D., Oddershede, L. B. et al. (2018). Cancer cells' ability to mechanically adjust to extracellular matrix stiffness correlates with their invasive potential. *Mol. Biol. Cell*. 29:20. doi:10.1091/mbc.E18-05-0319
116. Zanutelli, M.R., Reinhart-King, C.A. (2018). Mechanical forces in tumor angiogenesis. *Adv Exp. Med. Biol.* 1092:91. doi:10.1007/978-3-319-95294-9_6
117. Zareei, A., Jiang, H., Chittiboyina, S., Zhou, J., Marin, B. P., Lelièvre, S. A. et al. (2020). A lab-on-chip ultrasonic platform for real-time and nondestructive assessment of extracellular matrix stiffness. *Lab Chip*. 20:4. doi:10.1039/C9LC00926D
118. Zhao, X., Gao, S., Ren, H., Sun, W., Zhang, H., Sun, J. et al. (2014). Hypoxia-inducible factor-1 promotes pancreatic ductal adenocarcinoma invasion and metastasis by activating transcription of the actin-bundling protein fascin. *Cancer Res.* 74:9. doi:10.1158/0008-5472.CAN-13-3009

CHAPTER 3. MATERIALS AND METHODS

3.1 Cell culture and medium

Three different types of human mammary epithelial cells (HMECs) were cultured and maintained as monolayers on plastic for regular use in chemically defined medium. Nonneoplastic S1 cells (1) between 52 and 60 passages (plating density: 2.3×10^4 cells/cm²) and invasive T4-2 cells (2) between passages 28 + 4 and 28 + 10 of the HMT-3522 progression series were cultured as monolayers on plastic (two-dimensional [2D] culture) in chemically defined H14 medium. For T4-2 cells, the flasks were precoated with a mixture of collagen I (Pure Collagen®, Advanced Biomatrix) : 1X PBS (1:44) for a minimum of 24 hours at 4 °C before use. On the day of using the flasks, collagen solution was aspirated out and briefly rinsed with DMEM solution. Chemically defined H-14 medium was prepared from Dulbecco's Modified Eagle Medium (DMEM) with the following additives: [5 µg/ml (or 0.15 IU/ml) prolactin, 250 ng/ml insulin, 1.4 µM hydrocortisone, 0.1 nM β-estradiol, 2.6 ng/ml sodium selenite, 10 µg/ml transferrin and 5 ng/ml epidermal growth factor (only used for S1 cells) as final concentrations in the DMEM] (3). Triple negative invasive HMECs MDA-MB-231 cells were plated between 29+2 and 29+10 passages initially in DMEM with 10% serum. A serum free batch of MDA-MB-231 that proliferated in the chemically defined medium (same as T4-2) was progressively created prior to the experiments as we previously reported (3).

3.2 3D cell culture and collagen matrix preparation

The following section is extracted from multiple pages of a protocol article, “Cell culture and coculture for oncological research in appropriate microenvironments”, that we published earlier and is in the journal's format for electronic submission (3). (Chhetri, A., Chittiboyina, S., Atrian, F., Bai, Y., Delisi, D. A., Rahimi, R., Garner, J., Efremov, Y., Park, K., Talhouk, R., & Lelièvre, S. A. (2019). Cell culture and coculture for oncological research in appropriate microenvironments. *Current Protocols in Chemical Biology*, e65. doi: 10.1002/cpch.65)

3.2.1 The following sections are included from pages 4 – 9 of the article: **Basic protocol 1**

Culture of cancer cells in collagen I matrix of specific stiffness level

The purpose of this method is to place cancer cells in a microenvironmental context that provides an optimal level of constraints for them to display their phenotype. For instance, cancer cells have different degrees of invasive capabilities, and a matrix too stiff or not stiff enough would influence such capabilities. A similar issue might occur with proliferation capabilities. Most cancer cells make their own ECM components, but carcinomas (the frequent cancers of glandular epithelial origin) grow within the interstitial matrix that normally delineates tissues in an organ; the basis for such matrix is collagen. There are many types of collagens depending on the organ (Kular, 2014). The protocol detailed below is focused on collagen type-I (collagen I), the major constituent of the microenvironment of carcinomas. We will use examples of breast carcinomas that recapitulate ductal carcinoma in situ (DCIS), a noninvasive form of cancer, and invasive ductal carcinomas (IDC) with low and high aggressiveness based on their invasive and metastatic potentials. The steps included in the Protocol are the management of cells prior to culture within collagen, the preparation of collagen and embedding of cells (to provide a layer thin enough for direct immunostaining), the observation of cells within collagen and the release of cells from collagen for further desired analyses.

This protocol and other cell culture protocols presented in this article require specific steps and good organization to prepare the appropriate cell culture medium if one wishes to work with serum-free medium. Please read the Reagents and Solutions section and view Table 1 in order to adequately prepare for serum-free cell culture.

Materials and cells

-HMT-3522 T4-2 cells: The IDC T4-2 cells belong to the HMT-3522 series containing non-neoplastic S1 cells, preinvasive S2 cells and invasive T4-2 cells (Briand, 1987; Briand, 1996; Rizki, 2008) and developed in H14 serum-free medium (see Reagents and Solutions and Table 1). They can be obtained from the European Collection of Authenticated Cell Cultures (ECACC)-Catalogue #98102212) or from Sigma-Aldrich (cells from ECACC), or by contacting Mina J. Bissell (Lawrence Berkeley National Laboratory, Berkeley, CA, USA). The T4-2 cells were established when after 238 passages the S2 cells in the series became tumorigenic in mice; the

tumorigenic status was confirmed via subculture *in vitro* of the cells from the tumor developed *in vivo*, and re-inoculation of these cells into mice that led to another tumor formation from which the cell line was ultimately derived (Briand, 1996).

Please note that Table 1 contains all cell culture additives used in the different protocols in this article. For the specific list of additives depending on the cell line please refer to protocol steps.

-Dulbecco's Modified Eagle's Medium (DMEM/F-12) (Thermo Fisher Scientific, Catalogue #12400-024)

-Prolactin (Sigma-Aldrich®, Catalog #L-6520)

-Insulin (Sigma-Aldrich® Catalog #I-4011)

-Hydrocortisone (Sigma-Aldrich® Catalog #H-0888)

-β-Estradiol (Sigma-Aldrich® Catalog #E-2758)

-Sodium selenite (BD Biosciences Catalog #354201)

-Transferrin (Sigma-Aldrich® Catalog #T-2252)

-Collagen type-I (Advanced Biomatrix: PhotoCol®, Catalog No #5201-1KIT for preparing tunable collagen I).

-Trypsin-EDTA (0.25% 1 mM EDTA-4Na) (Gibco, REF: 25200-056)

-Soybean trypsin inhibitor (SBTI), T-6522 type I-S (BD Biosciences #354201)

-Collagenase (Advanced Biomatrix, Catalog #5030-50 mg bottle)

-Ice bucket containing ice

-Pipettor with 1, 5, 10 ml pipets

-Micropipette with 10-20, 200, 1 ml tips

-Eppendorf tubes

-Cell culture compatible plastic tubes (15 and/or 50 ml) (Falcon, ref 352095)

-4-well chambered slides (used for direct immunostaining of cultures) (Falcon, ref 354104)

-Petri dishes to contain the chambered slides (VWR 734-2321)

Table 3.1. Stock, Working and Final Concentrations of Cell Culture Additives with their Storage Conditions

Additive	Company	Initial stock concentration		Aliquot with working stock concentration		Final concentration	
		Expiration at -80°C		Expiration at 4°C		In cell culture medium	
Prolactin	Sigma L-6520	30.03 I.U./ml (1 mg/ml)	1 year	1 mg/ml	1 month	5 $\mu\text{g/ml}$	
Insulin	SIGMA I-4011	2 mg/ml	6 months	100 $\mu\text{g/ml}$	1 month	250 ng/ml	
β -estradiol	SIGMA E-2758	8 mg/ml (0.03 M stock)	1 year	2.67×10^{-5} $\mu\text{g/ml}$	1 month	2.67×10^{-8} $\mu\text{g/ml}$ (or 0.1 nM)	
Hydrocortisone	SIGMA H-0888	5 mg/ml (1.4×10^{-2} M)	1 year	0.5 mg/ml	1 month	0.5 $\mu\text{g/ml}$ (or 1.4 μM)	
Sodium selenite	BD-Biosciences 354201	20 mg/ml	3 months	2.6 $\mu\text{g/ml}$	1 week	2.6 ng/ml	
Transferrin	SIGMA T-2252	20 mg/ml	3 months	20 mg/ml	1 month	10 $\mu\text{g/ml}$	
Epidermal growth factor	Coming Life Sciences 354001	20 $\mu\text{g/ml}$	3 months	20 $\mu\text{g/ml}$	1 week	5 ng/ml	
Fibroblast growth factor	ThermoFisher PHG0264	10 $\mu\text{g/ml}$	1 year	10 $\mu\text{g/ml}$	1 week	2.5 ng/ml	
Transforming growth factor- β	ThermoFisher PHG9204	300 ng/ml	1 year	60 ng/ml	1 week	7.5 pg/ml	
Soybean trypsin inhibitor	SIGMA, T-6522 type I-S	10 mg/ml	6 months	10 mg/ml	2 weeks	0.18 mg/ml	

Protocol steps

Management of cells prior to culture within collagen I

1. Use T4-2 cells at 80% confluence from a T-25 or T-75 flask depending on the number of cells needed for an experiment. The number of cells depends on the type of culture vessel (refer to Table 2 for information on cell numbers). Usually, 4-5 million cells are expected from a T75 flask at 80% confluence.

It is essential to control the passage number of these cells for experiments and we recommend keeping all experiments within a window of 10 passages as phenotypic drifts are typically observed in 3D cell cultures when cells are used beyond a certain number of passages. DO NOT allow the cells to exceed 70-80% confluency before using or for routine passages otherwise you will enrich the population with cells that are less aggressive. This phenotypic drift is usually only seen in 3D culture and by the time the drift in phenotype is observed, it is impossible to recover the original phenotype. To avoid phenotypic drift it is very important to perform standard cell cultures for passages very carefully, with always the same number of cells seeded in flask for each passage and always the same confluence chosen to split the cell population for propagation (Plachot, 2009; Vidi, 2013; see Table 2 for cell seeding concentration in 2D culture). 3D cell culture is usually done no sooner than after one passage of the cells in standard 2D culture if they were thawed from their liquid nitrogen storage.

2. Observe the cells using a light microscope. At 80% confluence, the T4-2 cells typically form large islands containing cells of irregular (but not fusiform) shape and sizes around 20 μm . Cells make contact within these islands, so it looks like a continuous sheet of cells (Vidi, 2013).

If the cells do not look as they do usually or if there are many floating (detached) cells, do not use this flask.

3. Sterilize the laminar flow hood with UV at least 30 minutes prior to use.

We do not use antibiotics for cell culture. The use of antibiotics is not recommended for cell culture as it might lead to the survival of resistant bacteria that could devastate cultures in the long run. It is better to use sterile cell culture elements (containers, pipettes, etc.), thoroughly clean every

piece of equipment before placing it in the hood and clean the hood before and after use (and make use of UV as appropriate).

Table 3.2. Example of Cell Seeding Depending on the Culture Mode

Culture container	Surface area	T4-2; S2; MDA-MB-231 cells	H-14 medium	S1 cells
<i>Standard 2D culture</i>				
4-well plate/ well	2.01 cm ²	23,500	300 µl	47,000
6-well plate/ well	9.08 cm ²	106,000	1.2 ml	212,000
12-well plate/ well	3.8 cm ²	44,500	500 µl	89,000
35 mm dish	9.62 cm ²	112,500	1.3 ml	225,000
60 mm dish	28.27 cm ²	330,000	3.8 ml	660,000
T-25 flask	25 cm ²	291,500	3 ml	583,000
T-75 flask	75 cm ²	875,000	10 ml	1,750,000
<i>Embedded culture in collagen I</i>				
4-well plate/ well	2.01 cm ²	86,700	500 µl	
4-well slide/ well	1.44 cm ²	62,100	500 µl	
35-mm dish	9.62 cm ²	415,100	1.5 ml	
60-mm dish	28.27 cm ²	1,220,000	4.5 ml	
<i>Drip culture with EHS gel</i>				
4-well slide/ well	1.44 cm ²	25,000	400 µl (on 60-µl gel coat)	50,000
35-mm dish	9.62 cm ²	200,000	1.2 ml (on 500-µl gel coat)	400,000
60-mm dish	28.27 cm ²	600,000	3.8 ml (on 1.5-ml gel coat)	1,200,000

^aFor 2D culture, cancer cell seeding for the indicated cell lines is usually 11,700 cells/cm² and non-neoplastic epithelial cell seeding is usually 23,300 cells/cm²; for EHS gel-drip culture, cancer cell seeding for the indicated cell lines is usually 17,400 cells/cm² and 34,700 cells/cm² for non-neoplastic epithelial cells on a gel coat of 42 µl/cm² and with 5% final EHS gel concentration in the cell culture medium; for collagen I-embedded culture, cancer cell seeding for the indicated cell lines is usually 43,150 cells/cm², in 55 µl of gel/cm², on a thin gel coat of 14 µl/cm²

4. Place an ice-filled bucket inside the laminar flow hood.

The bucket must be cleaned before taking it inside the laminar flow hood by wiping it down with ethanol.

5. Prepare Collagen I according to **SUPPORT PROTOCOL 1**. The amount to be prepared depends on the culture vessel and experiment (see Table 2 for detailed information). This step takes between 10 and 20 minutes depending on whether different degrees of gel stiffness need to be prepared.

Removal of cells from their 2D culture device in preparation for embedding in collagen

6. Prepare fresh H14 medium (DMEM/F12 medium including additives) as outlined in the Reagents and Solutions section. For T4-2 breast cancer cells we use 5 µg/ml (or 0.15 IU/ml) prolactin, 250 ng/ml insulin, 1.4 µM hydrocortisone, 0.1 nM β-estradiol, 2.6 ng/ml sodium selenite, 10 µg/ml transferrin as final concentrations in the cell culture medium (see Table 1).

Note that this cocktail works well for the T4-2 and MDA-MB-231 cell lines that we will use as examples of breast IDC in this protocol.

7. Detach cells with trypsin. To do so, discard the medium from the flask and add 750 µl (for T-75) or 250 µl (for T-25) of Trypsin and spread evenly on the cell layer for a quick rinse at room temperature.
8. Immediately remove the trypsin rinse from the flasks (no cells but dead cells will have time to be in suspension).
9. Add 1 ml or 330 µl of trypsin to the T-75 or T-25 flask, respectively and gently spread the solution. Incubate the flask at 37°C for no more than 5-10 minutes.

We recommend you using a timer and removing the flask from the incubator at the 5-minute mark to check for floating cells with a microscope after gently tapping on the sides of the flask. Please continue the incubation for up to five more minutes if the cells were not detached; within 10 minutes the trypsin should have detached most of the cells.

10. After the incubation period is over, add 3 ml (T-25) or 9 ml (T-75) of DMEM containing SBTI at 0.18 mg/ml final concentration. Mix the solution with the pipettor two or three times, washing the entire surface where the cells were cultured and ensure that all the cells are detached and within the solution.

When the cells are removed from their culture vessels, trypsin is used like for other cells, but since there is no serum in the culture, SBTI needs to be added to cancel the effect of trypsin after the few minutes incubation necessary to detach the cells.

SBTI is prepared in milli-Q water to make a stock concentration of 10 mg/ml (see Table 1 and Reagents and Solutions for details). Once an aliquot is thawed and stored in the fridge, this SBTI should be no older than two weeks to be used.

11. Add 100 µl of the above cell suspension into a prelabeled Eppendorf tube for cell counting. Based on the number of cells counted, the necessary volume of suspension can be calculated for cell seeding purposes. (For detailed information on cell seeding concentration and numbers see Table 2).
12. Spin the cells down for five minutes at 3000 g at room temperature and resuspend the cell pellet in 5 µl of H-14 medium.

There should be no significant dilution effect in the collagen I gel. The final volume here usually corresponds to no more than 10 % of the total volume in which the cells are embedded in the next step.

Embedding of cells in collagen I (thin layer)

13. Fill an ice bucket dedicated to the “cell culture” room with ice and transfer the collagen-containing tube (see **SUPPORT PROTOCOL 1**) from the 4°C (refrigerator) to the ice bucket inside the laminar flow hood if you had stored the collagen I there after preparing it (see step 5).
14. Label the tissue culture devices inside the laminar flow hood (e.g., 4-well chambered slides are used for immunostaining purposes) with indication of the cell type, the collagen stiffness and any specific treatment for each well as appropriate; indicate the date.
15. Coat the surface of each well with an ultrathin layer of collagen-I (14 µl/cm², thus 20 µl per well of 4-well chambered slide) and incubate at 37°C for five minutes until the gel becomes opaque.

For the coating step, first add a few drops of the calculated volume of the prepared collagen solution so that they cover all the surface of the well. Use the tip of the pipettor to mix the drops together by gently moving the tip back and forth between the drops. If you keep the tip attached to the micropipette, ensure that the plunger is pushed down to the first notch all the time and avoid taking back the solution into the tip. Keep a small volume of solution in the tip (then the plunger is not pushed all the way down to the first notch) so that it can be added in the final step all around the surface of the well. In that case the remaining collagen solution is slowly released to prevent bubble formation (as usual stop pushing on the plunger when you reach the second notch to avoid making bubbles).

- 16.** Mix the resuspended cells (in the small volume of medium ~5 μ l mentioned in step 12) with the collagen I suspension (55 μ l/cm², thus 80 μ l per well of a 4 well chambered slide; see Table 2) by gentle mixing inside a pipette tip (once or twice). Add the mixture immediately as per the note below on top of the ultrathin coat of collagen.

Briefly, take 10 μ l of collagen and add this volume into the ~5 μ l of cell suspension (see step 12), mixing up-and-down with the plunger only once. This step will allow the cells to get accustomed to the collagen environment. Then, add the necessary volume of collagen (you may subtract the initial 10 μ l volume that was just added). As the collagen solution is viscous, you will have to push the plunger of the micropipette down and stop at the second notch, then release the plunger just a little and wait for a few seconds for the solution to go up the tip, then release the plunger a little more, etc., until the whole volume is taken. Carefully release the collagen solution into the cell suspension, use slow release by maintaining pressure on the plunger of the micropipette. Do not add the last drop of the solution as it creates bubbles. Now mix the solution up and down with the plunger only once. Take the entire volume of collagen solution containing the cells and slowly release the solution on top of the well that is precoated with collagen. Add two drops next to each other in the well (and mix the drops together by moving the tip of the micropipette across the drops if necessary, with no more than one or two back and forth tip movement to avoid disturbing the cells). You should do this step very gently to drag the gel solution also to the sides or towards the edges of the well.

17. Incubate the chambered slides at 37°C in the cell culture incubator for 25 minutes.
18. After incubation, carefully add 500 µl of H-14 culture medium by bringing the pipette tip close to the side of culture vessel, without disturbing the gel.
19. Place the 3D cultures in the cell culture incubator and replace the cell culture medium every two to three days unless the experiment necessitates changing the medium every 24 hours (depending on the type of reagent used for certain treatments).
20. Keep the cells in culture for the necessary length of time.

To obtain tumors we usually wait at least three days before stopping an experiment since they are formed by cell division and not aggregation of cells; but routinely we leave our cells in culture for eight days so that we can compare with other cells that require longer cell culture. T4-2 cells can be kept in culture for weeks since the tumors they form do not grow beyond day 15 or so (there is an equilibrium between the percentages of cells that divide and cells that die at some point).

The following sections are extracted from Pages 13-17 of the article. (Chhetri, A., Chittiboyina, S., Atrian, F., Bai, Y., Delisi, D. A., Rahimi, R., Garner, J., Efremov, Y., Park, K., Talhouk, R., & Lelièvre, S. A. (2019). Cell culture and coculture for oncological research in appropriate microenvironments. *Current Protocols in Chemical Biology*, e65. doi: 10.1002/cpch.65)

3.2.2 Support protocol 1

Collagen type-I Preparation

Here we report a method used to prepare tunable collagen I from Advanced Biomatrix. Other types of collagen I matrix are available, like the Collymers (Geniphs Inc.) that we used for stiffness measurement in **SUPPORT PROTOCOL 3**. The gels vary depending on the origin of the collagen I and the level of purification. Collagen obtained from both companies are polymerized at acidic pH and room temperature leading to the formation of a gel. Polymerization via the kits purchased provide an appropriate ECM of a determined stiffness. The preparation follows the manufacturer's instruction based on the stiffness needed. The resulting stiffness can be confirmed by measuring it as described in **SUPPORT PROTOCOL 3**.

Materials

- Advanced Biomatrix kit (PhotoCol®, Catalogue No #5201-1KIT (formerly #5201-1EA)
- Acetic acid, 20 mM (Advanced Biomatrix, Catalogue Number: 5079-50ML)
- Neutralizing Solution (Advanced Biomatrix, Catalogue Number: 5205-10ML)
- Pure Collagen I (PhotoCol[®], Advanced Biomatrix, Catalogue Number: 5198-100MG)
- Ice bucket containing ice
- Pipettor with 1, 5, 10 ml pipets
- Micropipette with 10-20, 200, 1 ml tips
- Eppendorf tubes

Protocol Steps

1. Place an ice bucket filled with ice to keep the collagen solution cold.

While holding the collagen bottle, care should be given to not touch the bottom part as the solution can solidify quickly at higher than ice-cold temperature.

2. Calculate the volume of pure collagen I to be placed into a prelabelled Eppendorf tube based on the desired matrix stiffness and the entire surface of culture needed for the experiment.

Refer to the manufacturer's guidelines to determine the volume of collagen, acetic acid and neutralizing solution to be added, which varies depending on the matrix stiffness that is desired for a specific experiment. For instance, to embed T4-2 cells in collagen I of stiffness 900 Pa in one well of a 4-well chambered slide, 200 µl of the collagen solution is desirable.

A photoinitiator component is used when photo cross-linking is desired to reach certain degrees of stiffness as per the manufacturer's instructions. Here we present a protocol that does not make use of the photoinitiator.

3. Remove the needed volume of solution carefully and gently since collagen is a viscous polymer, to avoid the formation of bubbles along the process. Place the Eppendorf tube on ice when not handled.

During handling make sure that the bottom of the tube is not touched to avoid raising the temperature of the solution. To take the volume of collagen I solution needed, bring the pipette tip inside the collagen stock bottle, making sure not to touch the neck of the bottle with the end of the tip. The collagen is viscous, thus take the pipette tip sufficiently inside the bottle (although not too deep). When you 'aspirate' the needed volume, wait a few seconds with the pipette tip plunged inside the solution for the needed volume to come up into the tip, then carefully remove it from the bottle. Take an Eppendorf tube and slowly release the content of the pipette tip at the very bottom of the tube without touching that part of the tube with your hand in order not to raise the temperature too quickly. Make sure not to release all the collagen from the pipette tip. As you are nearing the last drop of the polymer in the pipette tip, stop its release (in other words, do not push through the second notch with the micropipette plunger). Acting this way will prevent the formation of bubbles. Place the Eppendorf tube immediately on ice.

4. Take the collagen I solution immediately back to the refrigerator after the desired volume has been taken and bring the 20 mM of acetic acid stock solution into the laminar flow hood from 4°C and place on ice.
5. Add the required volume of acetic acid, depending on the stiffness chosen, into the Eppendorf tube containing the collagen I. Place the tube on ice.

Take the necessary volume of acetic acid from its storage bottle. Carefully and slowly release the acetic acid into the collagen solution of the Eppendorf tube. Make sure that you are releasing the content to the side wall towards the bottom of the tube (not directly within the gel at the very bottom of the tube, otherwise a bubble will form). Do not release the last drop (second notch when pushing on the plunger), to avoid bubble formation.

6. Store the acetic acid back in the refrigerator after use.
7. Bring the neutralizing solution into the cell culture hood. (It is stored at room temperature).
8. Add the required volume of neutralizing solution carefully into the Eppendorf tube containing the mixture of collagen I and acetic acid, in a similar manner as the one used to add the acetic acid.

The neutralizing solution is used to reach a final pH of 7.0 to 7.4. In the mixing steps with acetic acid and neutralizing solution, mixing up-and-down with the pipettor should only be done once to avoid bubble formation.

9. Place this final solution on ice or in the fridge until used for the experiment.

If gel coating will be delayed by more than 30 minutes compared to the preparation of the solution, we usually wait to add the neutralizing solution so that there is no gel formation with time in the tube. We only add the neutralizing solution when we know that we will coat the gel within 30 minutes of preparation.

3.2.3 Support protocol 2

Choosing the appropriate matrix depending on the type of cancer

For each type of cancer, it is important to identify the matrix stiffness that should be used. In the protocol below, we give a step-by-step plan to obtain matrix stiffness information and help choose an appropriate matrix. Literature search will be necessary to gather some of the necessary information. If information on stiffness is not available in the literature, measurement from real tumors is feasible with the appropriate knowledge and equipment (*see SUPPORT PROTOCOL 3*). If the stiffness and composition of the matrix has been correctly chosen, the tumors should display phenotypic (notably architectural) traits that are similar to those observed *in vivo*.

Materials and resources

- Computer with internet access
- Histology resources (book, online information, a pathologist)
- ECM molecules and culture medium depending on the type of tumors
- 4-well chambered slides (used for direct immunostaining of cultures) (Falcon, ref 354104)
- 4-well plate (Nunc TM Thermo Fisher Scientific REF 176740)
- Pipettors and micropipettors with pipets and tips
- 4% Paraformaldehyde solution in PBS (Santa Cruz Biotechnology, SC281692)
- Phosphate Buffered Saline (PBS)

Protocol Steps

1. Determine the origin of the cells to be used (e.g., preinvasive or invasive cancer, subtype of a specific cancer).

*If the cancer type is preinvasive, a basement membrane type molecule (e.g., laminin) will be usually necessary to provide initial signaling for basal polarity to be established. It might also be necessary to have a stiffness higher than normal using collagen I, as it is the case, for instance for breast DCIS that may require a matrix twice as stiff as normal (Lopez, 2011). EHS-based gels typically have a stiffness close to the normal breast stroma (i.e., Young's modulus of 700-800 Pa measured by indentation of unconstrained matrix; see **SUPPORT PROTOCOL 3**). To reach a stiffness around 1,400 Pa and maintain basal polarity, we mix basement membrane component laminin 111 (76 µg/ml) with the collagen of appropriate stiffness prior to embedding the cells (Chittiboyina, 2018).*

2. Proceed with a literature search to identify articles that report measurements of matrix stiffness

*If this information is available, make sure it is the matrix that was measured and not the whole tumor, as stiffness would be different between the two types of samples. It is also important to know how the measurement was performed since results might vary greatly depending on how the measurements were performed (see **SUPPORT PROTOCOL 3**). Very often the information might be in term of fold increase rather than exact values, which is useful if we know the normal matrix stiffness for the location site.*

3. Perform additional literature search to determine any specific content of the ECM in the case of an invasive type of cancer (e.g., molecules other than collagen I that are abundant in the microenvironment of this type of cancer). If necessary, talk with a pathologist since there are tumors for which histochemical staining has been performed to identify the matrix content.

The type of molecules to include beyond collagen I vary depending on the type of cancer; these molecules might be fibronectin, tenascin, hyaluronic acid, etc. It might not be necessary to add these molecules at first since the cancer cells might be able to synthesize and secrete them. Adding

these molecules should only be done if the use of standard collagen I at the expected stiffness is not giving an in vivo-like phenotype upon immunostaining and/or histological analysis.

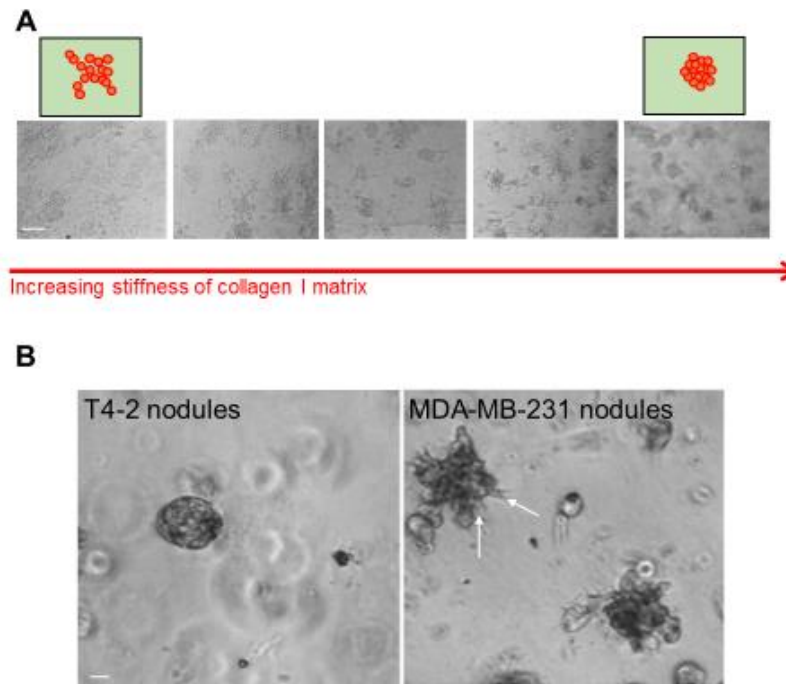


Figure 3.1. Influence of matrix stiffness on cancer cells.

(A) T4-2 cells were seeded in collagen I with a range of stiffness degrees (100 to 1500 Pa). Bright-field images at day 6 of culture show increasing cohesion of cancer cells with increasing matrix stiffness. Drawings display the cellular organization at low and high stiffness degrees. Size bar, 100 μ m. (B) T4-2 cells (poorly invasive) and MDA MB-231 (highly invasive) cells were seeded within the collagen I matrix with stiffness adjusted to 2000 Pa to mimic the in vivo tumor environment. Bright-field images are shown for day 6 of culture. Arrows indicate invasive arms formed by the nodules from MDA MB-231 cells. Scale bar, 25 μ m

4. Test the selected matrix stiffness, possibly performing a range of stiffness degrees (if the protocol for these cells was not established in the literature), with cancer cells of interest. Starting from individual cells as in **BASIC PROTOCOL 1**; follow the growth of tumors over the first six days of culture and take pictures if possible. If tumors grow to reach at least 100 μ m in size you may stop the cultures for analysis.

The characteristics of IDC types of breast carcinomas are invasiveness and a stiffer matrix (at least 2000 Pa if measured on unconstrained samples; Lopez, 2011). For instance, The T4-2 cells are mildly invasive and a triple negative subtype of breast cancer (Estrogen Receptor (ER),

Progesterone Receptor (PR) and Human Epidermal Growth Factor 2 (HER2) negative). The formation of tumors and the invasive phenotype of these cells greatly depend on the collagen I matrix stiffness (Fig. 2A). In contrast to T4-2 cells, triple negative MDA-MB-231 cells (available from American Type Culture Collection, ATCC, HTB-26TM) are highly aggressive (which is also characterized by resistance to treatment; Amaro, 2016). This aggressiveness is easily visible when comparing T4-2 and MDA-MB-231 cells for the same matrix stiffness of 2,000 Pa (Fig. 2B). Note that these tumors grow relatively fast (over a few days); but, other types of tumors might take a couple of weeks to reach an acceptable size for experiments.

5. Remove the cell culture medium, wash once quickly with PBS and add a fixing solution to the cultures for immunofluorescence staining and for future embedding in paraffin, sectioning and Hematoxylin & Eosin (H&E) staining. Then, proceed with (immuno)staining (protocols depend on the laboratories and/or the antibodies) or give the samples to the histology laboratory.

*For direct fluorescence immunostaining, tumors are usually grown in a thin layer of collagen I in 4-well chambered slides (see **BASIC PROTOCOL 1** and Table 2). The fixing solution used depends on the molecules to be stained. Typically, measurement of proliferation (e.g., Ki67) and apoptosis (e.g., caspase 3) might be done along with any characteristic marker of the cancer of interest. We often use 4% paraformaldehyde solution as a fixative. For embedding of the cell cultures in paraffin, tumors are usually cultured in 4-well plates. Then, we give the fixed samples to the Tissue Core or Histology facility for further processing.*

6. Proceed with the analysis of the fluorescence staining (around 150 to 300 cells per sample over several tumors for stainings that can be assessed on a per cell basis; Chittiboyina, 2018).
7. Send the H&E stained slide or a scan of the slide (e.g., using Aperio Digital Pathology) prepared in the histology laboratory to a pathologist for review if the histological analysis of the tumor cannot be done at the Tissue or Histology Core.

The remaining methods that were used in the experiments of the thesis project are described here:

3.3 Treatments with conditioned medium and cisplatin

In our study design, we first cultured non-neoplastic breast epithelial cells (S1 cells of the HMT-3522 series) using collagen I embedding method in a 4-well chamber slide. The chamber slides were precoated with laminin 111 that was added on top of a thin layer of collagen 1 (see section 1.1) and left to dry (with the lid open) in the laminar flow hood for two hours. After the coating was dry, S1 cells were cultured on top of the laminin layer. The stiffness of Collagen I used to culture S1 cells was 770 Pa. The cultures were maintained at 37°C (supplied with 5% CO₂), with regular medium change every two days. On day seven of S1 culture, we cultured MDA-MB-231 cells embedded in collagen I gel of two different stiffnesses – 900 and 2000 Pa with regular medium change for three days. Starting from the third day of cancer cell culture, medium was collected from the S1 cell monocultures and centrifuged to obtain the supernatant. Similarly, MDA-MB-231 medium from the four-well plates was collected and centrifuged to obtain the supernatant. The collected supernatant from S1 cell culture was mixed with fresh H-14 medium (ratio maintained at 50:50) and introduced to the MDA-MB-231 cultures on four-well chamber slides. Collected MDA-MB-231 supernatant (control conditioned medium) was also mixed with fresh H-14 and introduced to other four-well chamber slides with MDA-MB-231 cells in culture. The number of cultures supplemented with each type of medium was kept constant between S1 and control conditioned. This process was repeated at 24-hour intervals until the end of the culture period.

After three days of culture with conditioned medium, the wells containing tumors were selected at random to receive three different doses of Cisplatin (50, 75 and 100 μ M) and one group was selected as control (100 μ M NaCl). The treatment was introduced in the cultures during medium change and lasted for 24 hours. The T4-2 cells were treated with either 50 μ M of Cisplatin or vehicle (50 μ M NaCl) for 24 hours after six days of first culture.

3.4 DAPI staining

Chamber slides containing tumors were washed briefly with PBS 1X and fixed with paraformaldehyde (4%) at room temperature – 1 hour. This was followed by 100X Triton permeabilization and brief wash with 1X Cytoskeletal buffer solution + Protease inhibitors (Aprotinin, NaF, Pefabloc) (4). After three washes with PBS-Glycine (1X), the slides were

incubated with 0.5 $\mu\text{g/ml}$ of DAPI (final concentration in PBS) for 5-10 min at room temperature in the dark. The solution was discarded, and the cells were briefly washed once with PBS-Glycine. After removal of the solution, Antifade was added to cover the slide with a coverslip. Slides were left to dry overnight in the dark (at room temperature) and the coverslips were sealed with nail polish. Slides were stored at -20 C until further use.

3.5 Nuclear morphometry and cell death assessment

DAPI images then were taken using an EVOS Cell imaging system at 20X magnification. For each experiment, 4-5 images were stored for analysis. Images were processed on the Image J platform (<https://imagej.nih.gov/ij/>) to obtain nuclear morphometry parameters – area and circularity and identify dead cells based on nuclear features (Fig 3.3.2). Alive and dead cells were counted using DAPI-stained nuclei on ImageJ. A total of ~150-200 nuclei were analyzed for each condition (biological replicate, $n=3$). “Cell counter” plugin was used to keep track of the total number of alive (type 1) and dead cells (type 2). The images were each zoomed in to get a clearer view. Only the nuclei that were part of a tumor were considered and single cells away from tumors were not included. Tumor regions with >4 cells in focus were selected for analysis. After delineating the periphery of each nucleus, ROI commands $>\text{Analyze} >\text{Measure}$ were used to select the nuclear area and circularity for measurement.

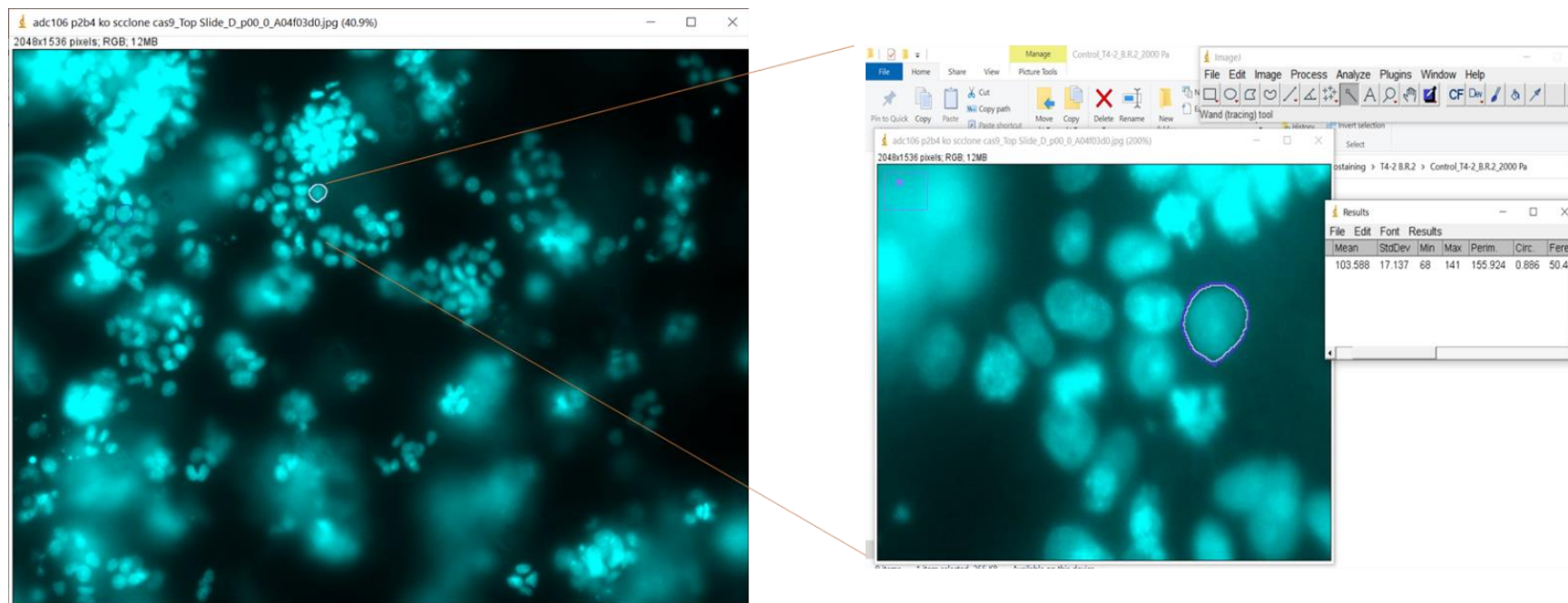


Figure 3.3.2 T4-2 tumors cultured in collagen I (2000 Pa) on H14 medium

The tumors were stained with DAPI and imaged on the sixth day (20X magnified image on the left), and morphometry parameters were identified using *ImageJ* using zoomed in images as on the right

3.6 References:

1. Briand, P., Petersen, O. W., & Van Deurs, B. (1987). A new diploid nontumorigenic human breast epithelial cell line isolated and propagated in chemically defined medium. *In vitro cellular & developmental biology*, 23(3), 181-188.
2. Briand, P., Nielsen, K. V., Madsen, M. W., & Petersen, O. W. (1996). Trisomy 7p and malignant transformation of human breast epithelial cells following epidermal growth factor withdrawal. *Cancer research*, 56(9), 2039-2044.
3. Chhetri, A., Chittiboyina, S., Atrian, F., Bai, Y., Delisi, D. A., Rahimi, R., ... & Lelièvre, S. A. (2019). Cell culture and coculture for oncological research in appropriate microenvironments. *Current protocols in chemical biology*, 11(2), e65.
4. Abad, P. C., Lewis, J., Mian, I. S., Knowles, D. W., Sturgis, J., Badve, S., ... & Lelièvre, S. A. (2007). NuMA Influences Higher Order Chromatin Organization in Human Mammary Epithelium. *Molecular Biology of the Cell*, 18(2), 348–361.
<https://doi.org/10.1091/mbc.e06-06-0551>

CHAPTER 4. RESULTS

Nuclear area and circularity parameters are dependent on extracellular matrix stiffness and the cell's phenotypic characters

We cultured two types of triple negative breast cancer cell lines with distinct cell proliferative and colony morphologic features – T4-2 (from the HMT-3522 series) and MDA-MB-231- in collagen I of different stiffnesses. Both cell lines resemble the basal B subtype of breast cancers (4), where MDA-MB-231 cells are identified as highly invasive (many of these cells typically adopt a mesenchymal shape) and metastatic while T4-2 cells are less aggressive (very mildly invasive) (2,4,5). Both cell lines were cultured in H14 medium (DMEM supplemented with additives) for breast tumors as described in detail previously (3); however, for some of the conditions (900 and 2000 Pa collagen I) MDA-MB-231 cells were cultured in H14 medium that was renewed at 50% instead of 100% every day for comparison with another set of experiments. The phenotypic characteristics. Phenotypically, the tumors formed from both types of breast cancer cell lines, cultured in the presence of methacrylated collagen I with adjustable stiffness, were similar to those reported earlier in matrigel, derived from Engelbreth-Holm-Swarm mouse tumors (3D culture) (4). MDA-MB-231 have stellate appearance (elongated cell body and invasive processes) (Fig 4.1), while the T4-2 cells have a mass-like appearance (robust cell-cell adhesion) (Fig1).

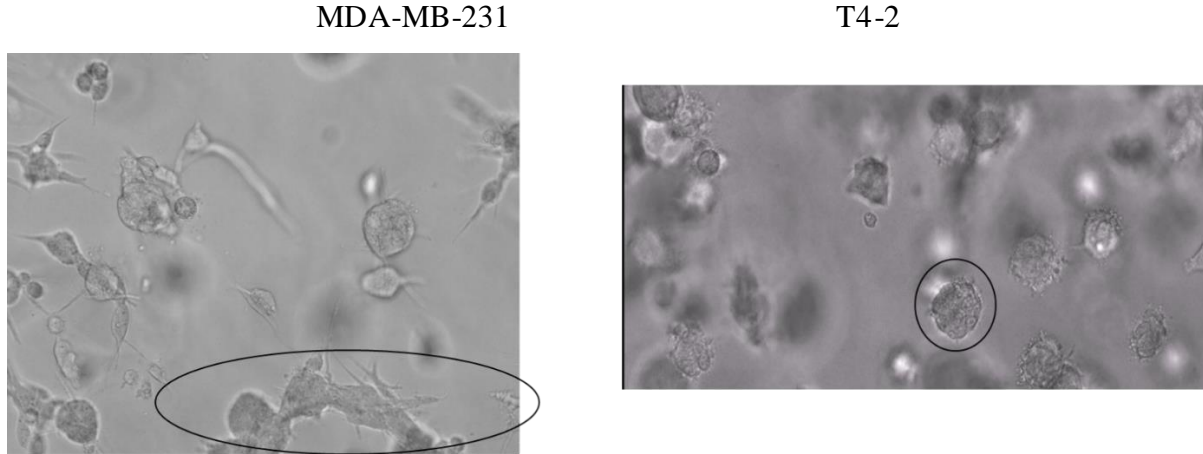


Figure 4.1. Tumor obtained from MDA-MB-231 and T4-2 cell lines are distinct. MDA-MB-231 tumors have invasive protrusions (encircled in left panel) while T4-2 tumors have mass-like appearance (encircled in right panel). Image taken with a brightfield microscope at 20X magnification after six days of culture in collagen I (2000 Pa).

After six days in 3D culture, the cells were fixed and stained with DAPI to perform nuclear morphometry measurements using ImageJ software (<https://imagej.nih.gov/ij/index.html>). The nuclear area and circularity (ratio of area to the square of the perimeter scaled by a factor of 4π) of the MDA-MB-231 tumors showed a more variable pattern when compared to nuclear morphometry features in T4-2 cells, in the presence of increased stiffness. In MDA-MB-231 cells, the mean nuclear area increased significantly from 900 Pa to 2000 Pa (with corresponding values as 155.8 and 164.88 μm^2 respectively), then, decreased significantly from 2000 Pa to 3300 Pa such that at 3300 Pa, the mean area of 148.33 μm^2 is comparable to that of 900 Pa stiffness (Fig 4.2).

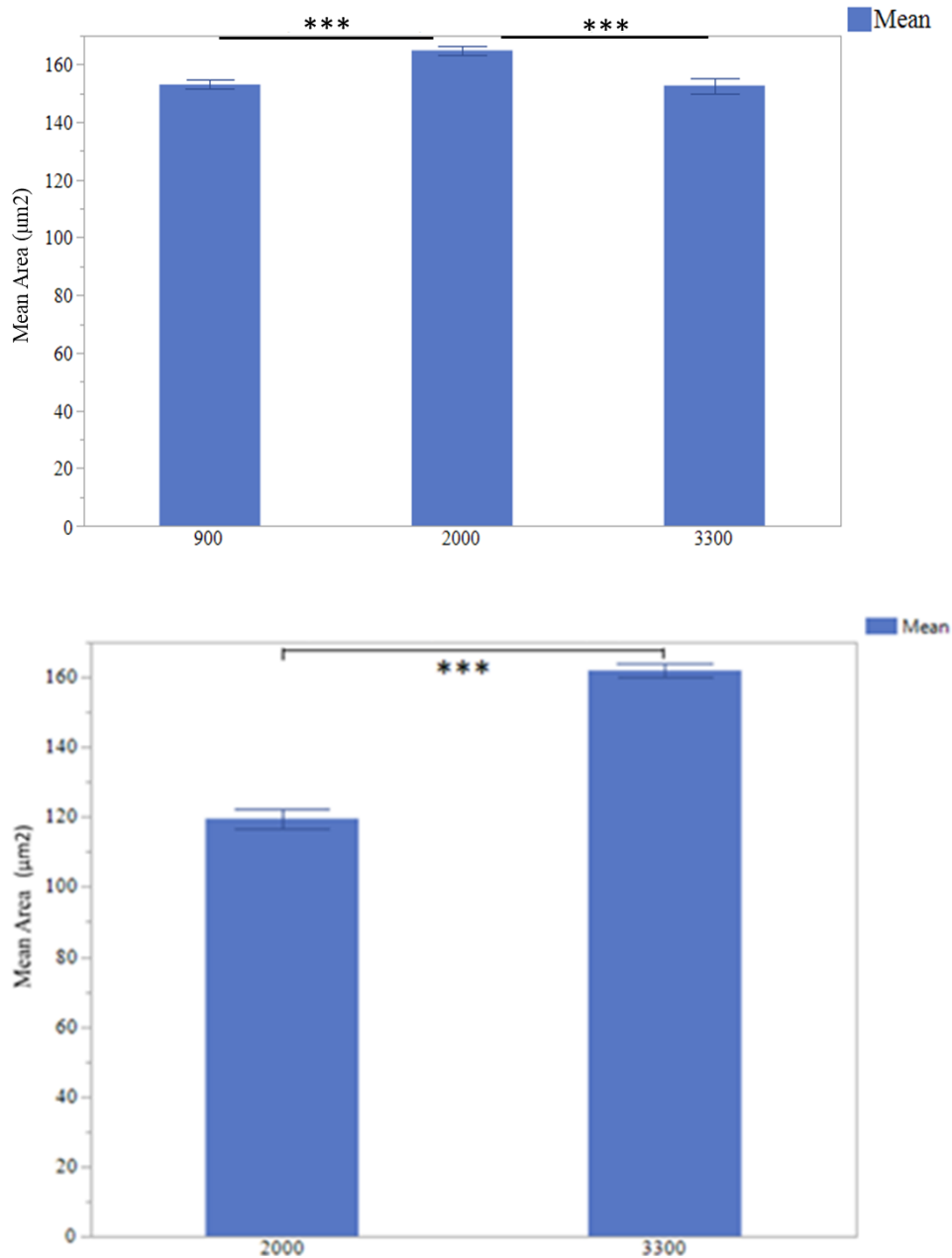


Figure 4.2. Mean nuclear area in MDA-MB-231(top panel) and T4-2 (bottom panel) is dependent on the stiffness of collagen I. MDA-MB-231cells were, embedded in collagen I at 900 Pa, 2000 Pa and 3300 Pa (for 900 and 2000 Pa conditions the medium was renewed by 50% every 24 hours after day three); T4-2 were embedded in collagen I at 2000 Pa and 3300 Pa supplemented regularly with fresh H14 medium. At day six, tumors were stained with DAPI and recorded images were analyzed using *ImageJ*. N = 3 for MDA-MB-231, N=2 for T4-2; 150 nuclei analyzed per replicate. *** $P < 0.001$.

Circularity, which provides a measure of the shape of the nucleus (with maximum 1 reflecting a perfectly circular nucleus) also changes significantly with increasing stiffness; it was 0.797, 0.765 and 0.800 for 900 Pa, 2000 Pa and 3300 Pa, respectively, in MDA-MB-231 tumors (Fig 4.3). While the mean area gives an idea about the spread of the nucleus, circularity brings information on the uniformity of that spread. In other words, at 2000 Pa, nuclei were more spread with smallest circularity, while at 900 Pa and 3300 Pa, the nuclei were more circular and less spread out. The stiffness of invasive ductal carcinomas (IDC) of the breast in real tissue seems to start around 2000 Pa (values around 900 Pa are close to normal tissue), thus, we only compared the T4-2 and MDA-MB-231 tumors cultured in collagen I of stiffnesses - 2000 and 3300 Pa. The nuclei in T4-2 tumors showed an opposite trend to MDA-MB-231 tumors. The nuclear area in T4-2 increased significantly from 2000 Pa ($119.47 \mu\text{m}^2$) to 3300 Pa ($161.87 \mu\text{m}^2$). Interestingly, there was no significant impact of increased stiffness on their nuclear circularity (Fig 4.3). Therefore, two basal-like tumors with notoriously different aggressiveness responded very differently to physical changes in the microenvironment.

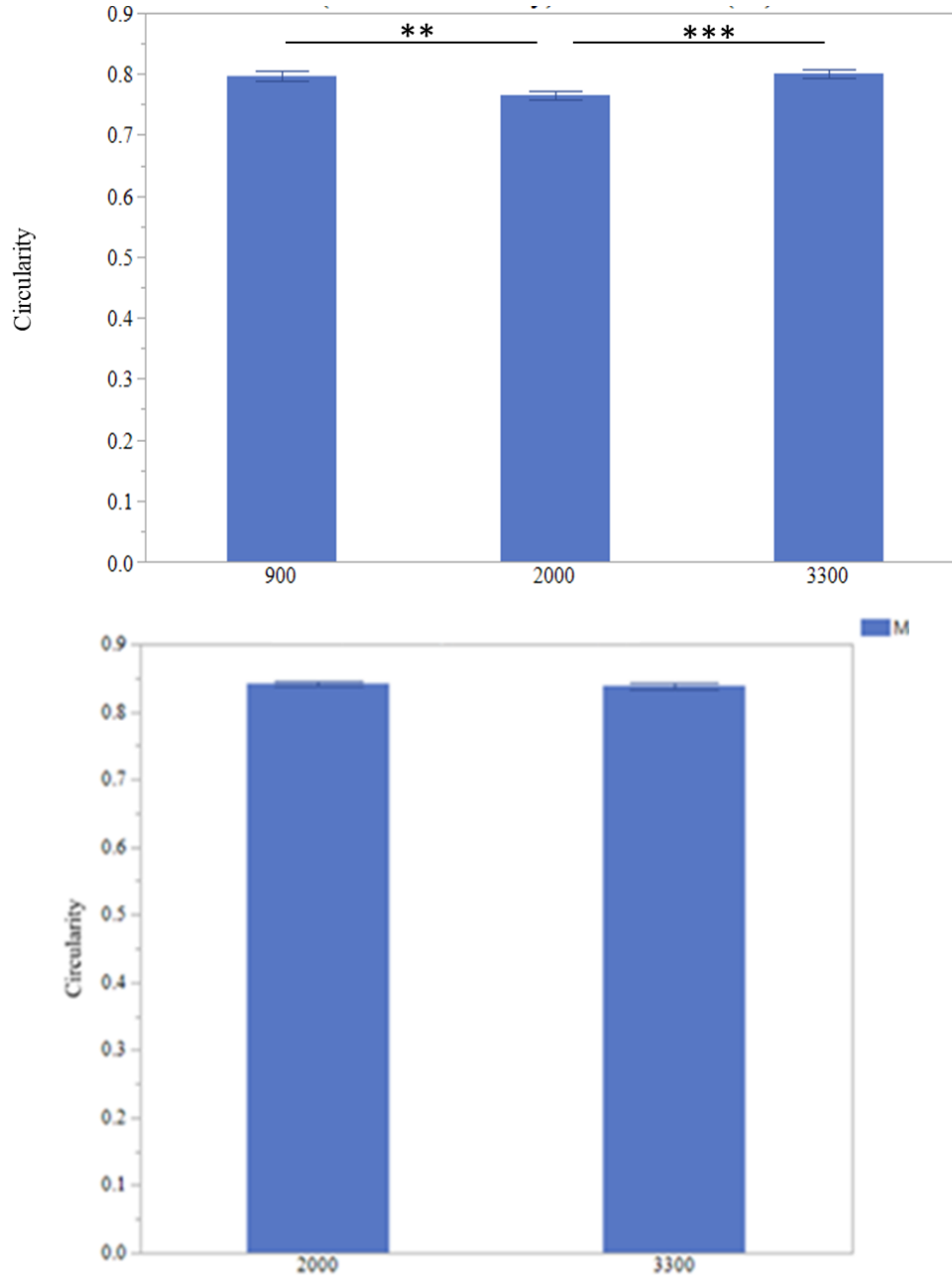


Figure 4.3. Mean nuclear circularity in MDA-MB-231(top panel) and T4-2 (bottom panel) is dependent on the stiffness of collagen I

MDA-MB-231 cells were embedded in collagen I at 900 Pa, 2000 Pa and 3300 Pa (for 900 and 2000 Pa conditions the medium was renewed by 50% every 24 hours after day three); T4-2 were embedded in collagen I at 2000 Pa and 3300 Pa, supplemented regularly with fresh H14 medium. At day 6, tumors were stained with DAPI and recorded images were analyzed using ImageJ. (N = 3 for MDA-MB-231, N=2 for T4-2); 150 nuclei analyzed per replicate. ** $P < 0.01$; *** $P < 0.001$.

The distribution of Nuclear Area and Circularity in the cancer cell population suggests distinct levels of heterogeneity depending on the aggressiveness of tumors and in response to increasing stiffness

We have previously used nuclear morphometry as a readout for phenotypic changes on a per cell basis (6–8). This type of measurement enables us to investigate the predominance or the variability of cell phenotypes within and across tumors. Two morphometric parameters – nuclear area and circularity were measured using ImageJ. Interestingly, we obtained a distinct pattern of nuclear morphometry with increasing stiffness even among the tumors cultured from same cell line (and same batch of culture). We also observed a variation in heterogeneity of nuclear phenotypes with increased stiffness across tumors of different levels of aggressiveness. Overall, the nuclear area values ranged from 60 to 250 μm^2 (Fig 4.4), and their nuclear circularity values ranged from 0.4 to 0.95 (Fig 4.5). The trends in heterogeneity of the nuclear area and circularity parameters were derived from the increased number of nuclei population that deviated from the median values, which is best captured by the boxplot above the histogram diagrams. The histograms were categorized with increments of 30 μm^2 for the area and 0.1 for the circularity.

We observed a trend for increased phenotypic heterogeneity for nuclear area and a slight decrease in heterogeneity for nuclear circularity with increased ECM stiffness in the MDA-MB-231 cell population cultured in 2000 Pa and 3300 Pa. In the case of T4-2 cell population, their nuclear area showed a decrease in heterogeneity as the collagen I stiffened (from 2000 to 3300 Pa). The distribution pattern for nuclear circularity was comparable for both stiffness levels (Fig 4.5). These responses to stiffnesses of two different basal-like breast cancers display an opposite trend in heterogeneity for nuclear morphometry. Such opposite behavior of nuclear heterogeneity for tumors with distinct degrees of aggressiveness is comparable to the behavior of the mean nuclear morphometry values (as illustrated in figures 4.2 and 4.3). These results also highlight a lack of obvious response of nuclear circularity to ECM stiffness increase in the less aggressive tumors.

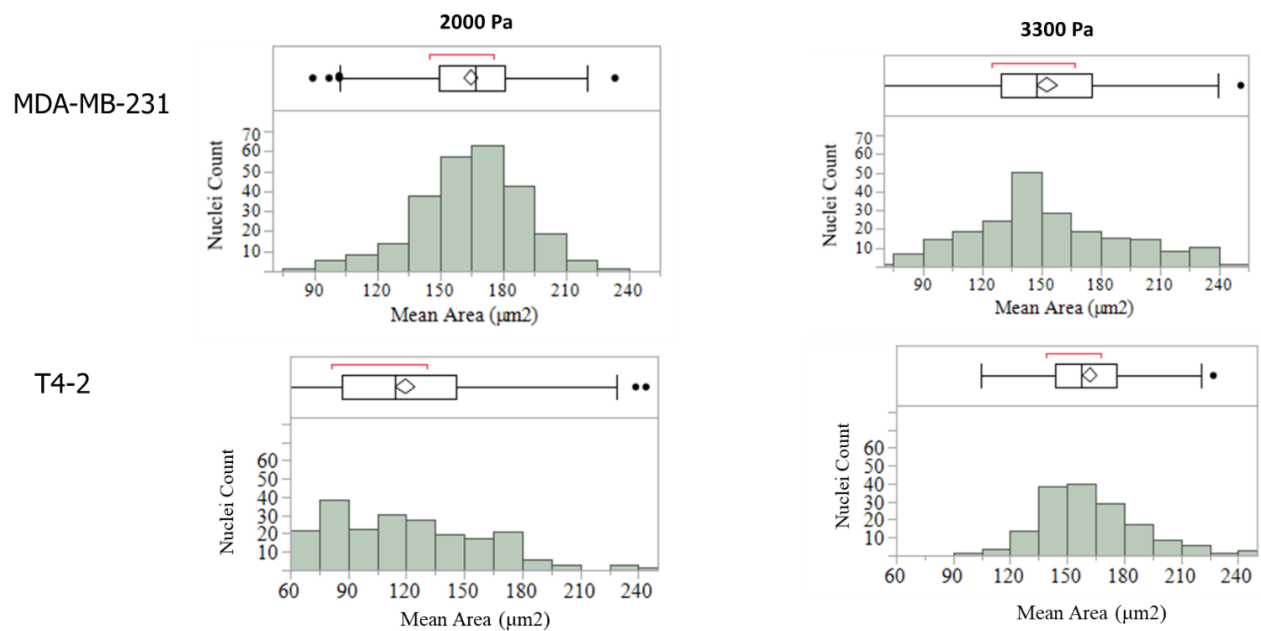


Figure 4.4. The distribution of nuclear area is influenced by the stiffness of collagen I in opposite manner depending on the degree of aggressiveness of the tumors.

Each histogram distribution accompanies an outlier boxplot indicating Q1, Q2, Q3. MDA-MB-231 cells (top panel) were embedded in collagen I at 2000 Pa and 3300 Pa, in H14 medium (Medium for MDA-MB-231 at 2000 Pa was renewed by 50% every 24 hours after day 3 with control conditioned medium). T4-2 cells (lower panel) were embedded in collagen I at 2000 Pa and 3300 Pa in regular H-14 medium. At day six, all the tumors were stained with DAPI and recorded images were analyzed using *ImageJ*. For MDA-MB-231 $n = 3$; for T4-2, $n=2$; 150 nuclei analyzed per replicate.

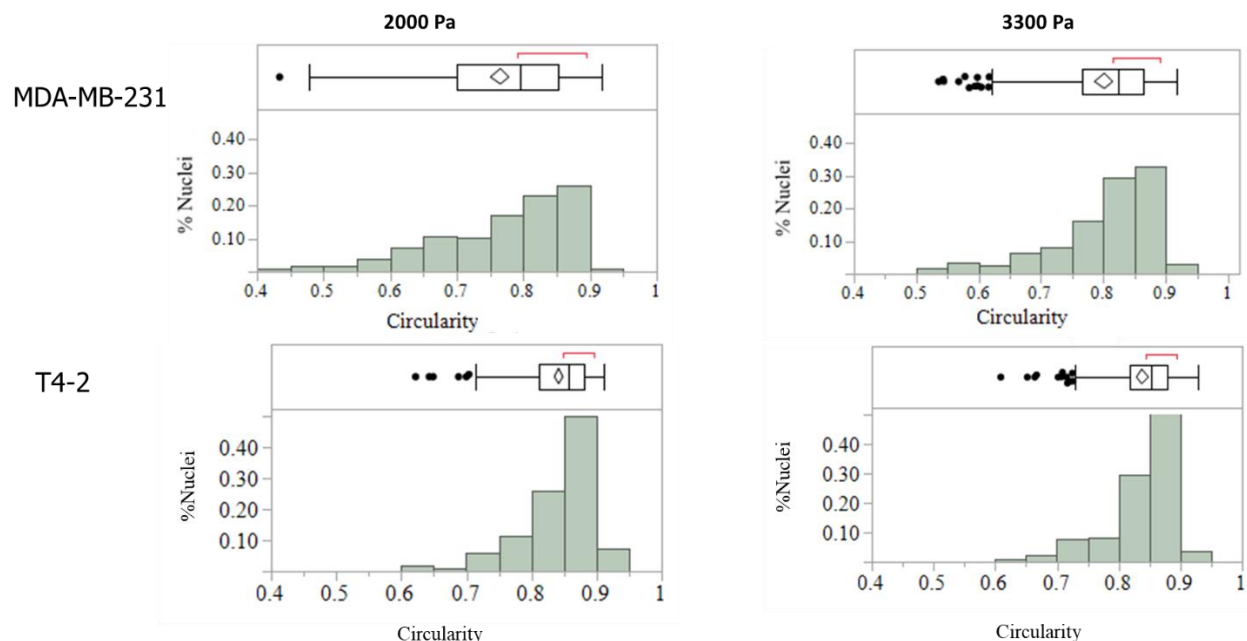


Figure 4.5. The distribution of nuclear circularity appears poorly responsive to increased matrix stiffness, especially in less aggressive tumors.

Each histogram distribution accompanies an outlier boxplot indicating Q1, Q2, Q3. MDA-MB-231 cells were embedded in collagen I at 2000 Pa and 3300 Pa, in H14 medium (medium for 2000 Pa was renewed by 50% every 24 hours after day three with control conditioned). T4-2 cells were embedded in collagen I at 2000 Pa and 3300 Pa in regular H-14 medium. At day six, all the tumors were stained with DAPI and recorded images were analyzed using *ImageJ*. For MDA-MB-231 $n = 3$; for T4-2, $n=2$; 150 nuclei analyzed per replicate.

Paracrine factors from non-neoplastic epithelial cells influence the physical response of nuclei to matrix stiffness increase in aggressive tumors.

Non-neoplastic epithelial cells are one of the major components of a tumor microenvironment besides the cancerous cells. The role of this cellular compartment is often undermined compared to other cells, like fibroblasts that are present within tumors or at their periphery. Yet, depending on the size of the tumor, the influence of the normal breast epithelium might be significant. Noting that ECM stiffness impacts cellular phenotype, and the secreted components of the non-neoplastic epithelial cells affect ECM dynamically, we were interested to study the interaction between cellular phenotype, stiffness, and paracrine influence. In our study design, we first cultured non-neoplastic breast epithelial cells (S1 cells of the HMT-3522 series) on top of laminin 111 (to ensure differentiation), itself coated on a thin layer of collagen I at 770 Pa (Fig 4.6).

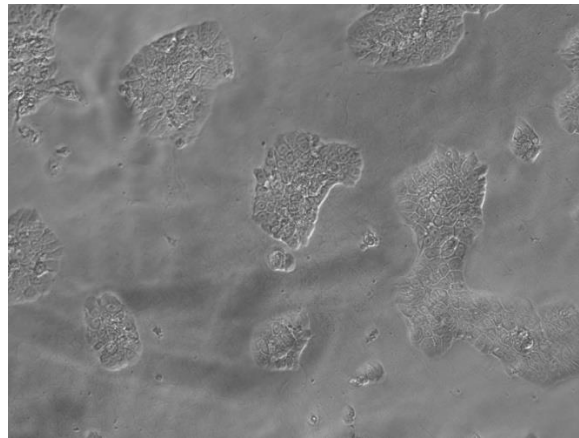


Figure 4.6. S1 cells monolayer culture on top of laminin 111 precoated with collagen I (770 Pa).

Image taken with a brightfield microscope at 20X magnification after seven days of culture.

After seven days of culture of S1 cells, we embedded MDA-MB-231 cells in collagen I of two different stiffnesses – 900 and 2000 Pa, with regular medium change every two days. Starting from the third day of cancer cell culture, S1 medium was collected and centrifuged to obtain only the supernatant, which was mixed in a 50-50 ratio with fresh H-14 medium and used to feed the MDA-MB-231 cultures regularly at 24-hour interval. The control cell cultures were supplemented

with fresh medium + MDA-MB-231 conditioned medium (50:50) (control conditioned medium) regularly at 24-hour interval. At day six of cultured in conditioned medium from non-neoplastic cells, morphometric analysis revealed that, the mean nuclear area at 2000 Pa ($177.19 \mu\text{m}^2$) was significantly higher than at 900 Pa ($160.93 \mu\text{m}^2$) (Fig. 4.7). These results were not statistically different from control cultures (MDA-MB-231 conditioned medium). However, nuclear circularity did not significantly change upon increasing stiffness from 900 to 2000 Pa (0.827 to 0.817) (fig 4.7) in contrast to what was observed in control conditioned medium. Therefore, it is possible that, if in large enough proportion, the non-neoplastic epithelial cells dampen the response of the cell nucleus to physical strains outside the tumor, at least for nuclear circularity.

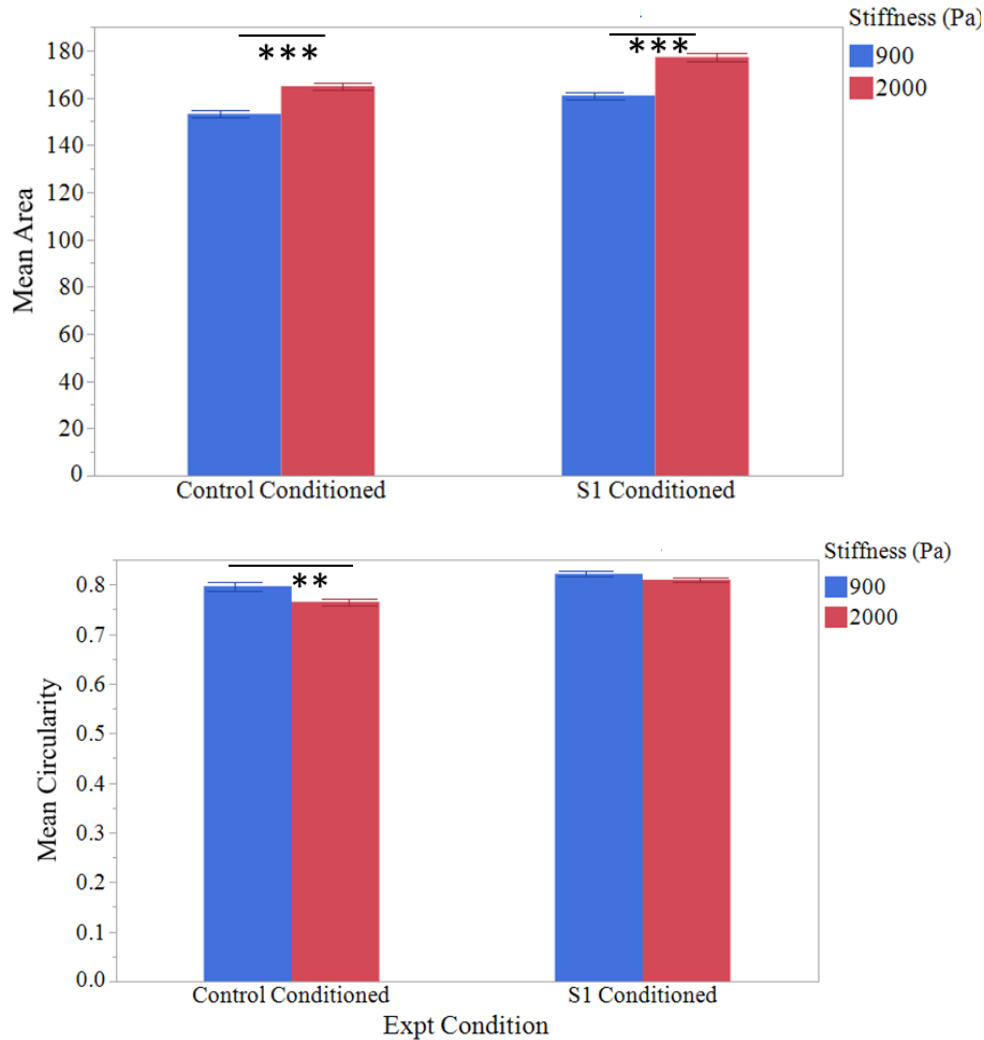


Figure 4.7. Conditioned medium from non-neoplastic cells prevents the effect of increasing collagen I stiffness on nuclear circularity.

MDA-MB-231 cells were cultured for six days, embedded in collagen I at 900 Pa and 2000 Pa in H14 medium. Cultures were supplemented with 50% S1 conditioned medium every 24 hours after day three in parallel with cultures supplemented with 50% MDA-MB-231 conditioned medium (control conditioned medium). At day six, tumors were stained with DAPI and recorded images were analyzed using *ImageJ*. S1 cells were cultured on top of collagen (770 Pa), coated with laminin111 to collect the conditioned medium. Shown are mean nuclear area (top panel) and mean nuclear circularity (bottom panel) of MDA-MB-231 cells. N = 3; 150 nuclei analyzed per replicate. ** $P < 0.01$; *** $P < 0.001$.

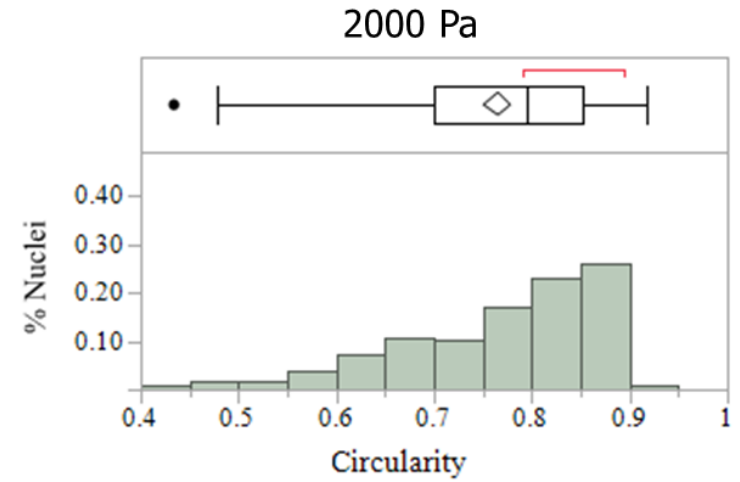
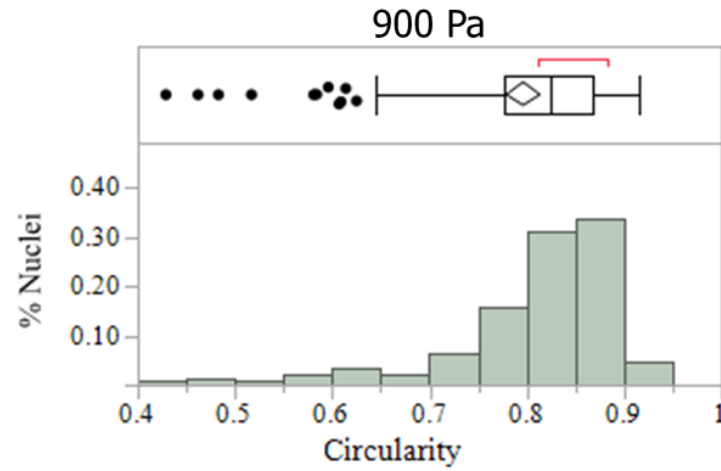
Interestingly, the conditioned medium from non-neoplastic cells also prevented the increase in heterogeneity for nuclear circularity induced by collagen I at 2000 Pa compared to 900 Pa (Fig 4.8). Whereas, the effect of the conditioned medium from non-neoplastic cells on the heterogeneity of nuclear area in MDA-MB-231 cells was mostly unremarkable (Fig 4.8).

Figure 4.8. The impact of ECM stiffness on the distribution of nuclear circularity in cancer cells is prevented by paracrine factors from the non-neoplastic cells.

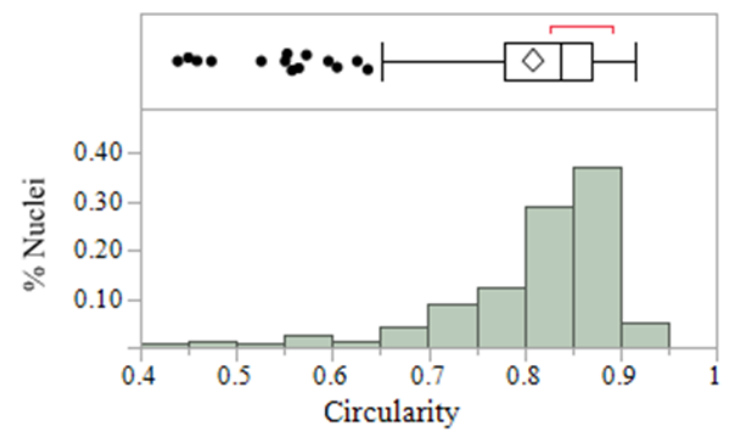
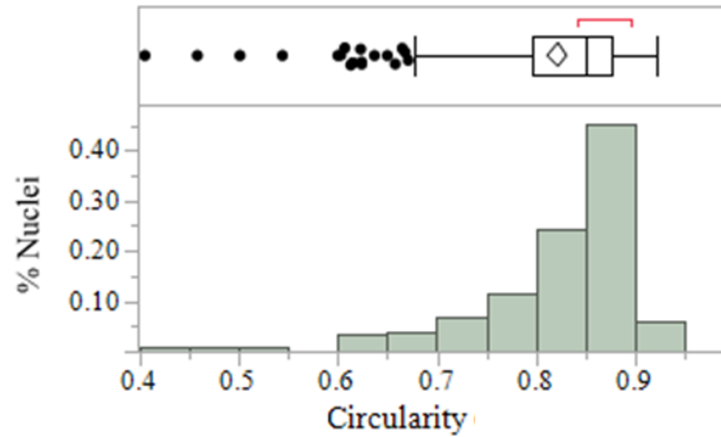
Each histogram distribution accompanies an outlier boxplot indicating Q1, Q2, Q3. MDA-MB-231 cells were embedded in collagen I at 900 Pa and 2000 Pa, in H14 medium (the medium was renewed by 50% every 24 hours after day three, either with control conditioned medium or with conditioned medium from non-neoplastic S1 cells). At day six, all the tumors were stained with DAPI, and recorded images were analyzed using *ImageJ*. N = 3. 150 nuclei analyzed per replicate.

Figure 4.8 continued

Control Conditioned Medium (MDA-MB-231)



S1 Conditioned Medium



Variation in heterogeneity of nuclear morphometry upon increase in matrix stiffness is not the result of selective pressure leading to cell death.

To determine if the microenvironment-induced changes in heterogeneity might be linked to cell survival, we calculated the percentage of dead cells based on DNA fragmentation and compaction shown by DAPI staining. For each culture condition used previously to assess phenotypic heterogeneity around 150 nuclei were analyzed per biological replicate. Our results indicate that the rate of survival of MDA-MB-231 cells organized into tumors is stiffness-dependent and varies significantly as stiffness increases in the presence of the control medium (Table 4.1). The observed percentages were comparable irrespective of the presence of conditioned medium from the non-neoplastic cells. Specifically, for the MDA-MB-231 cells, maximum cell death (around 40%) was observed at 2000 Pa, which was significantly higher than the observed cell death at 3300 Pa (26%) but comparable to the cell death at 900 Pa (33.17%). Thus, maximum cell death occurred under a condition corresponding to the most heterogeneous population when looking at nuclear circularity, which suggest that heterogeneity may not be induced by the disappearance of certain phenotype due to lack of cell survival.

A similar conclusion can be made for T4-2 cells. The percentage of T4-2 cells that died after six days of culture in collagen I (2000 and 3300 Pa) was statistically similar across stiffness, yet increasing stiffness strongly changed the level of heterogeneity in the cell population based on nuclear area.

Table 4.1. Percentage of cell death in MDA-MB-231 and T4-2 tumors based on microenvironmental conditions

Cell lines	Stiffness	% Cell Death (M \pm SE)	<i>P</i> value
MDA-MB-231	900 Pa	33.17 \pm 3.25	0.25
	2000 Pa	39.17 \pm 0.92	
MDA-MB-231	2000 Pa	39.17 \pm 0.92	*0.0026
	3300 Pa	25.59 \pm 0.64	
T4-2	2000 Pa	24.97 \pm 1.02	0.189
	3300 Pa	30.43 \pm 0.585	

Stiffness mediated response to cisplatin in aggressive tumors is modified by the paracrine influence of non-neoplastic cells

The aggressiveness of tumors is usually linked to the speed of growth and the potential for invasiveness. For some tumors, additional aggressiveness might be linked to their resistance to cytotoxic drugs, which in many cases is also linked to their proliferation status but might also be dependent on the expression of genes that promote survival. Both types of breast cancer cell lines – T4-2 and, MDA-MB-231- were cultured as described in the above sections for six days in a 4-well chamber slide in H-14 medium (MDA-MB-231 were supplemented with a 50% conditioned medium that was either S1 conditioned or control conditioned on day three until day 6, with medium change every 24 hours) . On the 6th day, Cisplatin was introduced during medium change for 24 hours, which was followed by fixation and DAPI staining for imaging. Four groups of tumors from each cell line were chosen at random to receive the doses prepared from a 3.3 mM stock of Cisplatin (50, 75 and 100 μ M for MDA-MB-231 and only 50 μ M for T4-2), or the vehicle (100 μ M NaCl)). Earlier experiments have shown that 50 μ M corresponds to the minimum lethal dose (LD₅₀) of Cisplatin required to kill 50% of the T4-2 cells. For MDA-MB-231, the LD₅₀ corresponds to 75 μ M of cisplatin.

We compared the percentages of apoptotic cells by counting the number of nuclei with specific features of DNA, i.e. condensation and fragmentation. The apoptotic cells usually have abnormally small nucleus and DAPI fluorescence may be very intense, covering a large focus representing a shrunken nucleus or there may be a few large foci (3-5) of DAPI fluorescence. In MDA-MB-231 cells we investigated whether there was a difference for the impact of cisplatin for two different collagen I stiffness levels (900 and 2000 Pa). The table 4.2 represents the percentage of apoptotic MDA-MB-231 cells (supplemented with control conditioned medium) with cisplatin treatment. From the table it is confirmed that the incremental doses of Cisplatin effectively caused apoptosis the cells. The sensitivity of aggressive MDA-MB-231 to 50, 75 and 100 μ M doses of cisplatin did not change with increased stiffness. However, when we compared the response to incremental drug concentrations and notably, the fold change as compared to control (this is represented by delta in table 4.2), sensitivity of the MDA-MB-231 tumors was observed to be higher in 900 Pa collagen I compared to 200 Pa collagen I. (Table 4.2 and Fig 4.9). This phenomenon was most distinct and only significant at higher concentration of Cisplatin treatment (100 μ M).

Table 4.2. Percentages of cytotoxicity response to cisplatin in collagen (900 Pa and 2000 Pa stiffnesses) for MDA-MB-231 cells in control conditioned medium.

Medium	Stiffness	Drug Concentration	%Cell Death (M \pm SE) (n=3 biological replicate)	Delta (M \pm SE) (Comparison of drug response with Control response)	P value (delta comparison)
Control Conditioned M.	900 Pa	Control	33.17 \pm 3.25	-	-
	2000 Pa	Control	39.17 \pm 0.92	-	-
Control Conditioned M.	900 Pa	50	39.53 \pm 3.71	1.20 \pm 0.05	0.56
	2000 Pa	50	50.16 \pm 1.7	1.29 \pm 0.08	
Control Conditioned M.	900 Pa	75	47.87 \pm 3.91	1.25 \pm 0.02	0.835
	2000 Pa	75	54.32 \pm 1.64	1.42 \pm 0.07	
Control Conditioned M.	900 Pa	100	60.12 \pm 4.27	1.83 \pm 0.08	*0.042
	2000 Pa	100	57.68 \pm 0.77	1.48 \pm 0.05	

We also compared the percentage of apoptotic MDA-MB-231 cells supplemented with S1 conditioned medium across the two stiffnesses (900 and 2000 Pa). There was no apparent difference in the response pattern to incremental doses of drugs (Table 4.3 and Figure 4.9) Thus, there is a paracrine influence from the conditioned medium of non-neoplastic epithelial cells on increased stiffness-mediated sensitivity to cisplatin. Interestingly, this influence was also reflected at the level of the mean and the heterogeneity of nuclear circularity under the same culture conditions.

Table 4.3. Percentage of cytotoxicity response to cisplatin in collagen I (900 Pa and 2000 Pa stiffnesses) for MDA-MB-231 cells in the presence of S1 conditioned medium:

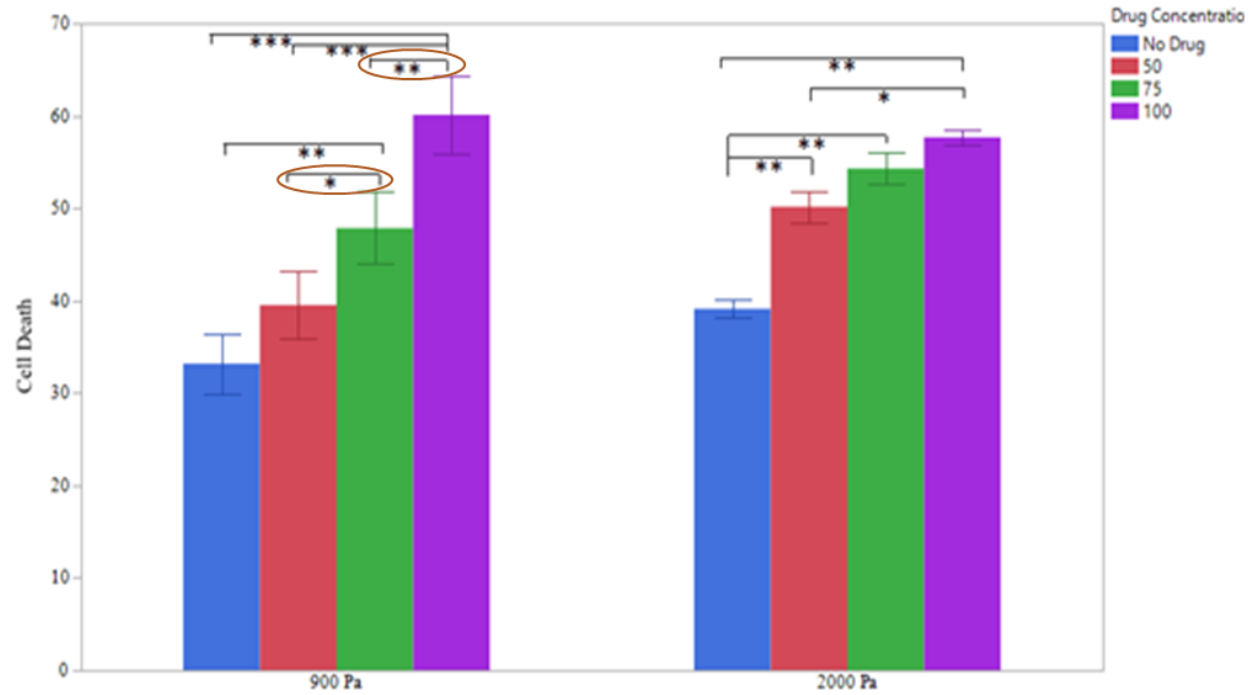
Medium	Stiffness	Drug Concentration	%Cell Death (M \pm SE) (n=3 biological replicate)	Delta (M \pm SE) (Comparison of drug response with Control response)	P value (delta comparison)
S1 conditioned M.	900 Pa	Control	34.5 \pm 4.6	-	-
	2000 Pa	Control	34.5 \pm 1.48		
S1 conditioned M.	900 Pa	50	43.42 \pm 5.74	1.22 \pm 0.005	0.39
	2000 Pa	50	39.84 \pm 3.62	1.14 \pm 0.07	
S1 conditioned M.	900 Pa	75	54.08 \pm 1.86	1.58 \pm 0.18	0.87
	2000 Pa	75	52.64 \pm 2.91	1.52 \pm 0.13	
S1 conditioned M.	900 Pa	100	57.52 \pm 2.04	1.67 \pm 0.19	0.83
	2000 Pa	100	60.39 \pm 2.83	1.74 \pm 0.09	

Figure 4.9. The percentage of viable cells in response to Cisplatin is influenced by collagen I stiffness and a paracrine effect from non-neoplastic cells.

After three days in culture half of the tumors was supplemented with fresh H14 + S1 conditioned medium (50:50) and half with fresh H14 + MDA-MB-231 conditioned medium (50:50) every 24 hours. To obtain the conditioned medium S1 cells were cultured on top of collagen (770 Pa), coated with laminin111. At day 6, culture plates with MDA-MB-231 cells were either treated with 50, 75 and 100 μ M of 3.3 mM Cisplatin or with vehicle (NaCl). After 24 hours tumors were stained with DAPI and recorded images were analyzed using ImageJ. N = 3; 150 nuclei analyzed per replicate. *P< 0.05, **P<0.01, ***P<0.001.

Figure 4.10 continued

a) Control Conditioned Medium (MDA-MB-231)

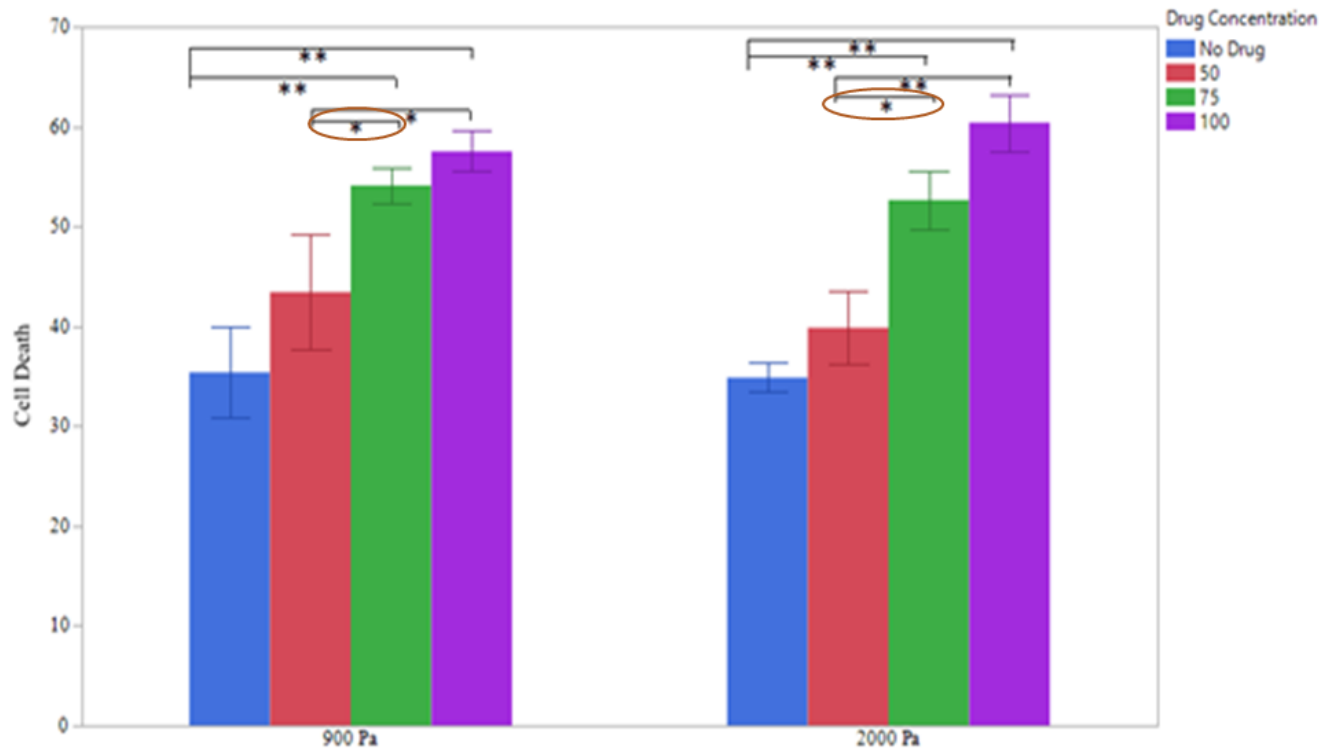


Nuclear circularity (mean)

Nuclear circularity (heterogeneity)

Figure 4.10 continued

b) S1 Conditioned Medium (MDA-MB-231)



Nuclear circularity (mean and heterogeneity)

Stiffness mediated response to cisplatin varies across tumors of different levels of aggressiveness

The tumors cultured from two different cell lines with different levels of aggressiveness showed distinct behaviors of nuclear morphometry with increasing stiffness. We were curious to observe if these phenotypes would be reflected in terms of cell's responses to cytotoxic treatment. We cultured T4-2 cells in collagen I (embedded method) of 2000 Pa and 3300 Pa for six days before treatment with cisplatin (50 μ M) for 24 hours and analyzed the percentage of apoptotic cells as described for MDA-MB-231 in the above section. Table 4.4 summarizes the apoptotic responses between the vehicle (NaCl) and Cisplatin treatment, indicating that the T4-2 cells were sensitive to the treatment at both the stiffnesses. Further, percentages of cell death were comparable for this dose of Cisplatin, even when stiffness was increased (Fig 4.10). Interestingly, in the less aggressive T4-2 tumors, we have observed, as shown in previous sections, that only nuclear area but not nuclear circularity was affected by increased stiffness, suggesting that like for the MDA-MB-231 cells the response of cells to drug sensitivity under the influence of increased stiffness parallels that of nuclear circularity.

Table 4.4. Percentage of cytotoxicity response to cisplatin in collagen I (2000 Pa and 3300 Pa stiffnesses) for T4-2

Medium	Stiffness	Drug Concentration	%Cell Death (M \pm SE) (n=2 biological replicate)	Delta (M \pm SE) (Comparison of drug response with Control response)	P value (delta comparison)
Regular H-14	2000 Pa	Control	24.97 \pm 1.02		
	3300 Pa	Control	30.43 \pm 0.585		
Regular H-14	2000 Pa	50	47.79 \pm 2.83	1.92 \pm 0.09	0.08
	3300 Pa	50	47.94 \pm 2.83	1.58 \pm 0.09	

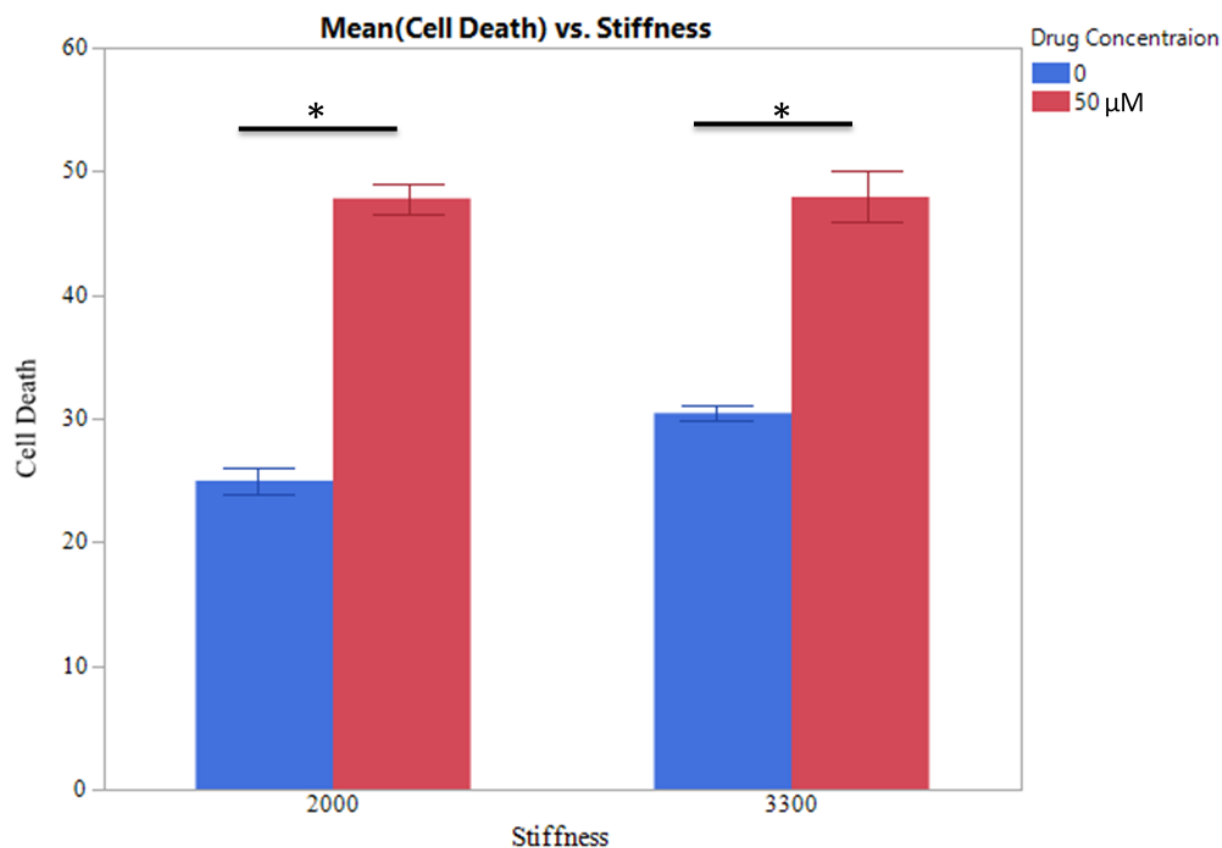


Figure 4.9. Increasing stiffness does not alter the sensitivity of T4-2 cell to LD₅₀ of cisplatin.

LD₅₀ for T4-2 is 50 μM in collagen at 2000 Pa. At day six, culture plates were either treated with 50 μM of Cisplatin or with vehicle (NaCl). After 24 hours tumors were stained with DAPI and recorded images were analyzed for apoptosis using *ImageJ*. N = 2; 150 nuclei analyzed per replicate. **P* < 0.05.

4.1 References:

1. Briand, P., Petersen, O. W., & Van Deurs, B. (1987). A new diploid nontumorigenic human breast epithelial cell line isolated and propagated in chemically defined medium. *In vitro cellular & developmental biology*, 23(3), 181-188.
2. Briand, P., Nielsen, K. V., Madsen, M. W., & Petersen, O. W. (1996). Trisomy 7p and malignant transformation of human breast epithelial cells following epidermal growth factor withdrawal. *Cancer research*, 56(9), 2039-2044.
3. Chhetri, A., Chittiboyina, S., Atrian, F., Bai, Y., Delisi, D. A., Rahimi, R., ... & Lelièvre, S. A. (2019). Cell culture and coculture for oncological research in appropriate microenvironments. *Current protocols in chemical biology*, 11(2), e65.
4. Kenny, P. A., Lee, G. Y., Myers, C. A., Neve, R. M., Semeiks, J. R., Spellman, P. T., ... & Bissell, M. J. (2007). The morphologies of breast cancer cell lines in three-dimensional assays correlate with their profiles of gene expression. *Molecular oncology*, 1(1), 84-96.
5. Rizki, A., Weaver, V. M., Lee, S. Y., Rozenberg, G. I., Chin, K., Myers, C. A., ... & Bissell, M. J. (2008). A human breast cell model of preinvasive to invasive transition. *Cancer research*, 68(5), 1378-1387.
6. Chittiboyina, S., Rahimi, R., Atrian, F., Ochoa, M., Ziaie, B., & Lelièvre, S. A. (2018). Gradient-on-a-Chip with reactive oxygen species reveals thresholds in the nucleus response of cancer cells depending on the matrix environment. *ACS biomaterials science & engineering*, 4(2), 432-445.
7. Becceneri, A. B., Fuzer, A. M., Plutin, A. M., Batista, A. A., Lelièvre, S. A., & Cominetti, M. R. (2020). Three-dimensional cell culture models for metallodrug testing: induction of apoptosis and phenotypic reversion of breast cancer cells by the trans-[Ru (PPh 3) 2 (N, N-dimethyl-N-thiophenylthioureaato-k 2 O, S)(bipy)] PF 6 complex. *Inorganic Chemistry Frontiers*, 7(16), 2909-2919.
8. Jain, R., Chittiboyina, S., Chang, C.-L., Lelièvre, S. A., & Savran, C. A. (2020). Deterministic culturing of single cells in 3D. *Scientific Reports*, 10(1), 10805. <https://doi.org/10.1038/s41598-020-67674-3>

CHAPTER 5. DISCUSSION

The influence of microenvironmental factors with physical impact, namely organization, density, and tensile properties of the ECM on tumor behavior has been revealed relatively recently. Increased stiffness of the ECM is associated with aggressive types of cancers, including cancers of the pancreas and the breast (1–3). However, it is not known whether the response to increasing stiffness depends on the level of aggressiveness of breast cancer that may be characterized by a different architecture of the tumors. Further, investigations of the TME's influence on tumors now include non-cancer cells, mainly immune cells, and fibroblasts (known to remodel the ECM). Influences from the non-neoplastic epithelial cells, that may constitute an important portion of the TME are suspected. Detailed investigations of such paracrine influences from non-neoplastic epithelial cells, especially with regards to a potential impact on the response of tumors to matrix stiffness are limited in the literature. Here, using breast models in 3D cell culture we have shown that the degree of tumor aggressiveness is associated with a differential behavior when ECM stiffness increases and that the non-neoplastic epithelial compartment is capable of influencing the effect of matrix stiffness even for tumors recognized as highly aggressive,

A cell's phenotype and its nuclear organizations are characteristic of the tissue microenvironment (valid for both normal and malignant cells) (4–6). Here, we investigated the impact of increasing collagen I stiffness within the low-level range of ECM stiffness, as experienced by breast tumors in the early stages of cancer progression (2000–3300 Pa) between two triple negative, basal-like breast cancers of different aggressiveness. Nuclear area and circularity of the aggressive **MDA-MB-231** tumors showed a more variable pattern than the less aggressive **T4-2** tumors upon increased ECM stiffness. Indeed, both nuclear area and circularity were modified in MDA-MB-231 cells, while only nuclear area was modified in T4-2 cells. A bigger nuclear area with increased stiffness as observed in T4-2 cells was an opposite trend when compared to the MDA-MB-231 cells. We also investigated whether the epithelial compartment may influence the impact of increasing stiffness on aggressive tumors in the extreme low range of stiffness increase for a cancerous tissue (900 to 2000 Pa), possibly corresponding to the early phase of tumor development when the impact of the remaining differentiated epithelium might be stronger. In the presence of paracrine factors from the non-neoplastic epithelium, the change in mean nucleus area between 900 Pa and 2000 Pa remained the same – i.e. – cells were bigger at

2000 Pa as compared to 900 Pa; however, there was no significant decrease in nuclear circularity anymore. Thus, it is possible that, if in large enough proportion, factors released by non-neoplastic epithelial cells might modify the response of the cell nucleus to physical strains outside the tumor, at least for nuclear circularity. Interestingly, the decrease of nuclear circularity is normally associated with enhanced aggressiveness in cancer.

Contextual synthetic lethality introduced by Bristow and colleagues (7) proposes the impact of non-genetic based tumor microenvironment on cancer cells' response to treatment. Therefore, one way to investigate the potential impact of changes in nuclear morphometry that are known indicators of potential changes in aggressiveness, is to assess sensitivity to cytotoxic anticancer drugs. Indeed, aggressiveness may not be only linked to an increase in invasive behavior, it might also be revealed by resistance to treatment. Stiffness mediated impact is largely favorable for aggressive forms of cancer as represented by MDA-MB-231, which resembles metastatic types of breast cancers (8). Our results show an impact of stiffness on drug-induced cell death as observed by others. Weaver and colleagues, who pioneered the field of mechanotransduction or the phenotypic impact of physical strains, including those imposed by the microenvironment, report an increased cell death in TNBCs in stiffer matrix in response to cytotoxic drugs as compared to softer matrices; they also report increased levels of NF- κ B (a major transcription factor involved in immune response) and activated JNK pathway (associated with regulation of apoptosis and proliferation) to be associated with resistance in softer matrices (9–11). In vivo, the metastatic behavior of tumors is known to be stiffness dependent, across different types of aggressive cancers of the breast and the liver. At the site of primary tumors, higher stiffness is shown to modulate invasive behavior with increased rate of proliferation and resistance behavior, while at the secondary sites of invasion (e.g., in the lungs) when tumors encounter softer stiffnesses, they enter a dormant, non-dividing state, often escaping the immune surveillance and therapy (most therapies aim to kill dividing cells) (10,12). The latter information suggests that tumors might also become resistant in stiffer matrix. Indeed, we measured decreased cell death for the highest dose of cisplatin (100 μ M) used with MDA-MB-231 cells at higher stiffness (2000 Pa) compared to a soft matrix (900 Pa). However, this slight 'resistance' was cancelled by the conditioned medium from the non-neoplastic epithelium. Interestingly, this change in behavior corresponded to the cancellation of the decrease in circularity observed at 2000 Pa compared to 900 Pa for these cells.

The existence of inter-tumor heterogeneity and of clonal populations within TNBCs is well known. The theory of clonal heterogeneity hypothesizes that higher heterogeneity increases the survival capabilities for cancer cells (higher genetic diversity, evolutionary selection of the most fit genetic and cell population mediated interactions) with an increased tendency towards forming more malignant/aggressive tumors, including resistant behaviors (13,14). Research exploring cellular/genetic/nuclear markers associated with heterogeneity is actively published, but the importance of nuclear morphometry features (which provide a general idea on possible alterations in phenotype) to assess heterogeneity linked to an aggressive behavior is not clearly established. We have previously used nuclear morphometry as a readout for phenotypic changes on a per cell basis (15–17). This type of measurement enables us to investigate the predominance or the variability of phenotypes within a tumor. With nucleus as the focus, our study aimed to understand the implications of increasing stiffness on the uniformity/ heterogeneity of the distribution of nuclear features (namely area and circularity). Further, we were interested to observe if the specific nuclear area and circularity distribution pattern had any association with overall cell viability. This information would be a steppingstone towards understanding the impact of heterogeneity on sensitivity/resistance at the cell nucleus level in the context of mechanotransduction. Distinct levels of heterogeneity in nuclear morphometry were observed across different stiffnesses for the tumors cultured from the same cancer cell line, suggesting a high plasticity in such population of cells. Heterogeneity in nuclear phenotypes linked with stiffness increase (2000 to 3300 Pa) was observed only for nuclear area for the less aggressive T4-2 cells. In contrast, MDA-MB-231 showed a heterogenous distribution of both nuclear area and circularity upon increasing stiffness. The change in heterogeneity level for nuclear area showed an opposite direction between the two types of tumors- it increased for MDA-MB-231 and decreased for T4-2 in a stiffer collagen I. The less heterogenous distribution of nuclear circularity of MDA-MB-231 cells at 3300 Pa also corresponds to their lowest percentage of cell death in this stiffness. This suggests that the change in heterogeneity level might be linked to phenotypic alterations rather than cell death induced by selective pressure that would make certain phenotypes disappear. A similar conclusion may be drawn for the increase in stiffness with the T4-2 cells for which the decrease in nuclear heterogeneity is not associated with a significant change in cell death. The presence of paracrine factors from non-neoplastic cells in MDA-MB-231 cultures impacted the mean and heterogenous distribution of nuclear circularity with increasing stiffness. Briefly, the differences that were

observed with nuclear circularity upon increasing stiffness in control conditioned medium disappeared in the presence of paracrine factors and the nuclei did not acquire a heterogeneous distribution pattern. These observations strengthen the claim for a phenotypic alteration of tumors with stiffness (one, that probably involves genes).

With the lowly aggressive T4-2 cells, although a change in heterogeneity was clear for nuclear area and might reflect its significant increase at 3000 Pa, it was not associated with a significant change in sensitivity to cisplatin (only measured with the LD50). Interestingly, the lack of change in sensitivity to the drug with increased stiffness was accompanied by the lack of change of circularity. This results warrants making a dose response curve for these conditions to better scrutinize sensitivity for both stiffness degrees. For MDA-MB-231 cells, the increase in heterogeneity for nuclear circularity between 900 and 2200 Pa was accompanied with the decreased impact of the highest dose of cisplatin used. It seems thus, that increased heterogeneity based on nuclear circularity might be linked to less sensitivity to cisplatin for these initially more aggressive cells. However, cisplatin treatment at 3000 Pa will need to be performed to verify this possibility.

Our results further substantiate recent revelations of the impact of ECM mechanics on nuclear shape and size. Earlier experiments which utilized force application (directly or indirectly) on the cytoskeleton, revealed a direct influence on nuclear shape using 2D based eukaryotic cell cultures (18). Here, we report an impact of an incremental stiffness, individually and in combination with paracrine factors, on nuclear morphometry. Perinuclear actin physically tethers the nuclear lamina to the cytoskeleton, hence providing a physical continuity from cell membrane and cytoskeleton linkers to the nucleus. Besides the physical linkage, perinuclear actin (formed through a strong integration of actin and myosin fibers) is also known to play dynamic biological roles, notably in resisting internal nuclear pressure (prominently during cell division) and in maintaining the cellular shape. Cytoskeletal actin fibers impact the formation of actin caps and, in response to stress (such as increased stiffness), they increase the transcription of homeostatic genes such as Glyceraldehyde-3-Phosphate dehydrogenase (*GADPH*) (19) by influencing the heterochromatin changes mediated through the nuclear distribution of histone acetylase and mechanoresponsive proteins like *MRTF* (20). Besides actin, other proteins involved in nuclear mechanics like Lamins A/C are also known to regulate heterochromatin. An important feature of the actin cap response to external stress is the regulation of nuclear shape. It progressively

decreases nuclear height as the stress filaments pass over the nucleus forming stress activated adhesion sites around it (21). The decrease in nuclear circularity for MDA-MB-231 cells when comparing 900 to 2000 Pa stiffnesses might be explained through this physical force modulation (should nuclear volume remain constant). Possibly, in a stiffer matrix of 3300 Pa, the increased nuclear pressure owing to the perinuclear stress caps around it could probably be mitigated by a homeostatic change in the nucleus at the level of heterochromatin or gene expression. Morphologically, this change would result in a more circular nucleus. It should be noted that the absence of, or any error in the structural proteins of the nucleus, such as lamins would impact the internal chromatin distribution, essentially by influencing DNA synthesis, DNA repair mechanisms, apoptosis and chromatin rearrangements (22). Further, lamins greatly impact the shape or spread of the nucleus, as a possible mechanism to release internally generated stress. Thus, nuclear homeostasis is essentially linked with the stability of structural nuclear proteins, and nuclear lamins are being investigated as prognostic markers of cancer (23). While we did not explore the expression and the distribution pattern of different lamins between the aggressive MDA-MB-231 and T4-2 cells, based on our results we can hypothesize that there might be significant differences in the expression/distribution pattern of at least one, if not more of these proteins. Breast cancer subtypes and the MDA-MB-231 cell line are known to have reduced and heterogeneous levels of lamin A in the cell population (24). The different types of lamins have been linked to oncogenes or tumor suppressor genes, indicating their importance in cancer cell's survival, apoptosis and proliferation. Lamin A was shown to interact with and regulate retinoblastoma protein pRb, (RB1), a tumor suppressor as well as the cell cycle proteins- ERB1 and ERB2. The competitive binding of pRb or Erb1/2 with lamin A ultimately directs the cell's entry into G0 phase or reentry into the cell cycle (25).

Both nuclear morphometry parameters investigated in the study provide a unique outlook on cellular phenotype and stiffness-mediated behavior. While nuclear area appears to reflect heterogeneity as a response to stiffness, which is more pronounced at higher stiffness for MDA-MB-231 (3300 Pa) and lower stiffness for T4-2 (2000 Pa), the nuclear circularity might reflect sensitivity to drug treatment. Changes in MDA-MB-231 cells' sensitivity to cisplatin in case of increased stiffness, depending on the presence or absence of conditioned medium, parallels the changes in nuclear circularity; the absence of a significant change in sensitivity to cisplatin in T4-2 cells upon increasing stiffness is also paralleled by the absence of a significant change in nuclear

circularity. However, additional experiments are needed to clearly establish whether nuclear circularity might be a marker of sensitivity to cytotoxic drugs and elucidate a potential to provide a cost-effective readout for matrix mediated mechanotransduction. Future studies should aim to establish a direct connection with histone modifications and gene transcription using next generation sequencing technologies, such as RNA-seq, on a per cell basis.

More aggressive cells are indeed impacted by stiffness for their response to cisplatin, but only mildly and this is mitigated by paracrine factors released by non-neoplastic epithelial cells. Paracrine factors may include cytokines, exosomes as extracellular vesicles that may be loaded with miRNA, growth hormones that act as cytokines, or metalloproteinases (MMPs). Increasingly, studies exploring the impact of paracrine factors from cancer associated fibroblasts (CAFs) indicate that these factors influence cancer cell migration and invasive properties, angiogenesis, and tumorigenesis through distinct pathways (26). The transforming growth factor (TGF- β) acting as a cytokine through canonical and non-canonical signaling pathways influences the migration and invasiveness of cancer cells (26,27). Stromal cell-derived factor 1-alpha (SDF1- α) is another paracrine factor identified in CAFs and is shown to influence the levels of MMP proteins that are known to influence ECM remodeling, thus promoting invasiveness and migration of tumors (28). MMPs in general are part of a family of proteases of various types, which are known to have tumor proliferating and also anti-proliferating properties, a newer revelation that emerged after clinical failures through MMP targeted therapies against cancer (29). Therefore, developing therapeutics through MMPs should consider their context-dependent roles, including cells that secrete them in the microenvironment (29-31). Non-cancerous stromal cells like epithelial cells are one of the major contributors of MMP in the microenvironment (32). The caveolin-1 (Cav-1) protein is a structural protein of the cell membrane that was identified as an important paracrine factor. Its role in cancer progression and resistance to cisplatin treatment as well as its ability to influence the ECM (and probably mechanotransduction) makes it a paracrine factor of interest. While its role in metabolic reprogramming (a hallmark of cancer, 33) has been known for several years, newer evidences indicate that Cav-1 is also secreted in exosomes. In these structures it contributes to the paracrine influence on neighboring cancer cell but is also a key player in determining the cargo selection of the exosomes (34,35). Depending on the stage and type of cancer progression Cav-1 suppresses tumors (early stages for tumorigenesis in breast cancer) or enhances metastatic potentials (for late stage pancreatic and ovarian cancers) and aggressive behaviors in benign

tumors. The paracrine influence of Cav1 is shown through coculture or monoculture studies in 2D and 3D cell culture systems (with EHS and collagen I gels) involving CAF and carcinoma cell lines of the pancreas and ovaries among others. Elevated Cav-1 in the TME promote CAF-mediated ECM architecture reorganization (through fibronectin organization) (36). Further, Cav-1 has been shown to promote resistance to cisplatin treatment across various types of cancers (pancreas and ovarian), potentially by regulating Notch-1/Ak strain transforming (Akt)/Nf- κ B apoptotic pathways (34,37). In contrast, a tumor inhibiting role of Cav-1 was identified in breast cancer by potential metabolic reprogramming of the Myc protein (38). Besides Cav-1, serum levels of cytokines such as Interleukin 6 (IL-6) and IL-8 are known to be elevated in breast cancers, and excessively in TNBCs. Like other cytokines, IL-6 and IL-8 both promote and inhibit tumors depending on the context and are explored in different types of cancer for therapeutic purposes. The inhibition of IL-6 and IL-8 in different types of breast tumors is being studied to improve the fight against treatment resistance (39). An *in vitro* study of TNBC showed that carcinoma cells survival is dependent on IL-6 and IL-8 in an NF- κ B dependent manner (40).

Based on our results, we highlight the importance of integrating multi-cellular factors and microenvironmental constrains such as stiffness in the design of future *in vitro* models of cancer. These models could be designed for investigating the behavior of individual cells leading to tumor formation, as described by Jain et al. (17). These models could also make use of a modified micro physiological system for a population of cells, with a gradient-based design to study known levels of soluble paracrine factors in conjunction with a specific ECM stiffness (15, 41-43). We report a phenotypic correlation of nuclear morphometry (mean circularity and its heterogeneity) to cisplatin sensitivity on tumors based on the level of aggressiveness as well paracrine influence on stiffness mediated response of aggressive tumors. Thus, further investigations of the mechanisms by which non-neoplastic epithelial cells influence the response to ECM stiffness less aggressive tumors are required to understand the importance of such influences across tumors of different levels of aggressiveness. We have shown that ECM mechanical strains impact nuclear architecture. Nuclear circularity, which reflects nuclear architecture, was shown to correlate with the aggressiveness of tumors linked to sensitivity to cytotoxic drugs across stiffness levels. Aggressive tumors showed smaller nuclear circularity and reduced sensitivity to Cisplatin treatment. The link between nuclear circularity and gene expression (notably for cell survival) requires investigations to understand whether nuclear morphometry could inform about specific cell behaviors. Future studies are

recommended to explore this relationship through mechanotransduction in physiologically relevant microenvironments.

5.1 References:

1. Lyons, T. R., O'brien, J., Borges, V. F., Conklin, M. W., Keely, P. J., Eliceiri, K. W., ... & Schedin, P. (2011). Postpartum mammary gland involution drives progression of ductal carcinoma in situ through collagen and COX-2. *Nature medicine*, 17(9), 1109-1115.
2. Rice, A. J., Cortes, E., Lachowski, D., Cheung, B. C. H., Karim, S. A., Morton, J. P., & Del Rio Hernandez, A. (2017). Matrix stiffness induces epithelial–mesenchymal transition and promotes chemoresistance in pancreatic cancer cells. *Oncogenesis*, 6(7), e352-e352.
3. Yoo, J., Seo, B. K., Park, E. K., Kwon, M., Jeong, H., Cho, K. R., ... & Cha, J. (2020). Tumor stiffness measured by shear wave elastography correlates with tumor hypoxia as well as histologic biomarkers in breast cancer. *Cancer Imaging*, 20(1), 1-10.
4. Weaver, V. M., Bissell, M. J., Fischer, A. H., & Peterson, O. W. (1996). The importance of the microenvironment in breast cancer progression: recapitulation of mammary tumorigenesis using a unique human mammary epithelial cell model and a three-dimensional culture assay. *Biochemistry and cell biology*, 74(6), 833-851.
5. Lelièvre, S. A., Weaver, V. M., Nickerson, J. A., Larabell, C. A., Bhaumik, A., Petersen, O. W., & Bissell, M. J. (1998). Tissue phenotype depends on reciprocal interactions between the extracellular matrix and the structural organization of the nucleus. *Proceedings of the National Academy of Sciences*, 95(25), 14711-14716.
6. Bissell, M. J., Weaver, V. M., Lelièvre, S. A., Wang, F., Petersen, O. W., & Schmeichel, K. L. (1999). Tissue structure, nuclear organization, and gene expression in normal and malignant breast. *Cancer research*, 59(7 Supplement), 1757s-1764s.
7. Chan, N., Pires, I. M., Bencokova, Z., Coackley, C., Luoto, K. R., Bhogal, N., ... & Bristow, R. G. (2010). Contextual synthetic lethality of cancer cell kill based on the tumor microenvironment. *Cancer research*, 70(20), 8045-8054.
8. Welsh, J. (2013, June 07). Animal models for studying prevention and treatment of breast cancer. Retrieved April 17, 2021, from <https://www.sciencedirect.com/science/article/pii/B9780124158948000403>
9. Weaver, V. M., Lelièvre, S., Lakins, J. N., Chrenek, M. A., Jones, J. C., Giancotti, F., ... & Bissell, M. J. (2002). $\beta 4$ integrin-dependent formation of polarized three-dimensional architecture confers resistance to apoptosis in normal and malignant mammary epithelium. *Cancer cell*, 2(3), 205-216.

10. Schrader, J., Gordon-Walker, T. T., Aucott, R. L., van Deemter, M., Quaas, A., Walsh, S., ... & Iredale, J. P. (2011). Matrix stiffness modulates proliferation, chemotherapeutic response, and dormancy in hepatocellular carcinoma cells. *Hepatology*, 53(4), 1192-1205.
11. Drain, A. P., Zahir, N., Northey, J. J., Zhang, H., Huang, P. J., Maller, O., ... & Weaver, V. M. (2021). Matrix compliance permits NF- κ B activation to drive therapy resistance in breast cancer. *Journal of Experimental Medicine*, 218(5).
12. Tilghman, R. W., Blais, E. M., Cowan, C. R., Sherman, N. E., Grigera, P. R., Jeffery, E. D., ... & Parsons, J. T. (2012). Matrix rigidity regulates cancer cell growth by modulating cellular metabolism and protein synthesis. *PloS one*, 7(5), e37231.
13. Karaayvaz, M., Cristea, S., Gillespie, S. M., Patel, A. P., Mylvaganam, R., Luo, C. C., ... & Ellisen, L. W. (2018). Unravelling subclonal heterogeneity and aggressive disease states in TNBC through single-cell RNA-seq. *Nature communications*, 9(1), 1-10.
14. Marusyk, A., & Polyak, K. (2010). Tumor heterogeneity: causes and consequences. *Biochimica et Biophysica Acta (BBA)-Reviews on Cancer*, 1805(1), 105-117.
15. Chittiboyina, S., Rahimi, R., Atrian, F., Ochoa, M., Ziaie, B., & Lelièvre, S. A. (2018). Gradient-on-a-Chip with reactive oxygen species reveals thresholds in the nucleus response of cancer cells depending on the matrix environment. *ACS biomaterials science & engineering*, 4(2), 432-445.
16. Becceneri, A. B., Fuzer, A. M., Plutin, A. M., Batista, A. A., Lelièvre, S. A., & Cominetti, M. R. (2020). Three-dimensional cell culture models for metallodrug testing: induction of apoptosis and phenotypic reversion of breast cancer cells by the trans-[Ru (PPh 3) 2 (N, N-dimethyl-N-thiophenylthiourea-to-k 2 O, S)(bipy)] PF 6 complex. *Inorganic Chemistry Frontiers*, 7(16), 2909-2919.
17. Jain, R., Chittiboyina, S., Chang, C.-L., Lelièvre, S. A., & Savran, C. A. (2020). Deterministic culturing of single cells in 3D. *Scientific Reports*, 10(1), 10805. <https://doi.org/10.1038/s41598-020-67674-3>
18. Haase, K., Macadangdang, J. K., Edrington, C. H., Cuerrier, C. M., Hadjiantoniou, S., Harden, J. L., ... & Pelling, A. E. (2016). Extracellular forces cause the nucleus to deform in a highly controlled anisotropic manner. *Scientific reports*, 6(1), 1-11.
19. Charó, N. L., Galigniana, N. M., & Pwien-Pilipuk, G. (2018). Heterochromatin protein (HP) 1 γ is not only in the nucleus but also in the cytoplasm interacting with actin in both cell compartments. *Biochimica et Biophysica Acta (BBA)-Molecular Cell Research*, 1865(2), 432-443.

20. Jain, N., Iyer, K. V., Kumar, A., & Shivashankar, G. V. (2013). Cell geometric constraints induce modular gene-expression patterns via redistribution of HDAC3 regulated by actomyosin contractility. *Proceedings of the National Academy of Sciences*, 110(28), 11349-11354.
21. Khatau, S. B., Hale, C. M., Stewart-Hutchinson, P. J., Patel, M. S., Stewart, C. L., Searson, P. C., ... & Wirtz, D. (2009). A perinuclear actin cap regulates nuclear shape. *Proceedings of the National Academy of Sciences*, 106(45), 19017-19022.
22. Singh, M., Hunt, C. R., Pandita, R. K., Kumar, R., Yang, C.-R., Horikoshi, N., ... & Pandita, T. K. (2013). Lamin A/C Depletion Enhances DNA Damage-Induced Stalled Replication Fork Arrest. *Molecular and Cellular Biology*, 33(6), 1210–1222.
<https://doi.org/10.1128/MCB.01676-12>
23. Foster, C. R., Przyborski, S. A., Wilson, R. G., & Hutchison, C. J. (2010). Lamins as cancer biomarkers. *Biochemical Society Transactions*, 38(1), 297–300.
<https://doi.org/10.1042/BST0380297>
24. Capo-chichi, C. D., Cai, K. Q., Smedberg, J., Ganjei-Azar, P., Godwin, A. K., & Xu, X.-X. (2011). Loss of A-type lamin expression compromises nuclear envelope integrity in breast cancer. *Chinese Journal of Cancer*, 30(6), 415–425.
<https://doi.org/10.5732/cjc.010.10566>
25. Rodríguez, J., Calvo, F., González, J. M., Casar, B., Andrés, V., & Crespo, P. (2010). ERK1/2 MAP kinases promote cell cycle entry by rapid, kinase-independent disruption of retinoblastoma-lamin A complexes. *The Journal of Cell Biology*, 191(5), 967–979.
<https://doi.org/10.1083/jcb.201004067>
26. Erdogan, B., & Webb, D. J. (2017). Cancer-associated fibroblasts modulate growth factor signaling and extracellular matrix remodeling to regulate tumor metastasis. *Biochemical Society Transactions*, 45(1), 229–236. <https://doi.org/10.1042/BST20160387>
27. Yu, Y., Xiao, C.-H., Tan, L.-D., Wang, Q.-S., Li, X.-Q., & Feng, Y.-M. (2014). Cancer-associated fibroblasts induce epithelial–mesenchymal transition of breast cancer cells through paracrine TGF- β signalling. *British Journal of Cancer*, 110(3), 724–732.
<https://doi.org/10.1038/bjc.2013.768>
28. Teng, F., Tian, W.-Y., Wang, Y.-M., Zhang, Y.-F., Guo, F., Zhao, J., Gao, C., & Xue, F.-X. (2016). Cancer-associated fibroblasts promote the progression of endometrial cancer via the SDF-1/CXCR4 axis. *Journal of Hematology & Oncology*, 9(1), 8.
<https://doi.org/10.1186/s13045-015-0231-4>
29. Kessenbrock, K., Plaks, V., & Werb, Z. (2010). Matrix Metalloproteinases: Regulators of the Tumor Microenvironment. *Cell*, 141(1), 52–67.
<https://doi.org/10.1016/j.cell.2010.03.015>

30. Egeblad, M., & Werb, Z. (2002). New functions for the matrix metalloproteinases in cancer progression. *Nature Reviews Cancer*, 2(3), 161–174. <https://doi.org/10.1038/nrc745>
31. Winer, A., Adams, S., & Mignatti, P. (2018). Matrix metalloproteinase inhibitors in cancer therapy: turning past failures into future successes. *Molecular Cancer Therapeutics*, 17(6), 1147–1155. <https://doi.org/10.1158/1535-7163.MCT-17-0646>
32. Sengupta, N., & MacDonald, T. T. (2007). The Role of Matrix Metalloproteinases in Stromal/Epithelial Interactions in the Gut. *Physiology*, 22(6), 401–409. <https://doi.org/10.1152/physiol.00027.2007>
33. Hanahan, D., & Weinberg, R. A. (2011). Hallmarks of Cancer: The Next Generation. *Cell*, 144(5), 646–674. <https://doi.org/10.1016/j.cell.2011.02.013>
34. Bartz, R., Zhou, J., Hsieh, J.-T., Ying, Y., Li, W., & Liu, P. (2008). Caveolin-1 secreting LNCaP cells induce tumor growth of caveolin-1 negative LNCaP cells in vivo. *International Journal of Cancer*, 122(3), 520–525. <https://doi.org/10.1002/ijc.23142>
35. Lin, C.-J., Yun, E.-J., Lo, U.-G., Tai, Y.-L., Deng, S., Hernandez, E ... & Hsieh, J.-T. (2019). The paracrine induction of prostate cancer progression by caveolin-1. *Cell Death & Disease*, 10(11), 1–15. <https://doi.org/10.1038/s41419-019-2066-3>
36. Goetz, J. G., Minguet, S., Navarro-Lérida, I., Lazcano, J. J., Samaniego, R., Calvo, E., ... & Del Pozo, M. A. (2011). Biomechanical Remodeling of the Microenvironment by Stromal Caveolin-1 Favors Tumor Invasion and Metastasis. *Cell*, 146(1), 148–163. <https://doi.org/10.1016/j.cell.2011.05.040>
37. Zou, W., Ma, X., Hua, W., Chen, B., & Cai, G. (2015). Caveolin-1 mediates chemoresistance in cisplatin-resistant ovarian cancer cells by targeting apoptosis through the Notch-1/Akt/NF-κB pathway. *Oncology Reports*, 34(6), 3256–3263. <https://doi.org/10.3892/or.2015.4320>
38. Wang, S., Wang, N., Zheng, Y., Yang, B., Liu, P., Zhang, F., ... & Wang, Z. (2020). Caveolin-1 inhibits breast cancer stem cells via c-Myc-mediated metabolic reprogramming. *Cell Death & Disease*, 11(6), 1–16. <https://doi.org/10.1038/s41419-020-2667-x>
39. Heo, T.-H., Wahler, J., & Suh, N. (2016). Potential therapeutic implications of IL-6/IL-6R/gp130-targeting agents in breast cancer. *Oncotarget*, 7(13), 15460–15473. <https://doi.org/10.18632/oncotarget.7102>
40. Hartman, Z. C., Poage, G. M., Hollander, P. den, Tsimelzon, A., Hill, J., Panupinthu, N., ... & Brown, P. H. (2013). Growth of Triple-Negative Breast Cancer Cells Relies upon Coordinate Autocrine Expression of the Proinflammatory Cytokines IL-6 and IL-8. *Cancer Research*, 73(11), 3470–3480. <https://doi.org/10.1158/0008-5472.CAN-12-4524-T>

41. Deiss, F., Mazzeo, A., Hong, E., Ingber, D. E., Derda, R., & Whitesides, G. M. (2013). Platform for high-throughput testing of the effect of soluble compounds on 3D cell cultures. *Analytical chemistry*, 85(17), 8085-8094.
42. Moon, H. R., Ospina-Muñoz, N., Noe-Kim, V., Yang, Y., Elzey, B. D., Konieczny, S. F., & Han, B. (2020). Subtype-specific characterization of breast cancer invasion using a microfluidic tumor platform. *PloS one*, 15(6), e0234012.
43. Herland, A., Maoz, B. M., Das, D., Somayaji, M. R., Prantil-Baun, R., Novak, R., ... & Ingber, D. E. (2020). Quantitative prediction of human pharmacokinetic responses to drugs via fluidically coupled vascularized organ chips. *Nature biomedical engineering*, 4(4), 421-436.

CHAPTER 6. CONCLUSION

We investigated two nuclear parameters used for decades in cancer pathology- nuclear circularity and area. These nuclear parameters were studied under a new light by modifying the ECM properties of tumors produced in 3D cell culture. Both nuclear parameters were responsive, possibly illustrating distinct phenotypes reflective of the ECM changes. We showed that reduced nuclear circularity in the cancer cell population overall and the degree of heterogeneity for this morphometric parameter seem associated with an aggressive tumor behavior, considering changes in sensitivity to the cytotoxic drug, cisplatin. Our results also indicated that a paracrine influence from non-neoplastic epithelium, although small, is possible for stiffness mediated changes in nuclear morphometry and drug sensitivity in aggressive tumors. The knowledge about the relation between physical elements of the cell nucleus and chromatin is currently limited; we argue that changes in the level of sensitivity to anticancer drugs in the presence of alterations in nuclear circularity or shape might be linked to modifications in gene expression. Future studies that combine live cell imaging of nuclear mechanotransduction proteins and next generation sequencing will help elucidate the underlying mechanisms. Technical advances to design gradients of the microenvironmental factors of interest, thanks to engineering, will be needed to identify thresholds in stiffness and paracrine factors that modulate gene expression within a certain range of nuclear circularity. Nuclear stress is strongly associated with nuclear shape and biological outcomes important for cancer progression, such as response to cellular stress induced by external factors leading to DNA damage and repair, etc. Understanding stress response using nuclear shape and corresponding stress gene expression profiles would be advantageous. In this regard, the distribution pattern of histone modifiers that influence the accessibility of chromatin becomes critical. How would the nuclear circularity of a same cell and its chromatin and genes associated with nuclear stress, react when exposed to different conditions (stiffer matrix or more paracrine influence)? Mina Bissell, who developed the concept of dynamic reciprocity between the microenvironment and genes, had said that '*context is everything*'. Context can be defined by the surroundings or circumstances in which an event occurs. By modulating physical and biochemical microenvironmental factors in a very precise manner thanks to engineered cell culture, we can now start recreating different scenarios to elucidate the context of cancer within the nucleus.

APEKSHYA CHHETRI

Curriculum Vitae

206 S Martin Jischke Drive,
West Lafayette, 47906, IN

EDUCATION

Purdue University , West Lafayette, IN Ph.D. , Interdisciplinary Biomedical Sciences Advisor: Joseph V. Rispoli	Expected May 2023
M.Sc. , Basic Medical Science Advisor: Sophie A. Lelièvre	Expected May 2021 GPA: 3.71/4.00
Kathmandu University , Kathmandu, Nepal B. tech. , Biotechnology Dissertation: "Characterization and optimization of physical parameters for maximum PHB yield from <i>Bacillus</i> species isolated from soil sample"	December 2016 GPA: 3.64/4.00

RESEARCH EXPERIENCE

College of Veterinary Medicine, Purdue University Graduate Research Assistant	2018- 2020
Research Institute for Bioscience & Biotechnology, Nepal Research Assistant	March-August 2017
Kathmandu University-Seoul National University Collaboration, Nepal	2018

PEER- REVIEWED PUBLICATIONS

- Chhetri A., Rispoli J.V., Lelièvre S.A. (2021). 3D cell culture for the study of microenvironment-mediated mechanostimuli to the cell nucleus: An important step for cancer research. *Front. Mol. Biosci.* doi:[10.3389/fmolb.2021.628386](https://doi.org/10.3389/fmolb.2021.628386).
- Chhetri, A., Li X. & Rispoli J.V. (2020). Current and emerging magnetic resonance-based techniques for breast cancer. *Front. Med.* doi:[10.3389/fmed.2020.00175](https://doi.org/10.3389/fmed.2020.00175).
- Chhetri, A., et al. (2019). Cell culture and coculture for oncological research in appropriate microenvironments. *Curr. Protoc. Chem. Biol.* doi:[10.1002/cpch.65](https://doi.org/10.1002/cpch.65).
- Upreti, A., et al. (2018). Evaluation of α -amylase, lipase inhibition and in-vivo pharmacological activities of *Eucalyptus camaldulensis* Dehnh leaf extract. *eJTCM*. doi:[10.1016/j.jtcme.2018.07.001](https://doi.org/10.1016/j.jtcme.2018.07.001).

UNIVERSITY TEACHING EXPERIENCE

Purdue University, West Lafayette, IN

Teaching Assistant, BME 39000

Teaching Assistant, BIOL 11000

January 2021- Current

Fall 2020

ACHIEVEMENTS

Fellowship Awards

Purdue University, Lynn Graduate Fellowship

August 2018- July 2019

Poster presentation awards

Purdue University, IN

CTSI Best Poster Award

January 2020

Poster title “Disease-on-a-chip platform for rapid screening of anticancer drugs”

TECHNICAL SKILLS

Mammalian cell culture

Techniques: 2D plate culture; 3D cultures (matrigel, collagen, tissue chips)

Cell lines: HMT-3522, MDA-MB-231, HMS-32

Medium and additive preparation:

DMEM-F12;

Prolactin, Insulin, β -estradiol, Hydrocortisone, Sodium selenite, Transferrin, Fibroblast Growth Factor, Epidermal Growth Factor, Transforming growth factor β , Soybean trypsin Inhibitor

Microbial culture and analysis:

Agar plate culture, stab culture, broth culture; gram staining, antimicrobial analysis (disk diffusion assay)

Bacteria: *Bacillus* species, *Streptomyces* species, *Escherichia coli*

Biological Assays:

Proficient: Immunostaining, DAPI staining, spectroscopy, nuclei acid extraction

Basic training and working knowledge: gel electrophoresis, western blot

Animal models: rat, mice, rabbit

Chemical Assays: Analytical chromatography

Microscopy: Optical microscopes (fluorescence and EVOS live cell imaging microscope), trained in confocal microscope (Zeiss LSM 710 with Zeiss Zen software)

Imaging: Trained on Bruker 7T MRI Scanner for animals

Software packages: Image J, Microsoft package, MATLAB (basic), FSL

LEADERSHIP POSITIONS

Purdue University, West Lafayette, IN

Co-instructor of 3D Cell culture workshop, 3D3C facility December 2019

Purdue Graduate Student Government
Vice Chair for Public Relations August 2020 - Present

Biomedical Graduate Student Association
Co-chair for Special Programs June 2019 – April 2020

Judge: Lafayette Regional Science and Engineering Fair March 2019

Kathmandu University, Nepal

AIESEC Kathmandu University
President 2015

LANGUAGES

Nepali – Native or Bilingual Proficiency

English – Full Professional Proficiency

Hindi – Professional Working Proficiency